Andrea Damascelli

UBC-MPI Quantum Matter Institute

ARPES on Correlated Electron Systems

CUSO Lecture – Lausanne 02/2011

Outline Part II

- Sr_2RuO_4: A Fermi liquid + spin-orbit coupling
- HTSC: Mott gap and strong correlations
- Sudden approx. and QP renormalization
- HTSC: The fate of quasiparticle strength
- References, slides, and lecture notes

CUSO Lecture – Lausanne 02/2011

Outline Part II

Sr_2RuO_4: A Fermi liquid with spin-orbit coupling

CUSO Lecture – Lausanne 02/2011

Strongly Correlated Electron Systems

d - f
open shells materials

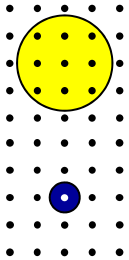

U<<W
Charge fluctuations

U>>W
Spin fluctuations

Control parameters

Bandwidth (U/W)
Band filling
Dimensionality

I	II	IIIb	IVb	Vb	VIb	VIIb	VIIIb		Ib	IIb	III	IV	V	VI	VII	0
H																He
Li	Be										B	C	N	O	F	Ne
Na	Mg										Al	Si	P	S	Cl	Ar
K	Ca	Sc	Ti	V	Cr	Mn	Fe	Co	Ni	Cu	Zn	Ga	Ge	As	Se	Br	Kr
Rb	Sr	Y	Zr	Nb	Mo	Tc	Ru	Rh	Pd	Ag	Cd	In	Sn	Sb	Te	I	Xe
Cs	Ba	La*	Hf	Ta	W	Re	Os	Ir	Pt	Au	Hg	Tl	Pb	Bi	Po	At	Rn
Fr	Ra	Ac**	Rf	Db	Sg	Bh	Hs	Mt									

Lanthanides*	Ce	Pr	Nd	Pm	Sm	Eu	Gd	Tb	Dy	Ho	Er	Tm	Yb	Lu
Actinides**	Th	Pa	U	Np	Pu	Am	Cm	Bk	Cf	Es	Fm	Md	No	Lr

Degrees of freedom

Charge / Spin
Orbital
Lattice

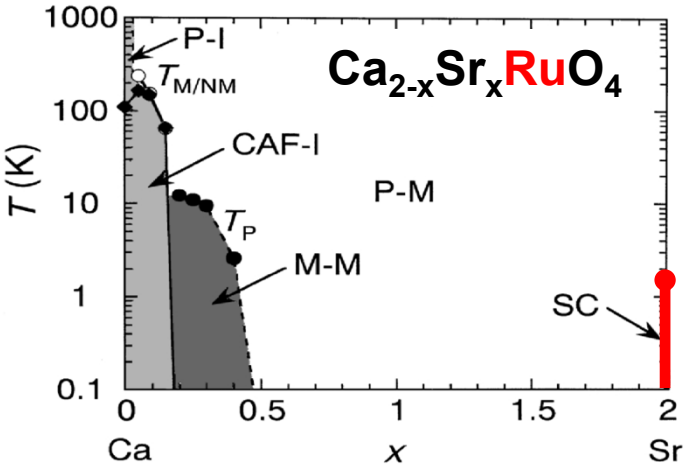

- **Kondo**
- **Mott-Hubbard**
- **Heavy Fermions**
- **Unconventional SC**
- **Spin-charge order**
- **Colossal MR**

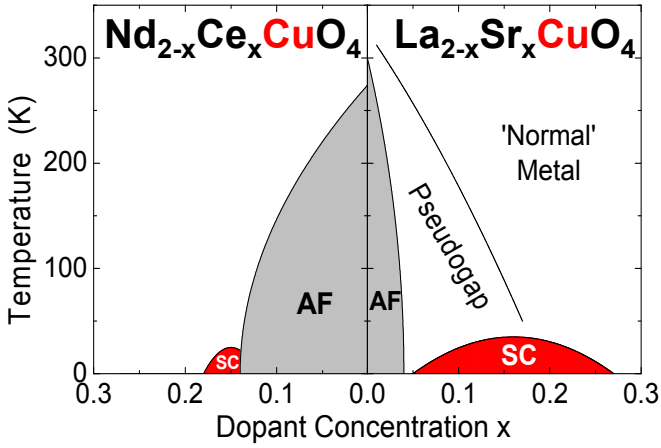

Strongly Correlated Electron Systems

d - f
open shells materials

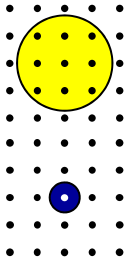

U<<W
Charge fluctuations

U>>W
Spin fluctuations

Control parameters

Bandwidth (U/W)
Band filling
Dimensionality

I	II	IIIb	IVb	Vb	VIb	VIIb	VIIIb		Ib	IIb	III	IV	V	VI	VII	0
H																He
Li	Be										B	C	N	O	F	Ne
Na	Mg										Al	Si	P	S	Cl	Ar
K	Ca	Sc	Ti	V	Cr	Mn	Fe	Co	Ni	Cu	Zn	Ga	Ge	As	Se	Br	Kr
Rb	Sr	Y	Zr	Nb	Mo	Tc	Ru	Rh	Pd	Ag	Cd	In	Sn	Sb	Te	I	Xe
Cs	Ba	La*	Hf	Ta	W	Re	Os	Ir	Pt	Au	Hg	Tl	Pb	Bi	Po	At	Rn
Fr	Ra	Ac**	Rf	Db	Sg	Bh	Hs	Mt									

Lanthanides*	Ce	Pr	Nd	Pm	Sm	Eu	Gd	Tb	Dy	Ho	Er	Tm	Yb	Lu
Actinides**	Th	Pa	U	Np	Pu	Am	Cm	Bk	Cf	Es	Fm	Md	No	Lr

Degrees of freedom

Charge / Spin
Orbital
Lattice

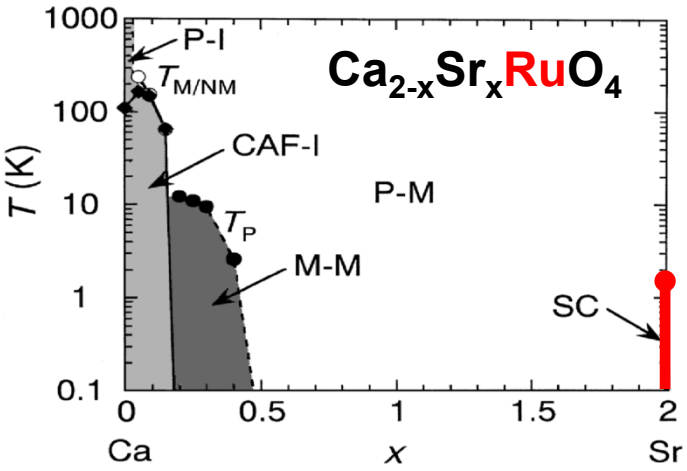

d-orbitals
radial extent

Spin-orbit coupling

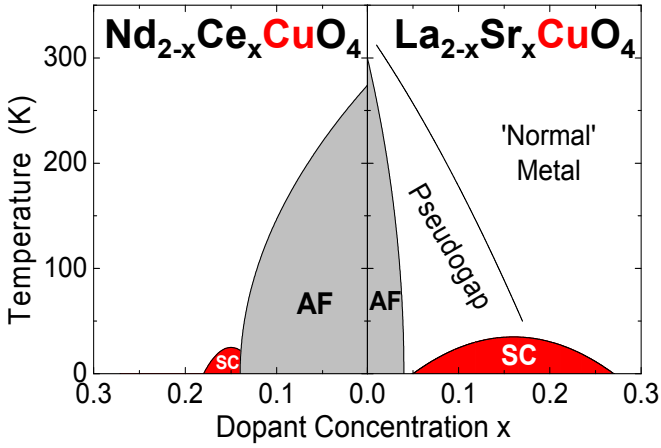

1D ($d_{xz,yz}$) versus 2D (d_{xy}) Superconductivity ?

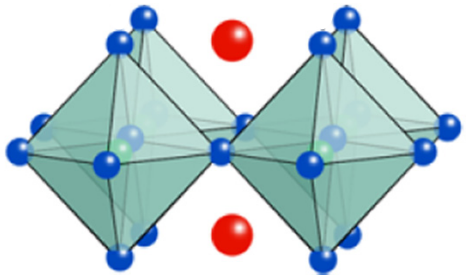

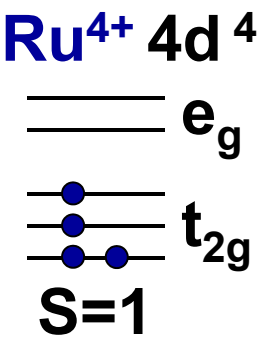

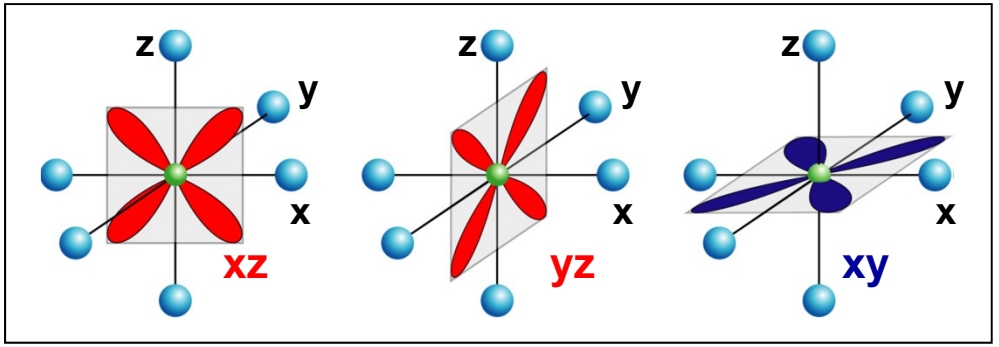

- Band structure calculation: **3 t_{2g}** bands crossing **E_F**

d_{xy}

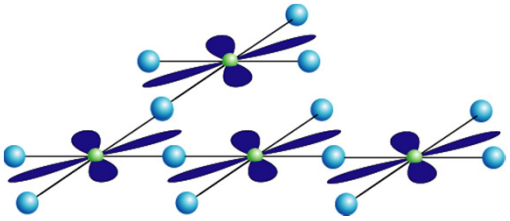

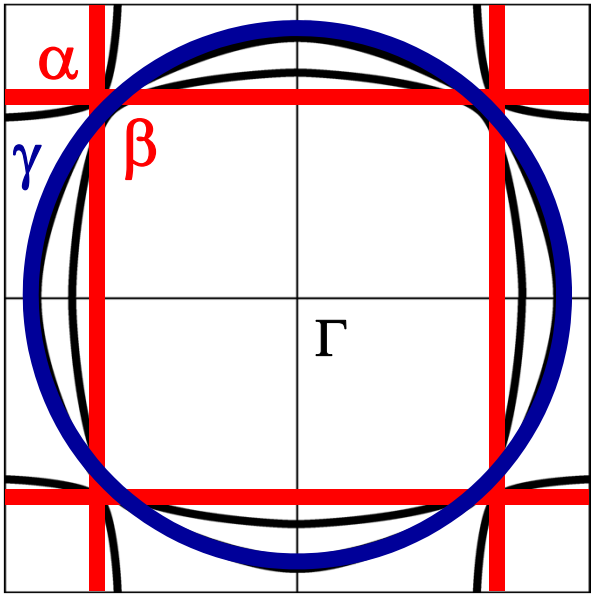

d_{yz}

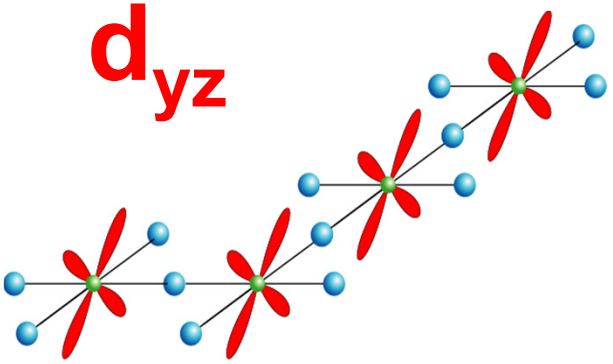

Mazin *et al.*, PRL **79**, 733 (1997)

Eigenstates with Spin-Orbit Coupling

Starting from degenerate t_{2g} orbitals

$\sqrt{1/2}\,(-d_{xz}-i\,d_{yz})=d_1$

$\sqrt{1/2}\,(d_{xz}-i\,d_{yz})=d_{-1}$

d_{xy}

3-orbitals with orbital momentum 0, +/- 1 like p-orbitals

Atomic relativistic SOC

Ru^{4+} ζ=161 meV

Rh^{4+} ζ=191 meV

Earnshaw, JCS **601**, 3132 (1961)

$$H = \zeta \sum_i l_i \cdot s_i$$

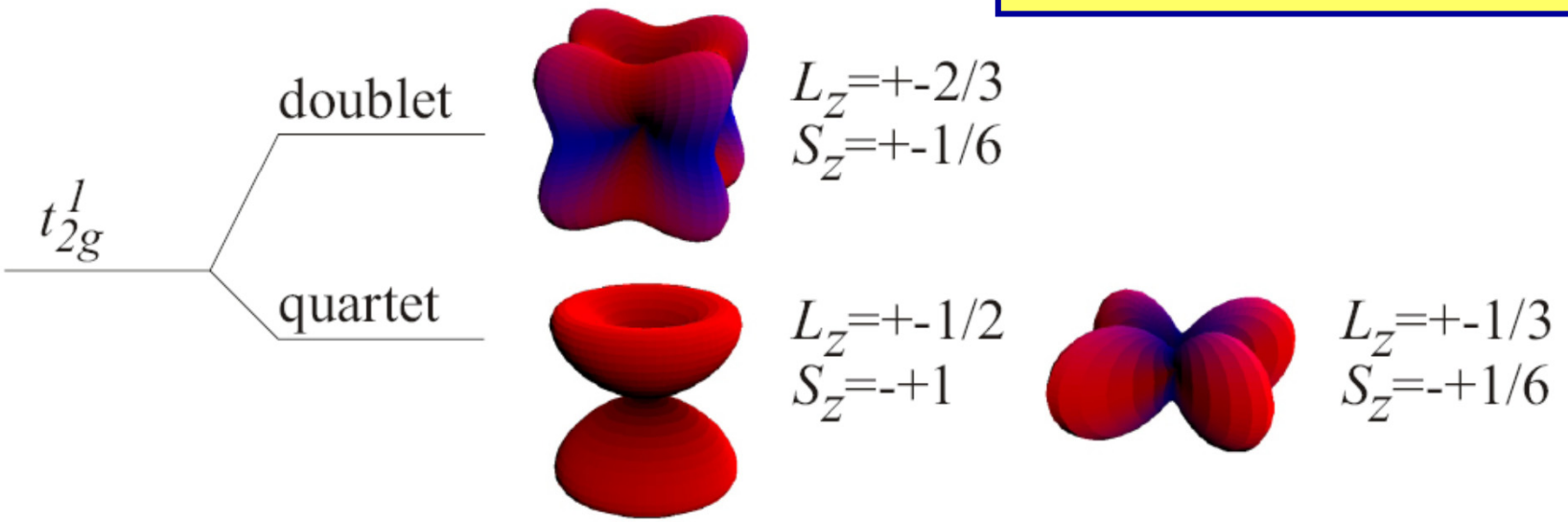

M.W. Haverkort, I.S. Elfimov, L.H. Tjeng, G.A. Sawatzky, A. Damascelli, PRL **101**, 026406 (2008)

Importance of Spin-Orbit Coupling in 4d Oxides

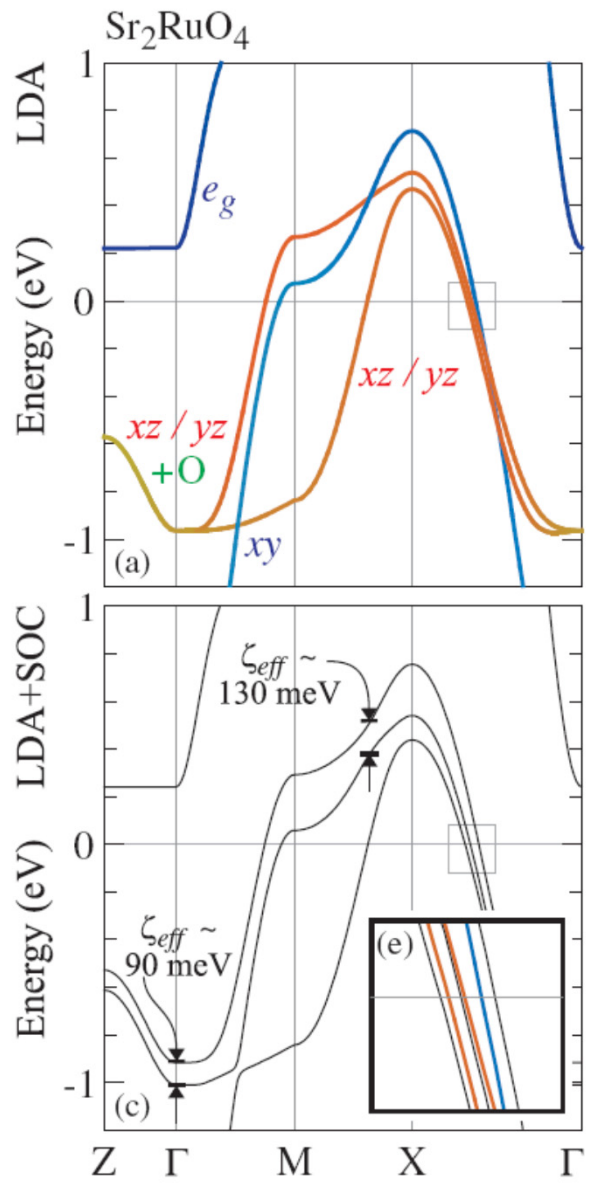

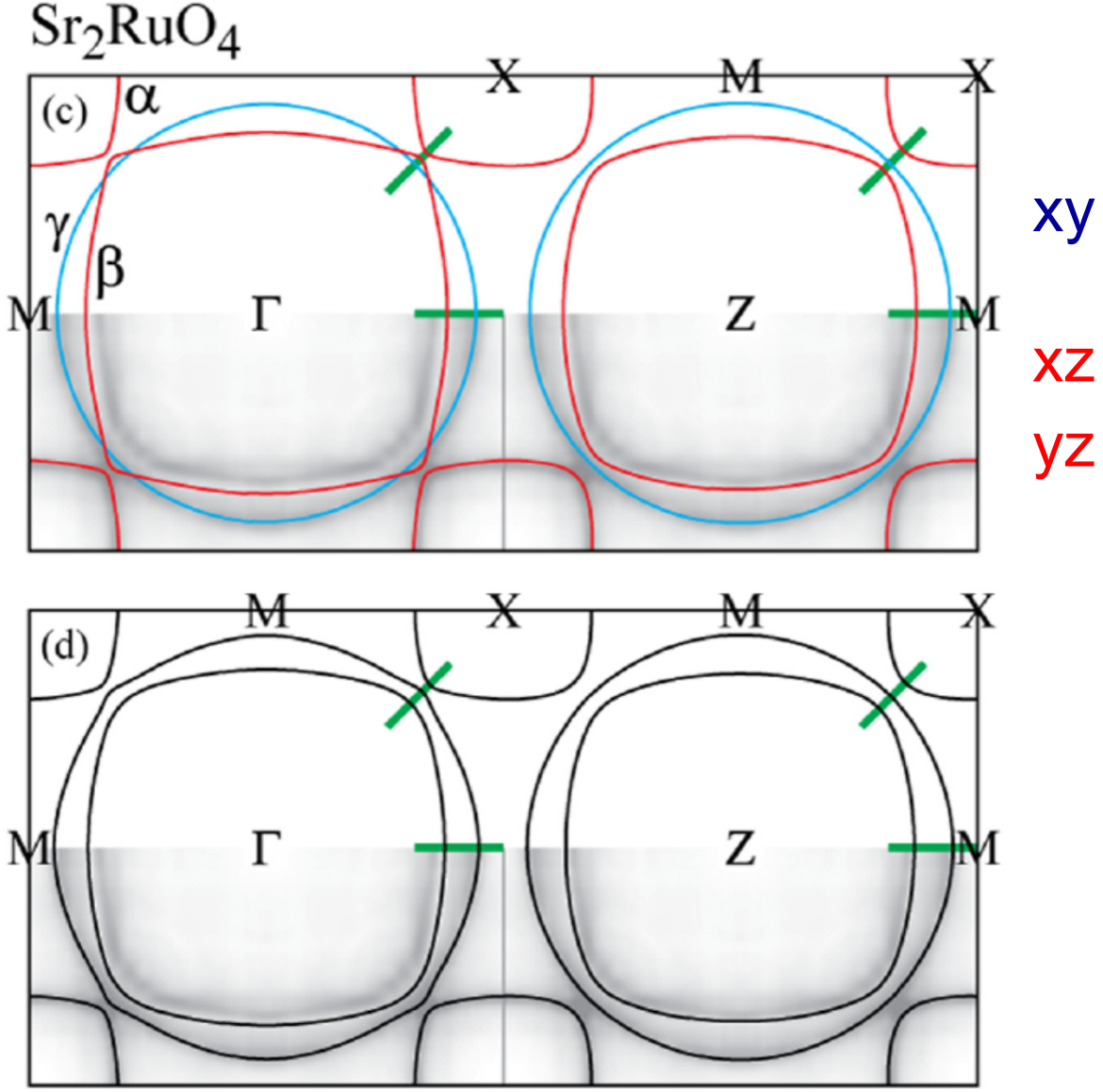

M.W. Haverkort, I.S. Elfimov, L.H. Tjeng, G.A. Sawatzky, A. Damascelli, PRL **101**, 026406 (2008)

“Classic Low-temperature” Superconductors

Metallic Density of States

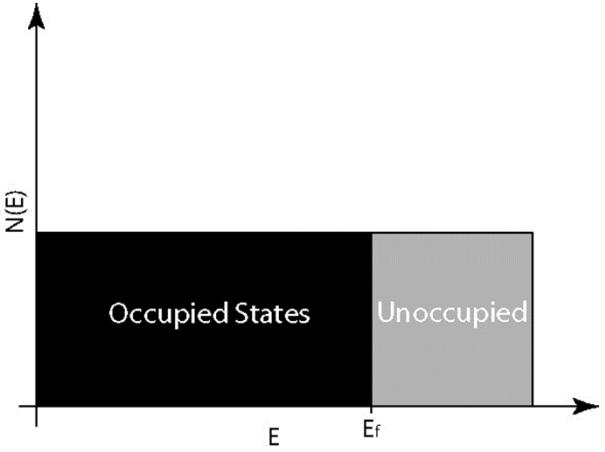

Superconducting Density of States

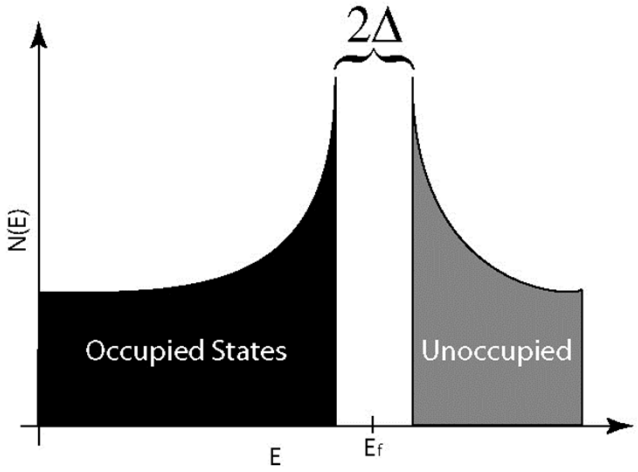

Superconductivity can only be seen on low energy scales and needs **high resolution**!

Superconductivity

2-electron bound state

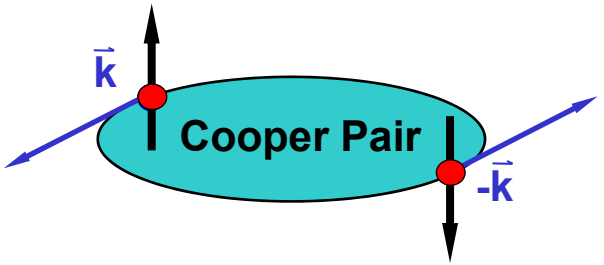

spin-singlet pairing

Spin-Triplet Superconductivity in Sr_2RuO_4

Mackenzie & Maeno, RMP **75**, 657 (2003)

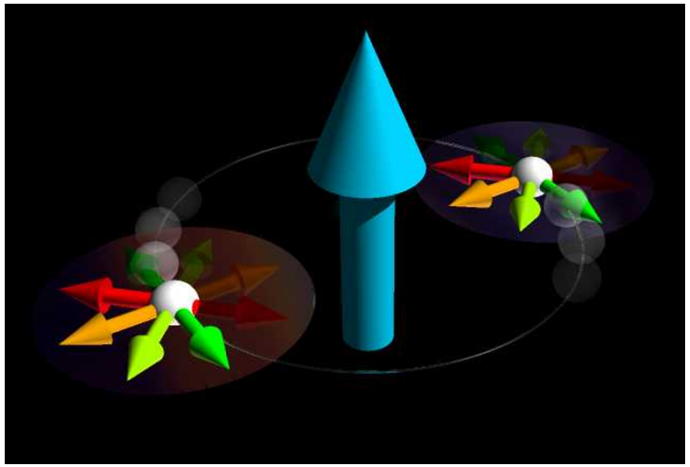

Xia et a., PRL **97**, 167002 (2006)

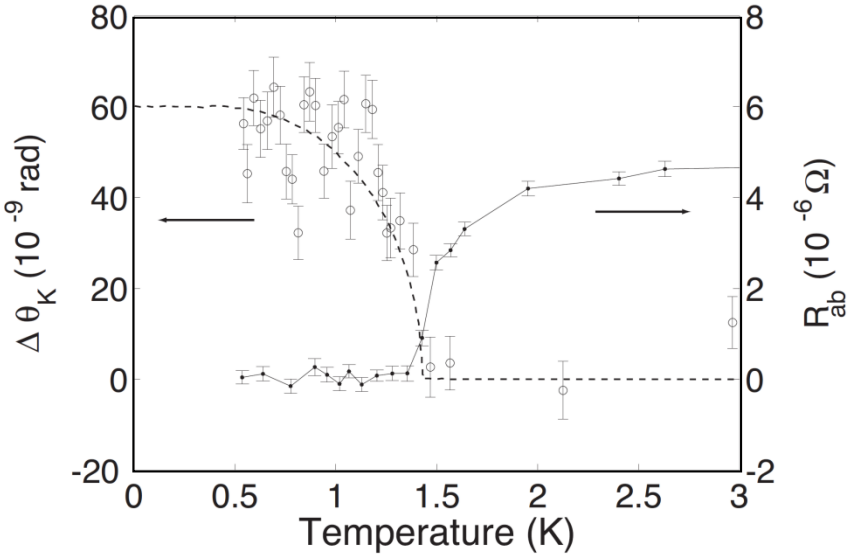

Weak SOC

- Equal spin-triplet pairing for any quantization axis
- Single-band (d_{xy}) isotropic p-wave order parameter
- TRSB: p_x+ip_y with no disorder gives zero Kerr signal

Strong SOC

- k-dependent spin-triplet mixing: order parameter?
- Orbital character mixing: multiband superconductivity?
- Is TRSB a signature of spin-orbit coupling?

Band Renormalization by Electronic Correlations

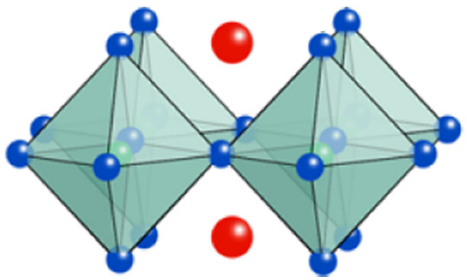

Ru^{4+} $4d^4$

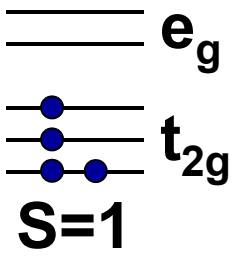

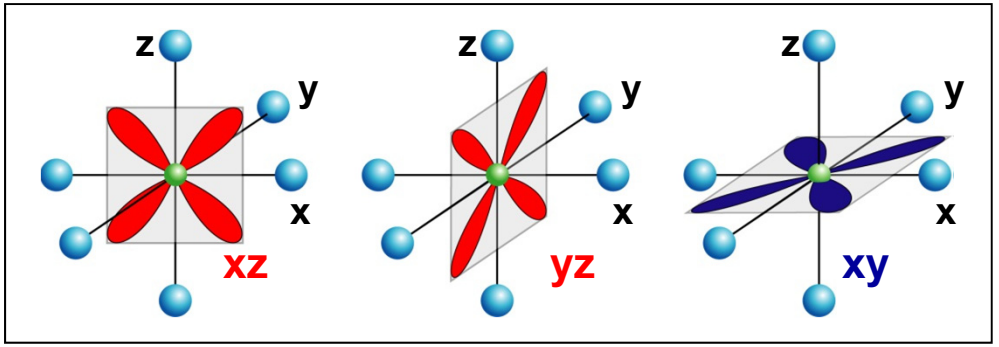

- Band structure calculation: **3 t_{2g}** bands crossing **E_F**

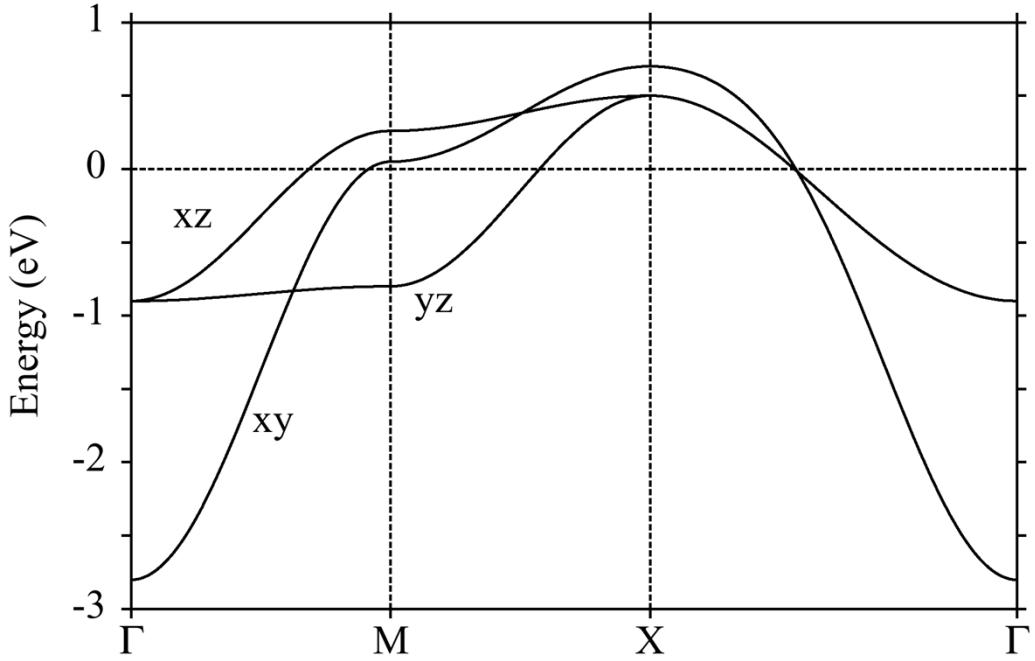

A. Liebsch *et al*, PRL **84**, 1591 (2000)

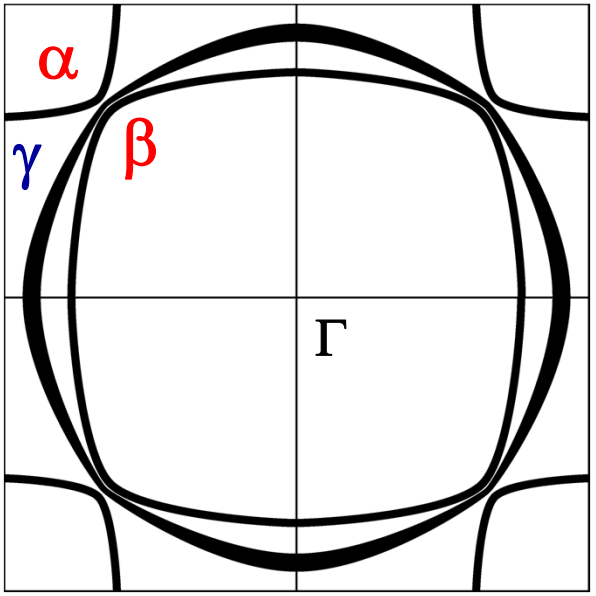

Mazin *et al.*, PRL **79**, 733 (1997)

Band Renormalization by Electronic Correlations

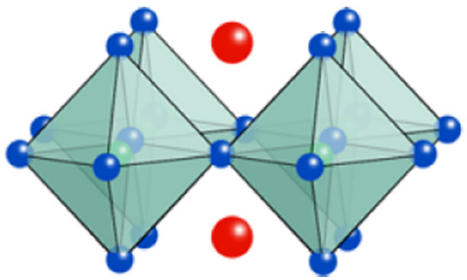

Ru^{4+} $4d^4$

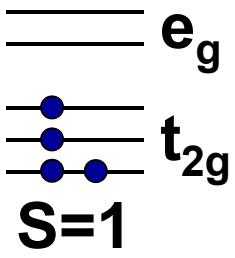

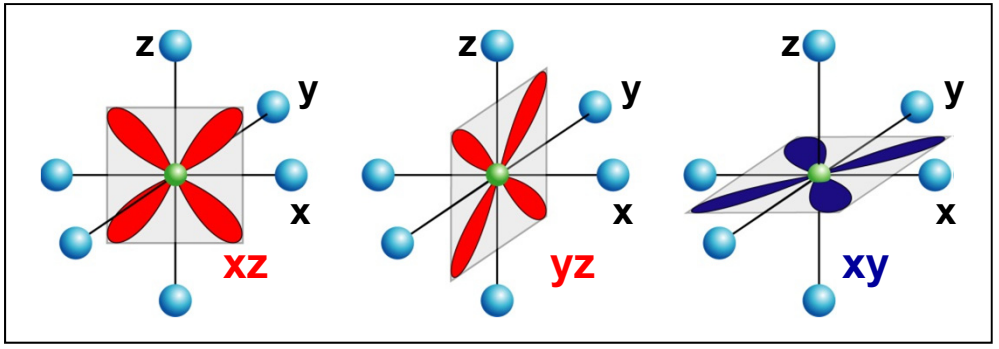

▶ The first indication of correlations is band narrowing

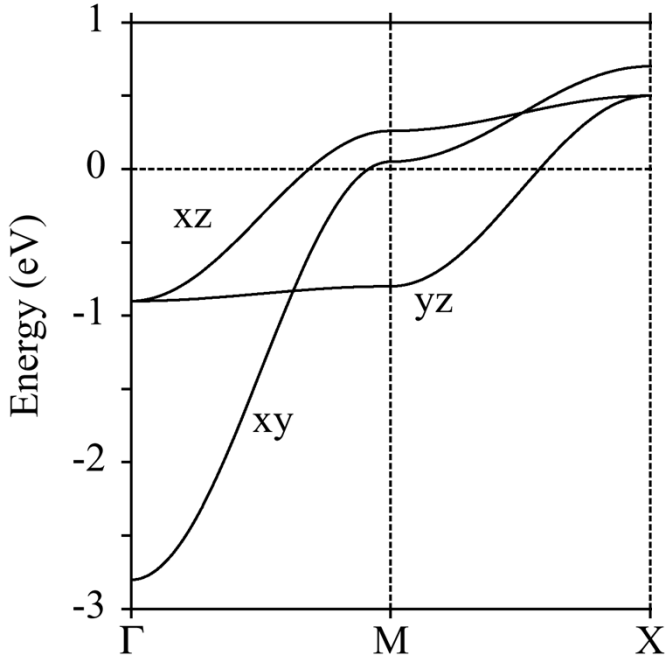

A. Liebsch *et al*, PRL **84**, 1591 (2000)

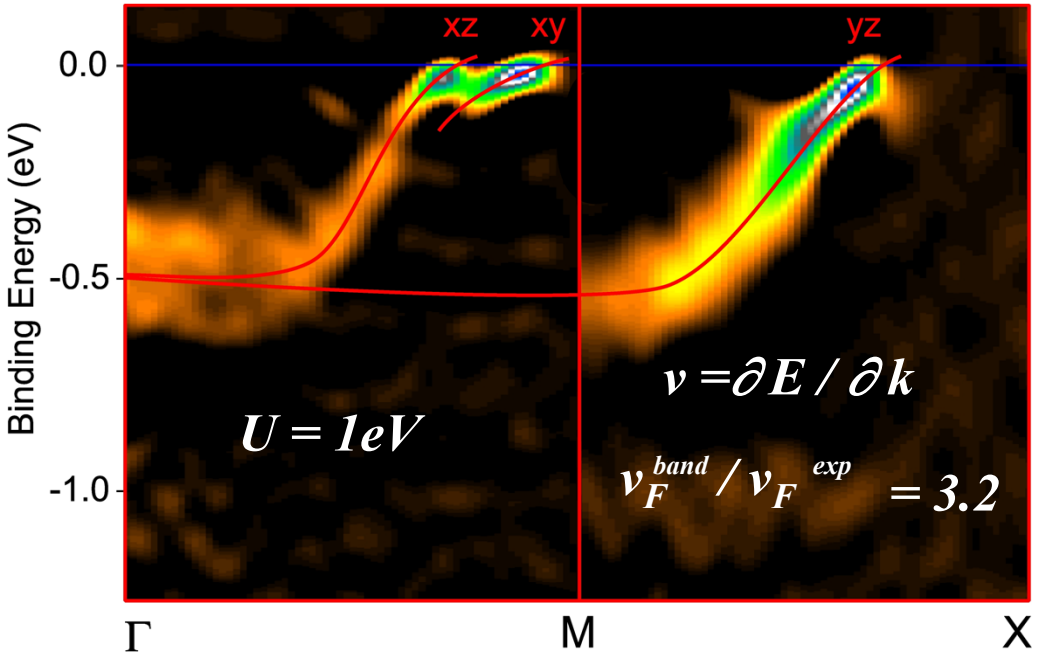

Damascelli et al., PRL **101**, 026406 (2008)

2H-$NbSe_2$: Normal State Electronic Structure

Corcoran *et al.*,JPCM **6**, 4479 (1994)

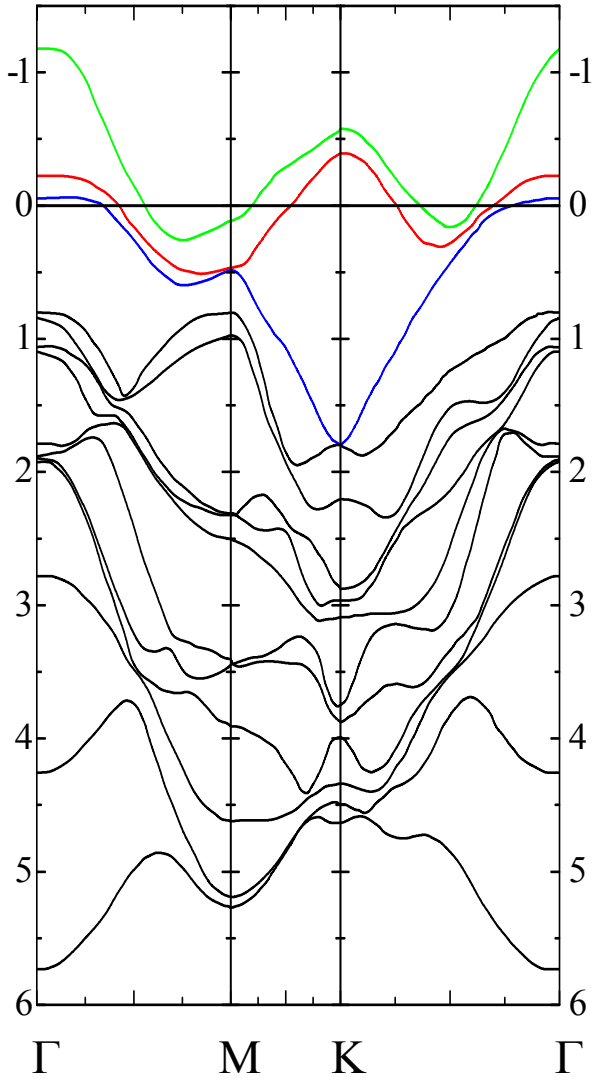

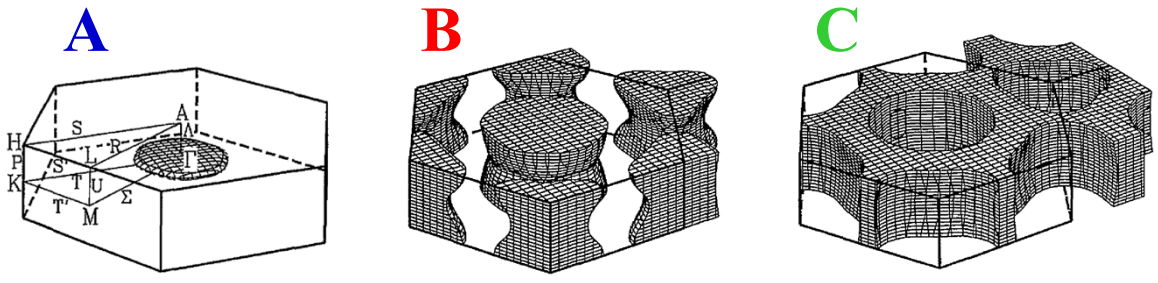

Damascelli *et al.* (2000)

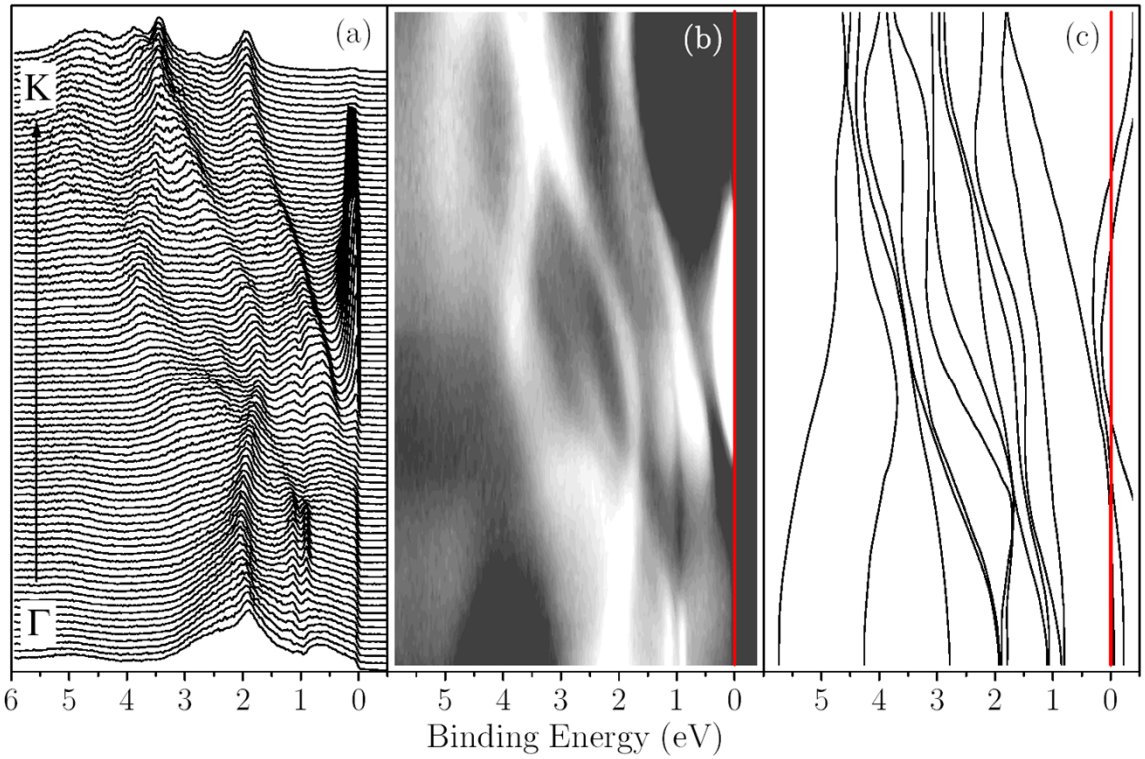

Here electronic correlations are weak: 1 to 1 matching with DFT

Many-Body Correlation Effects in Sr_2RuO_4

Single-particle spectral function

$$A(\mathbf{k},\omega) = -\frac{1}{\pi}\frac{\Sigma''(\mathbf{k},\omega)}{[\omega - \epsilon_{\mathbf{k}} - \Sigma'(\mathbf{k},\omega)]^2 + [\Sigma''(\mathbf{k},\omega)]^2}$$

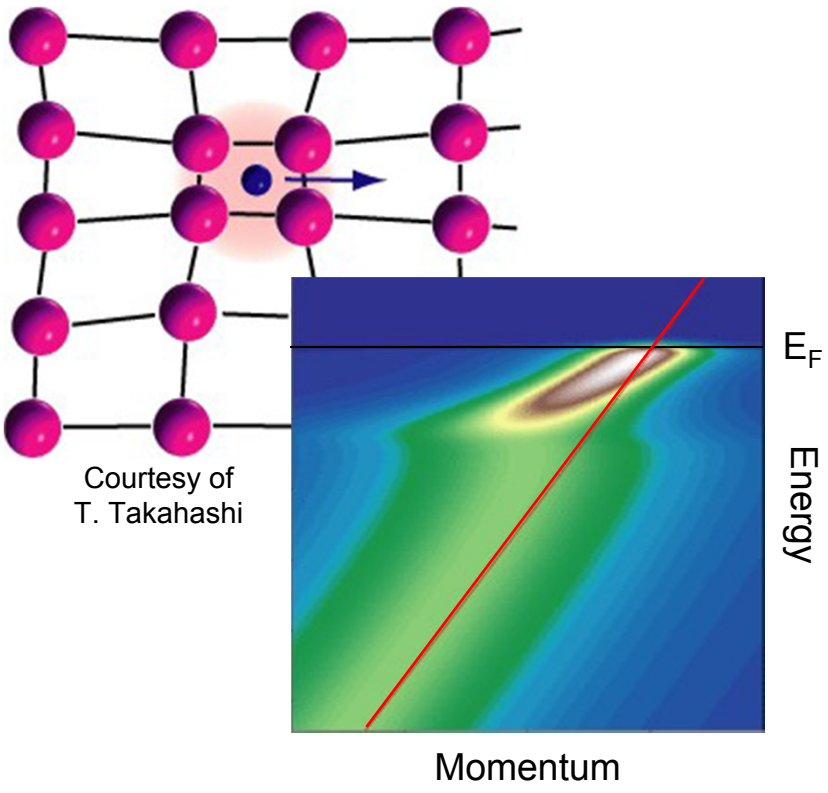

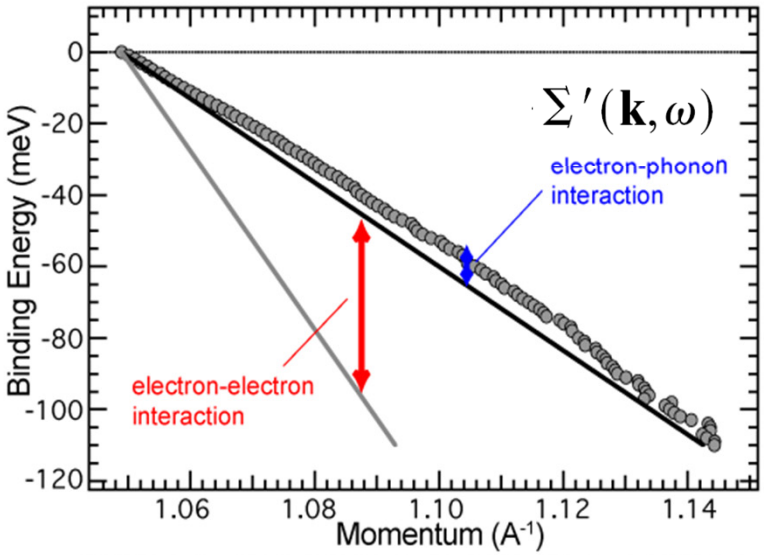

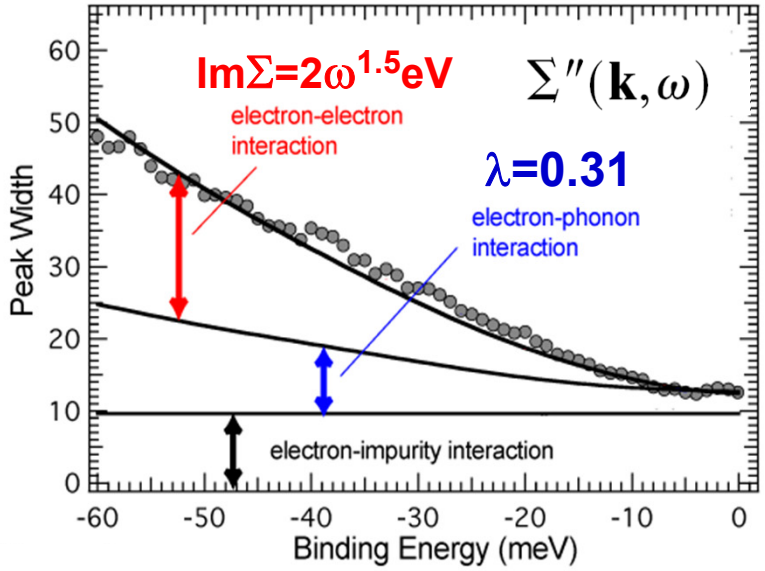

N.J.C. Ingle, K.M. Shen, A. Damascelli *et al.*, PRB **72**, 205114 (2005)

Outline Part II

HTSC: Mott gap and strong correlations

CUSO Lecture – Lausanne 02/2011

From Fermi Liquid to Mott Insulator

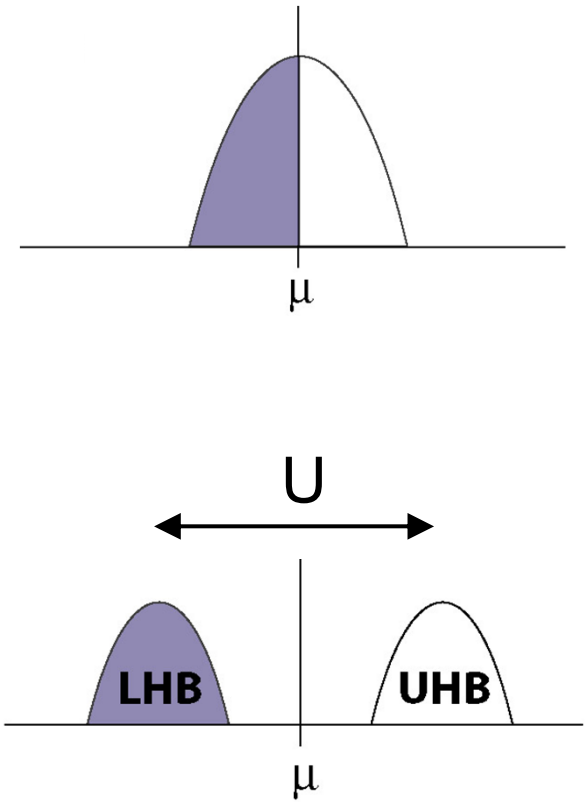

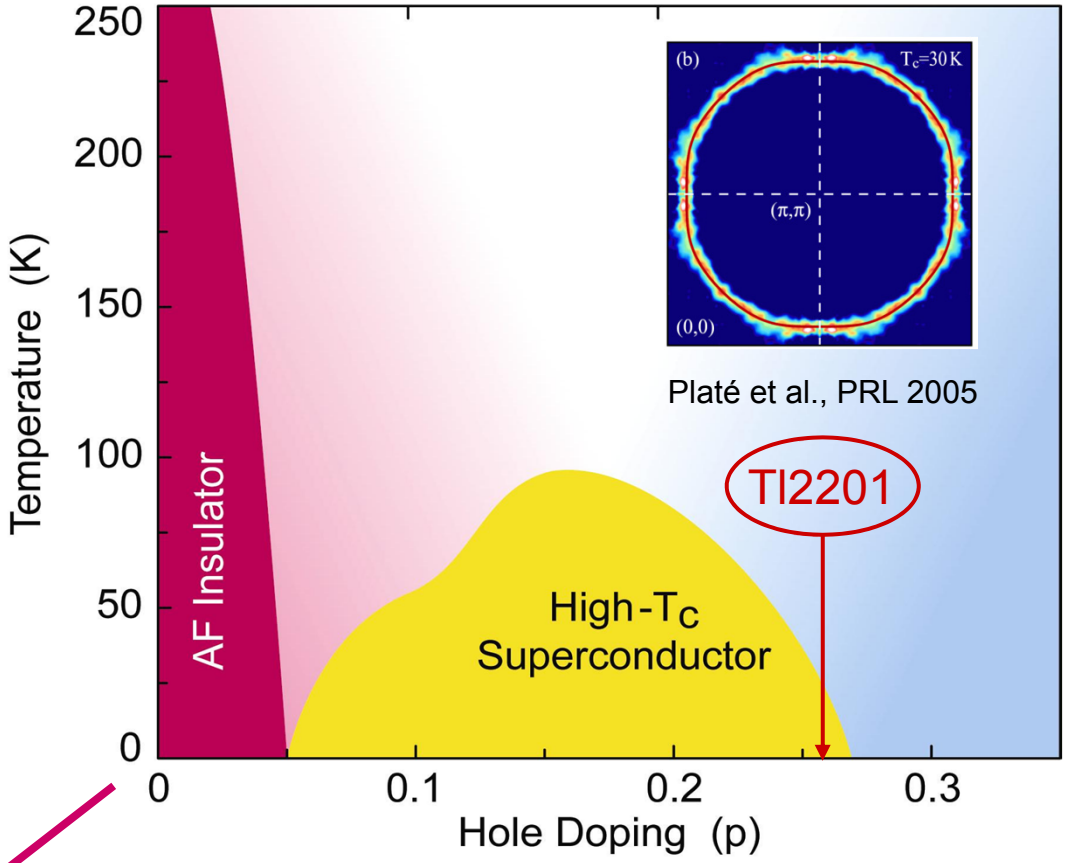

Mott insulator

Normal state properties

From Fermi Liquid to Mott Insulator

Correlations suppress Z_k

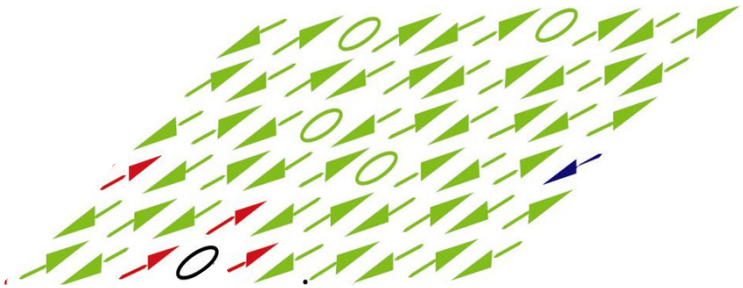

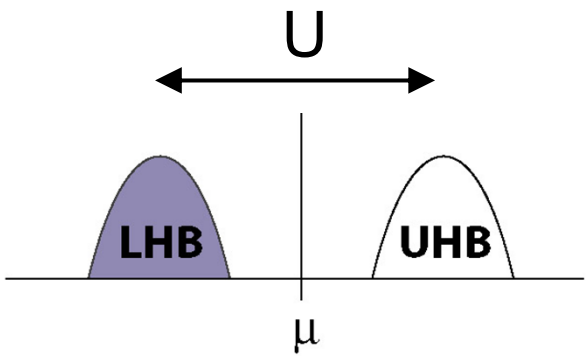

$$Z \simeq 2p/(p+1)$$

Sawatzky, Anderson, Randeria,
Paramekanti, Yang, Rice, et al.

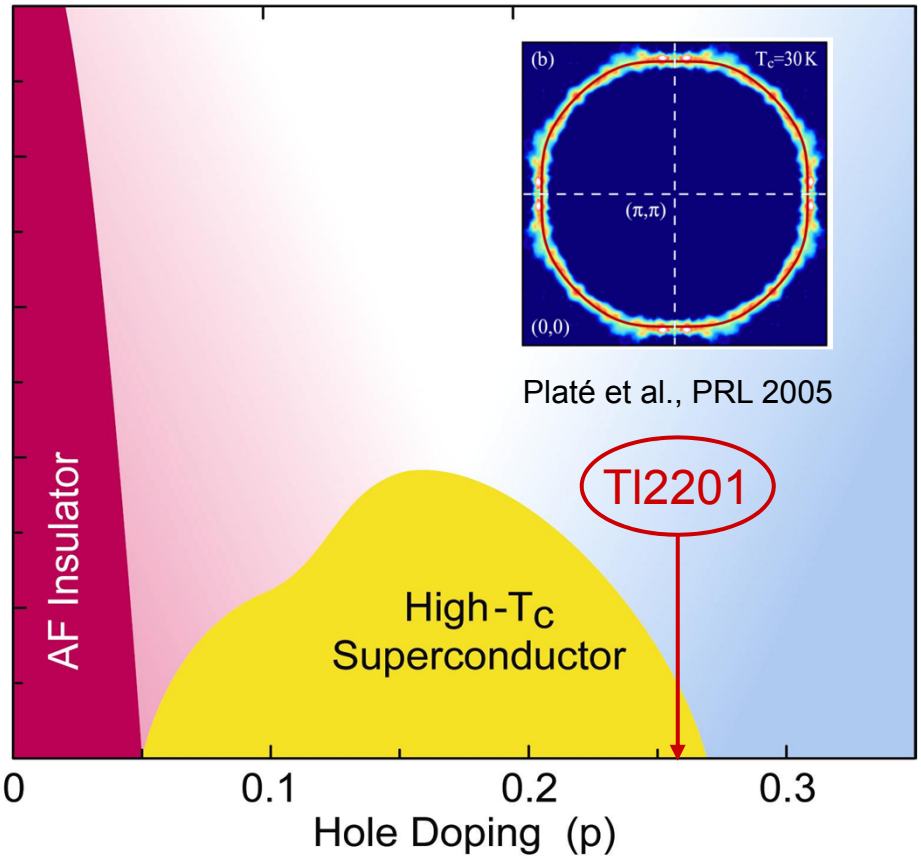

Normal state properties

Mott-Hubbard Insulating Behavior

Half-Filled Metal

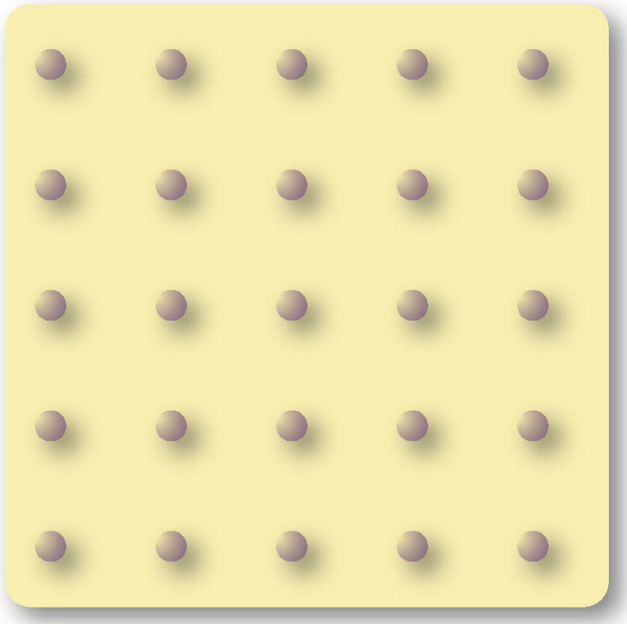

Increase inter-electron Coulomb repulsion (**U**)

Mott Insulator

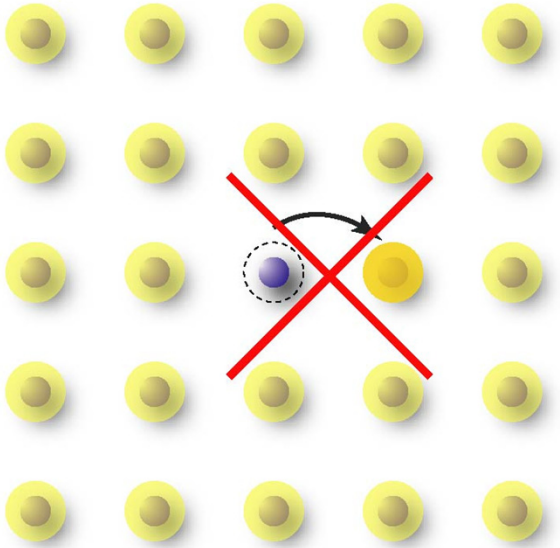

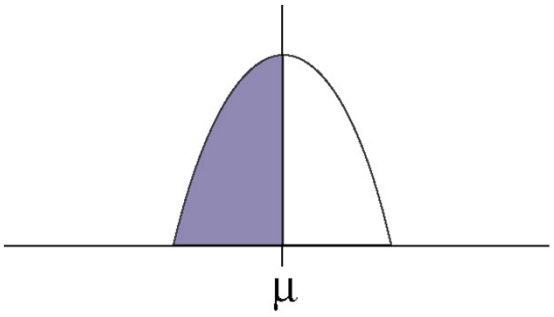

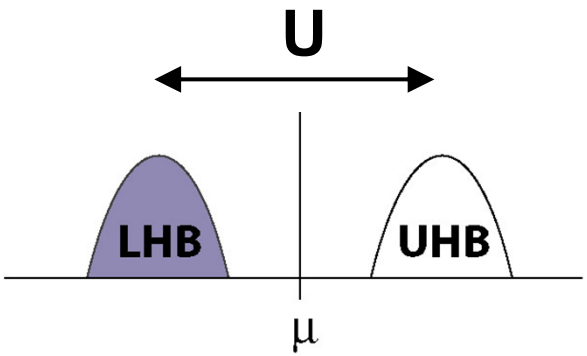

High-T_c Superconductors: A Minimal Model

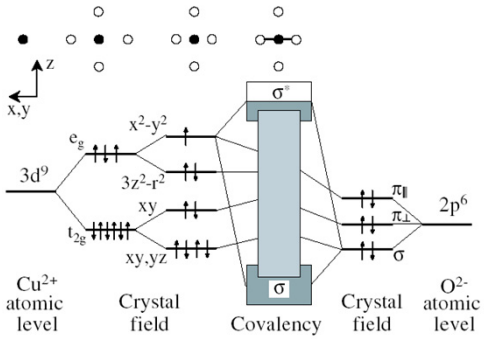

Density functional theory
5d Cu orbitals and 3 O orbitals
8-band model

1987 Anderson: the essential physics of the cuprates is captured by the 1-band Hubbard model

$$H = -t \sum_{\langle ij \rangle, \sigma} (c^{\dagger}_{i\sigma} c_{j\sigma} + \text{H.c.}) + U \sum_{i} n_{i\uparrow} n_{i\downarrow}$$

3-band model

Cu $3d_{x^2-y^2}$ O $2p_x$ and $2p_y$

1987 Emery: since the HTSCs are charge transfer insulators, both O and Cu have to be accounted for

---

1988 Zhang & Rice: projecting out double occupancy, Cu-O hybridization leads to an effective 1-band model

$$H = -t \sum_{\langle ij \rangle, \sigma} (\tilde{c}^{\dagger}_{i\sigma} \tilde{c}_{j\sigma} + \text{H.c.}) + J \sum_{\langle ij \rangle} \left(\mathbf{S}_i \cdot \mathbf{S}_j - \frac{n_i n_j}{4} \right)$$

A. Damascelli, Z. Hussain, Z.-X Shen, Rev. Mod. Phys. **75**, 473 (2003) -- see pgs 486-490

HTSCs: Charge Transfer Insulators

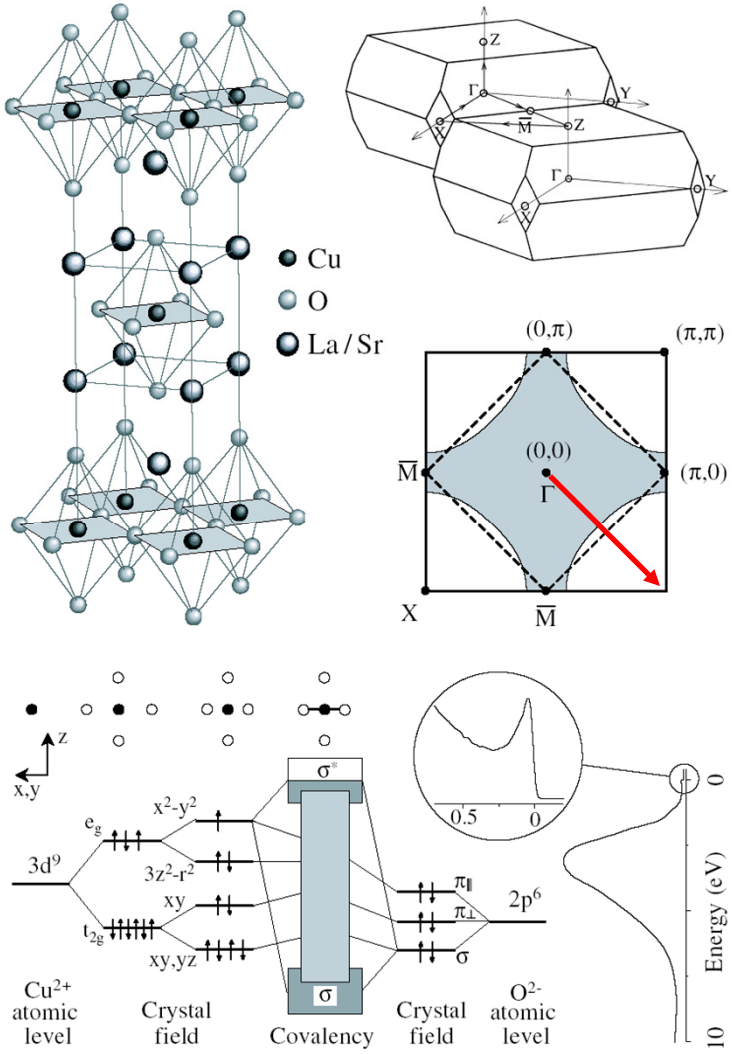

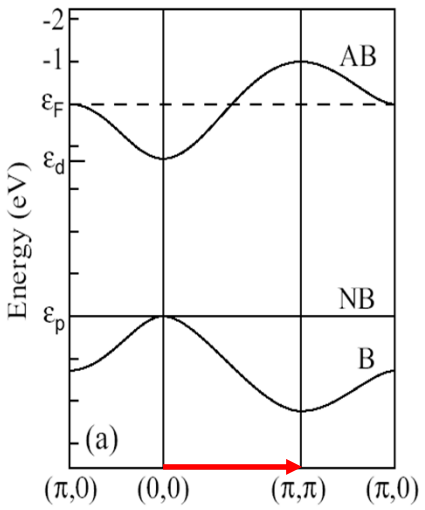

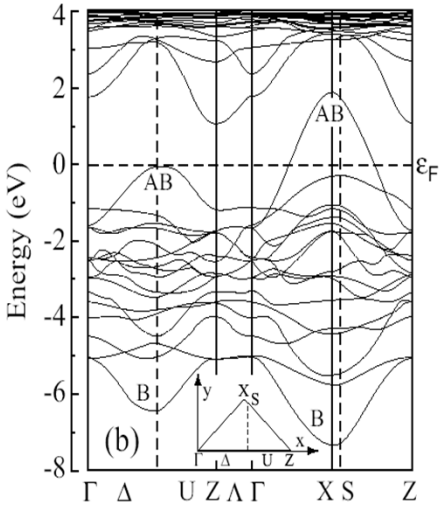

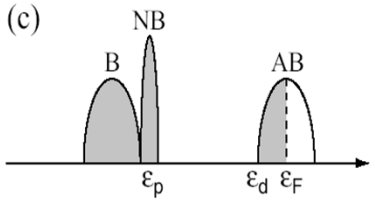

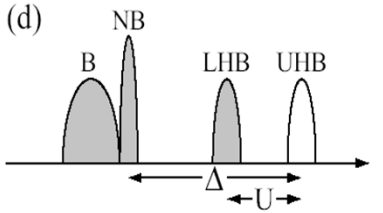

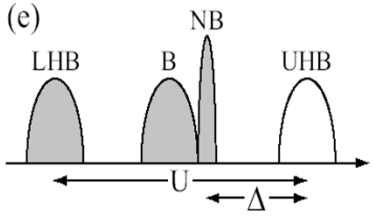

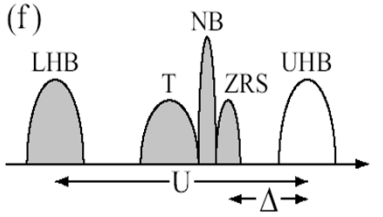

High-T_c Superconductors: A Minimal Model

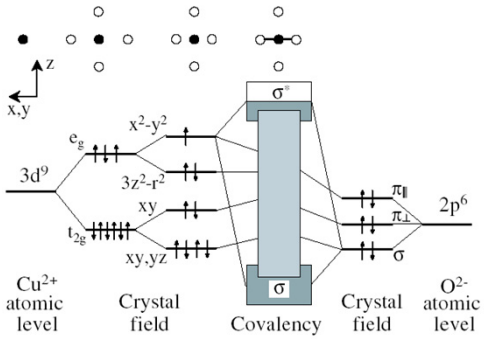

Density functional theory
5d Cu orbitals and 3 O orbitals
8-band model

1987 Anderson: the essential physics of the cuprates is captured by the 1-band Hubbard model

$$H = -t \sum_{\langle ij \rangle, \sigma} (c^{\dagger}_{i\sigma} c_{j\sigma} + \text{H.c.}) + U \sum_{i} n_{i\uparrow} n_{i\downarrow}$$

3-band model

Cu $3d_{x^2-y^2}$ O $2p_x$ and $2p_y$

1987 Emery: since the HTSCs are charge transfer insulators, both O and Cu have to be accounted for

---

1988 Zhang & Rice: projecting out double occupancy, Cu-O hybridization leads to an effective 1-band model

$$H = -t \sum_{\langle ij \rangle, \sigma} (\tilde{c}^{\dagger}_{i\sigma} \tilde{c}_{j\sigma} + \text{H.c.}) + J \sum_{\langle ij \rangle} \left(\mathbf{S}_i \cdot \mathbf{S}_j - \frac{n_i n_j}{4} \right)$$

A. Damascelli, Z. Hussain, Z.-X Shen, Rev. Mod. Phys. **75**, 473 (2003) -- see pgs 486-490

HTSCs: Charge Transfer Insulators

½ Filled Metal

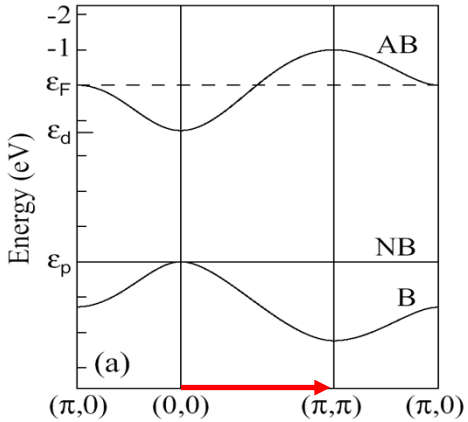

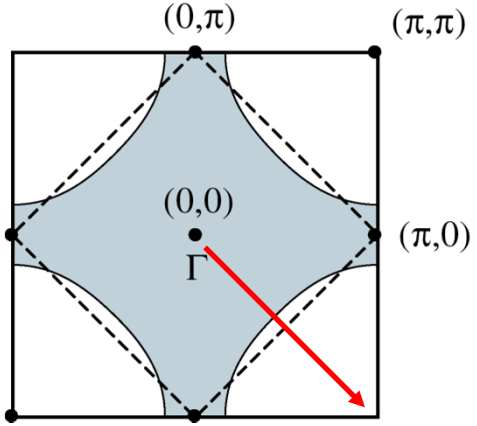

ARPES Spectra of Insulating $Ca_2CuO_2Cl_2$ along $(0,0)$–(π,π)

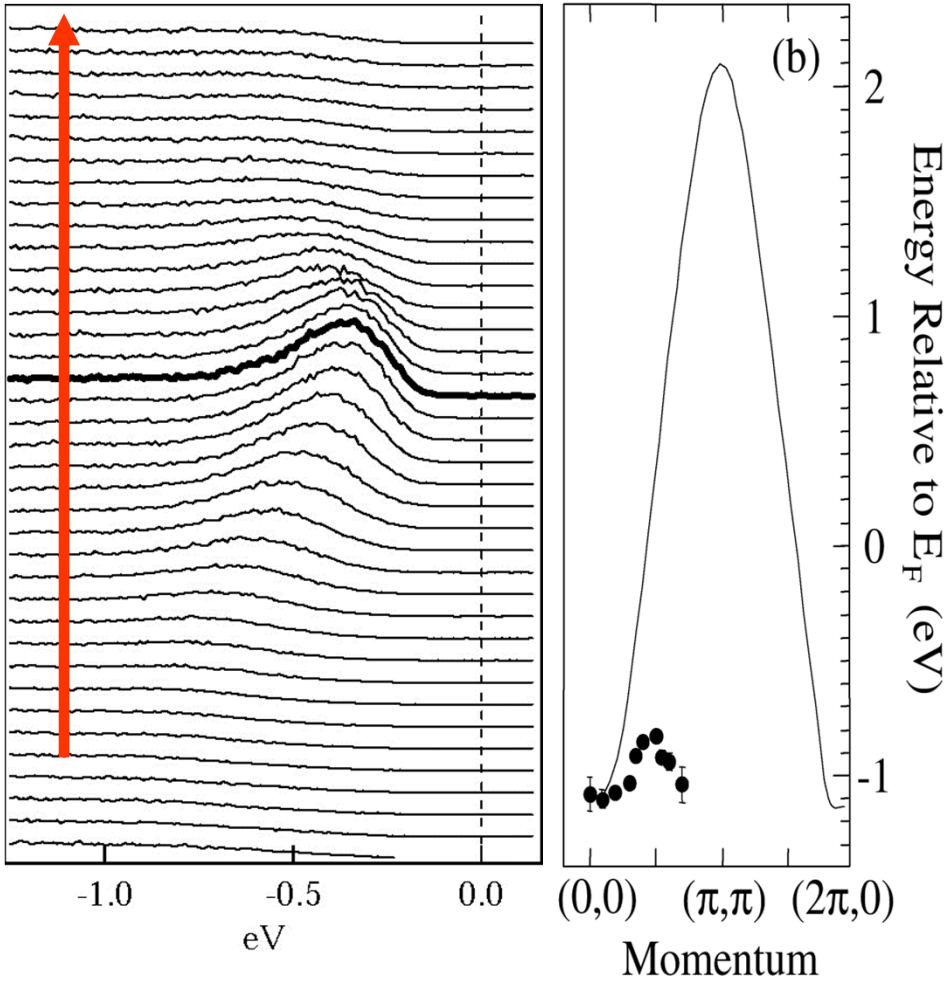

The dispersion instead of being the 2D tight-binding 8t (t~350meV) is 2.2J (J~125meV)

HTSCs: Charge Transfer Insulators

½ Filled Metal

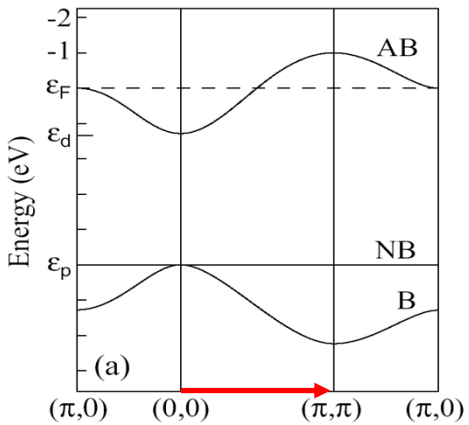

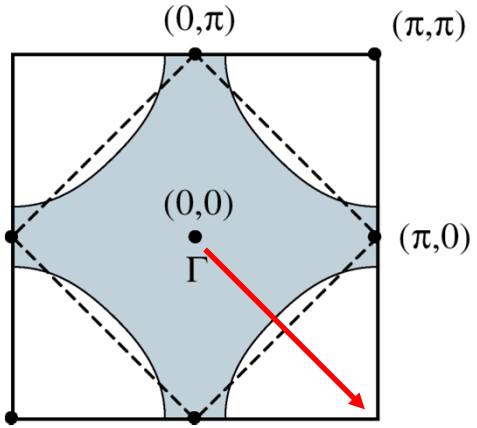

ARPES Spectra of Insulating $Sr_2CuO_2Cl_2$

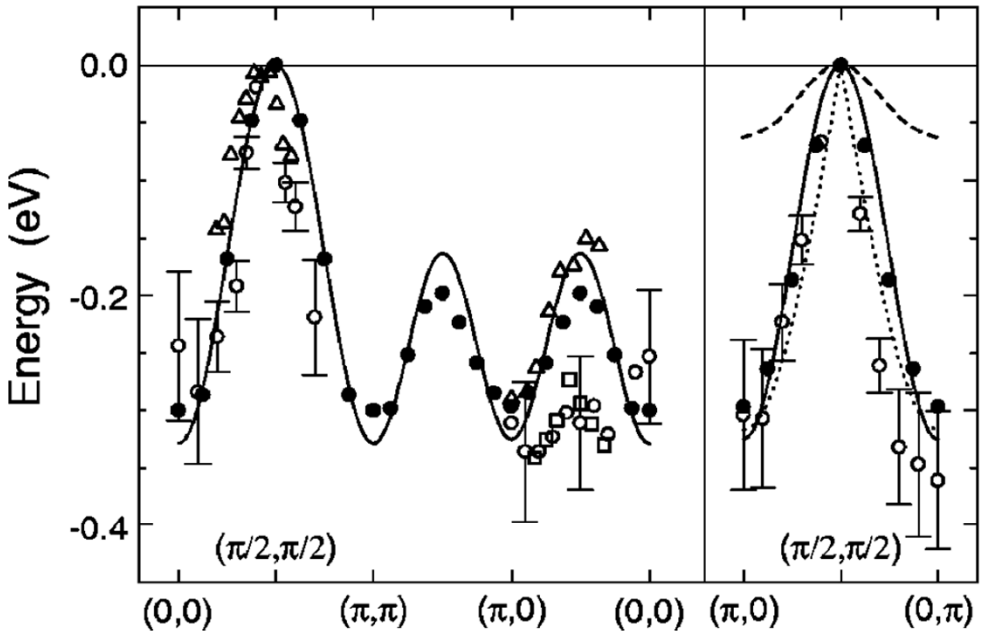

FIG. 17. Electronic dispersion for SCOC ($E=0$ corresponds to the top of the band). Experimental data: ○, Wells *et al.*, 1995; △, La Rosa *et al.*, 1997; □, Kim *et al.*, 1998. Dashed line, t-J model calculations (Wells *et al.*, 1995); ●, self-consistent Born approximation for the t-t'-t''-J model ($t=0.35$ eV, $t'=-0.12$ eV, $t''=0.08$ eV, and $J=0.14$ eV); solid lines, fits of the self-consistent Born approximation data (Tohyama and Maekawa, 2000); dotted line along $(\pi,0)$-$(0,\pi)$, spinon dispersion (Laughlin, 1997).

The dispersion instead of being the 2D tight-binding 8t (t~350meV) is 2.2J (J~125meV)

HTSCs: Charge Transfer Insulators

½ Filled Metal

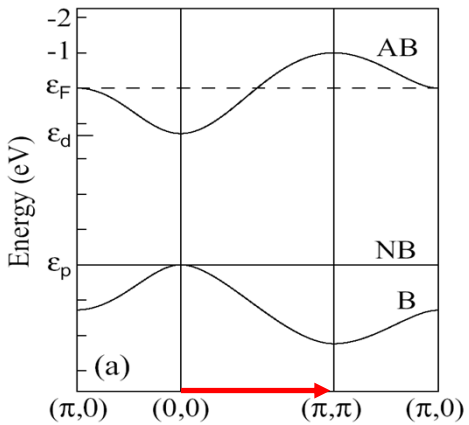

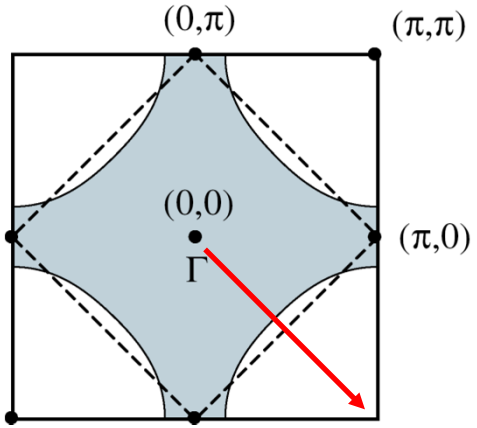

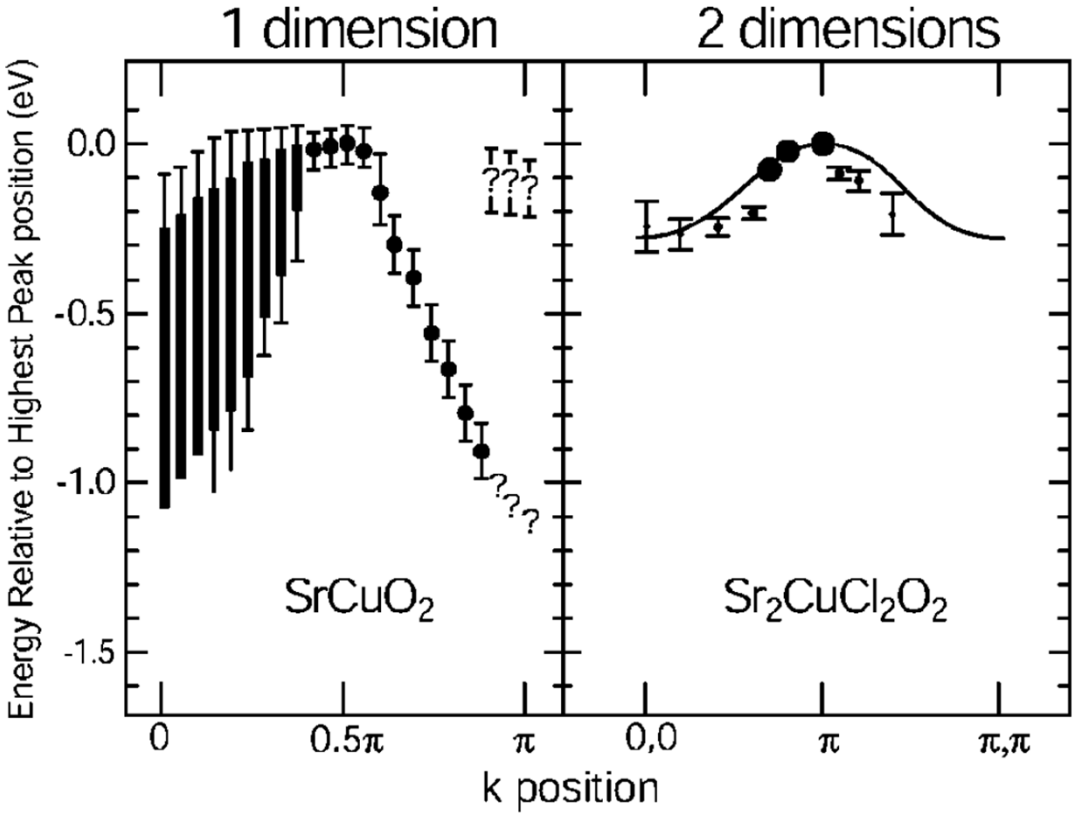

FIG. 18. Experimental dispersion for quasi-1D (Kim *et al.*, 1996) and quasi-2D (Wells *et al.*, 1995) insulating systems.

The dispersion instead of being the 2D tight-binding 8t (t~350meV) is 2.2J (J~125meV)

High-T_c Superconductors: Electronic Structure

½ Filled Metal

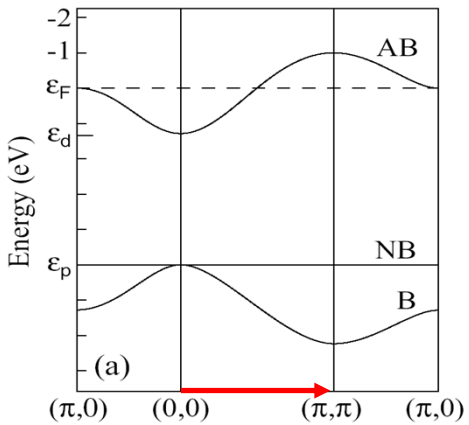

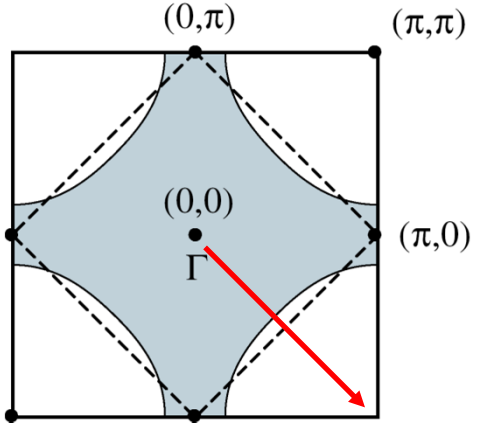

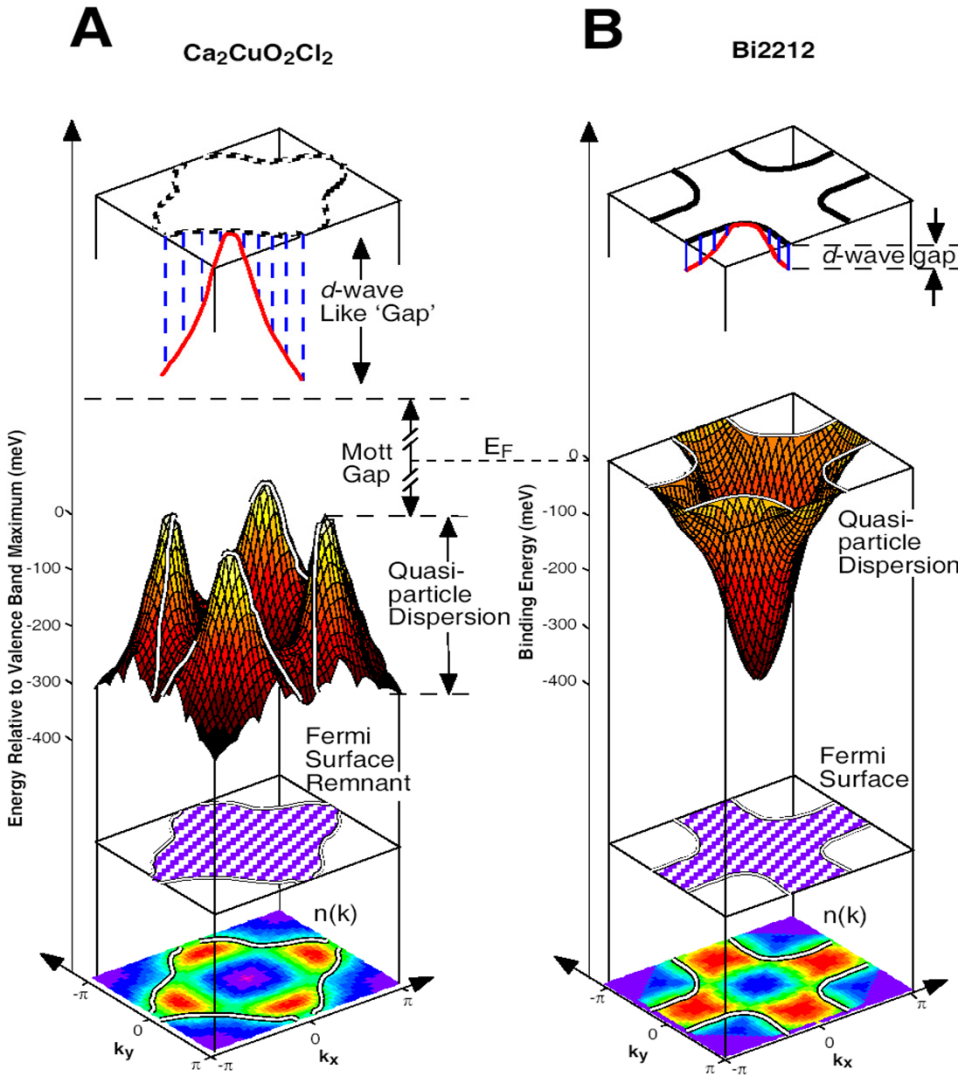

A. Damascelli, Z. Hussain, Z.-X Shen, Rev. Mod. Phys. **75**, 473 (2003) -- see pgs 486-490

How Can One Measure the Mott Gap?

Definition of Conductivity Gap

$$E_{gap} = (E_{gr}^{N-1} - E_{gr}^{N}) + (E_{gr}^{N+1} - E_{gr}^{N})$$

$$= E_{gr}^{N-1} + E_{gr}^{N+1} - 2\,E_{gr}^{N}$$

$E_{gr} \longrightarrow$ Ground state

How Can One Measure the Mott Gap?

Optics

- photon in – photon out
- electric dipole transition
- particle-hole excitations
- collective modes
  (phonons, magnons, plasmons)
- number of particles is conserved

Photoemission

- photon in – electron out
- electric dipole transition
- electron removal excitations
- collective modes?
  only as dressing of quasiparticles
- number of particles not conserved

Electron transition

Electron removal

Particle-hole excitations
of the N-particle system

Single-particle excitations
of the (N-1)-particle system

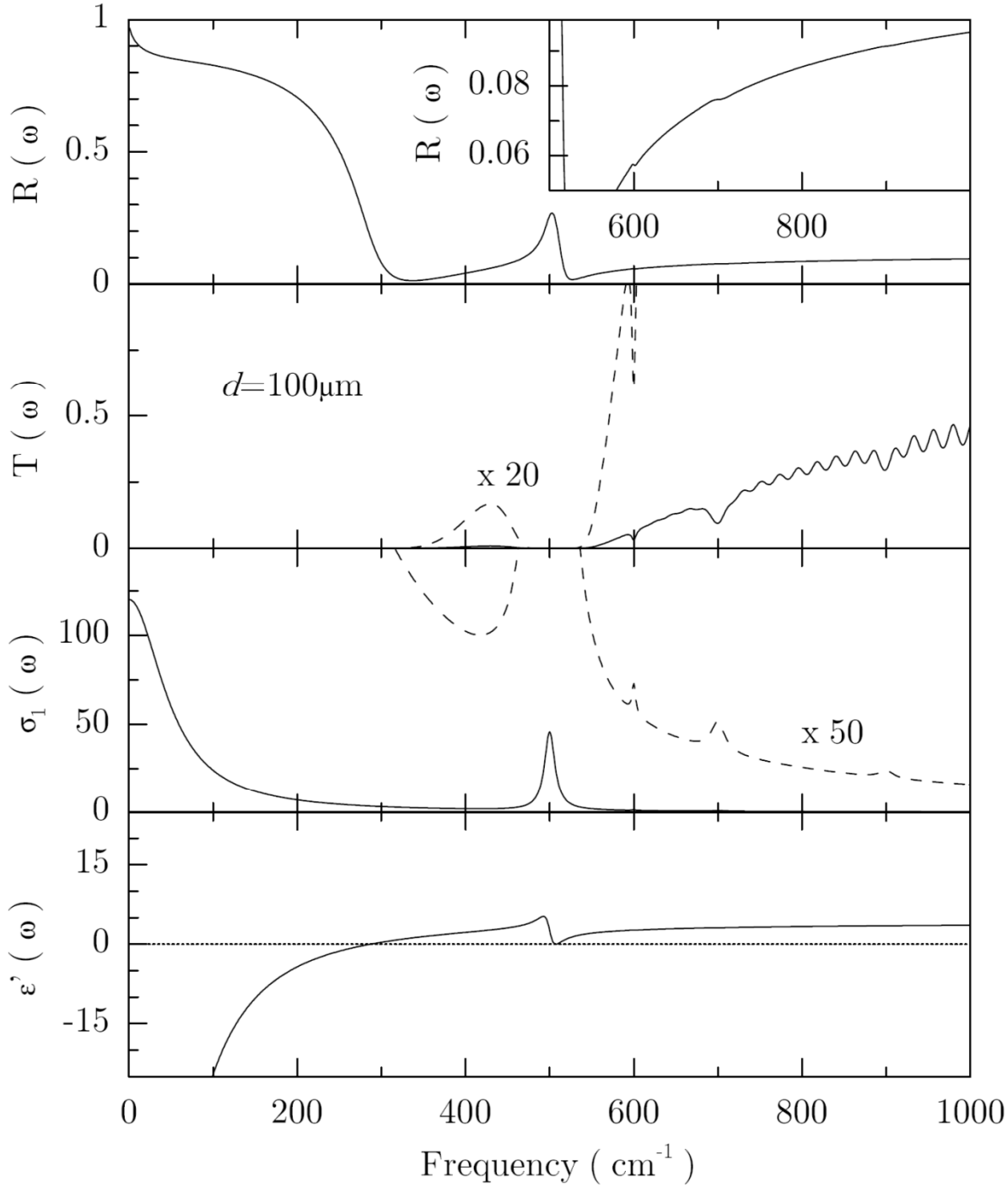
R (ω)
1
0.5
0
R (ω)
0.08
0.06
600
800
T (ω)
0.5
0
d=100μm
x 20
σ1 (ω)
100
50
0
x 50
ε' (ω)
15
0
-15
0
200
400
600
800
1000
Frequency (cm-1)

Optics

Second-Harmonic Generation, a Selective Probe for Excitons

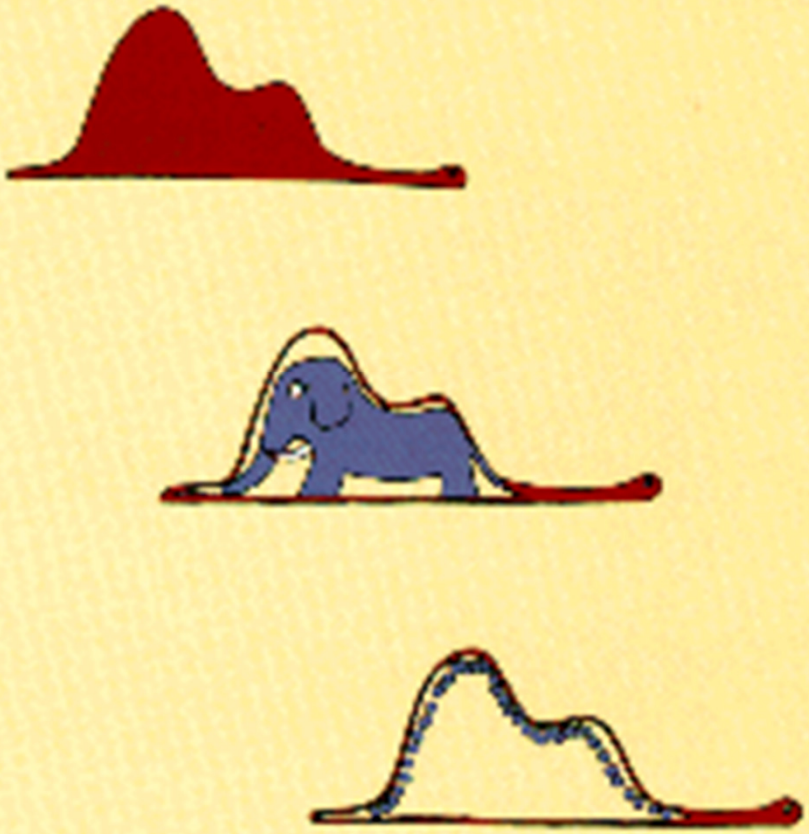

Anna-Maria Janner

General Elementary Excitations?

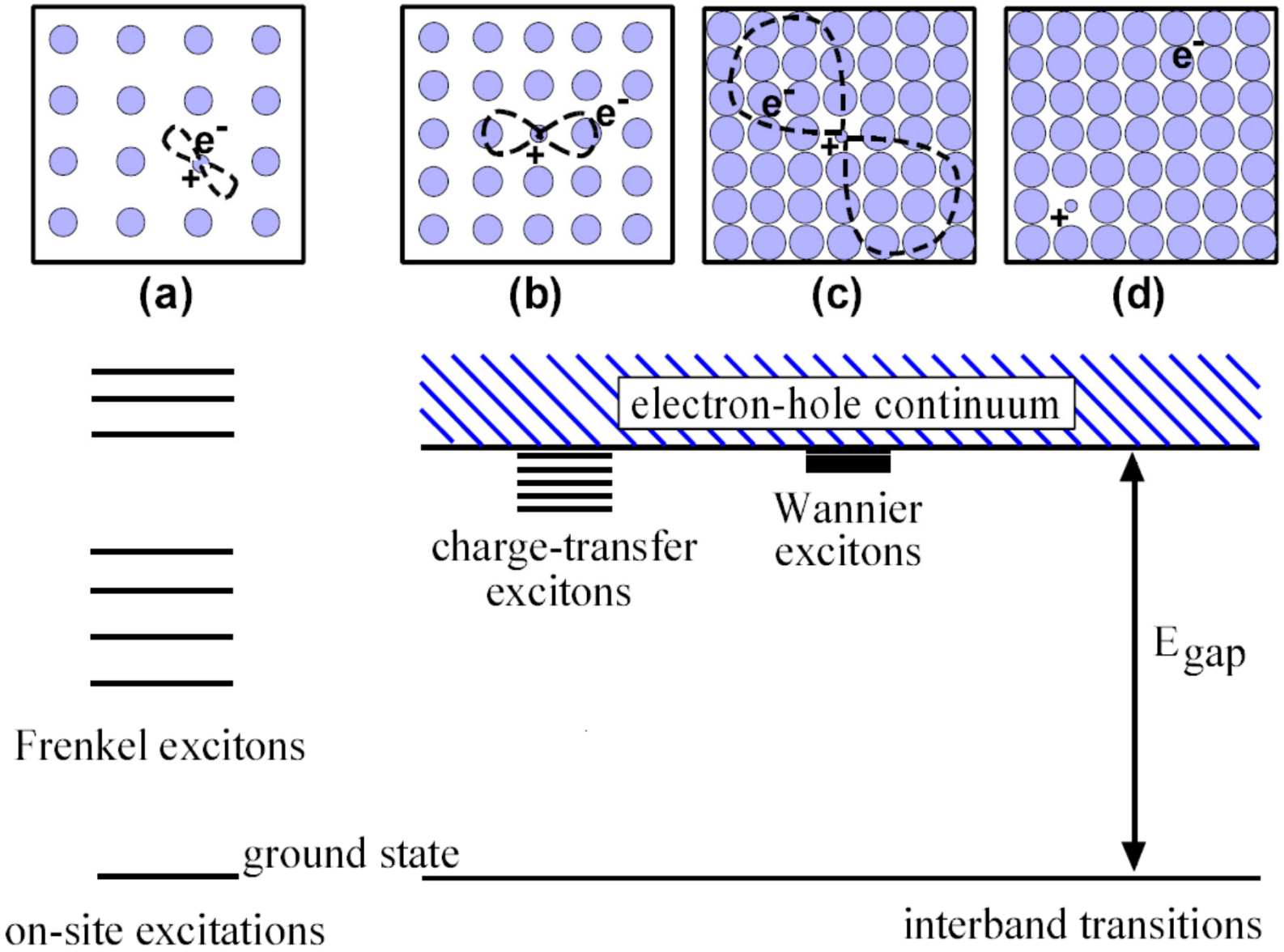

Courtesy of George Sawatzky

General Elementary Excitations?

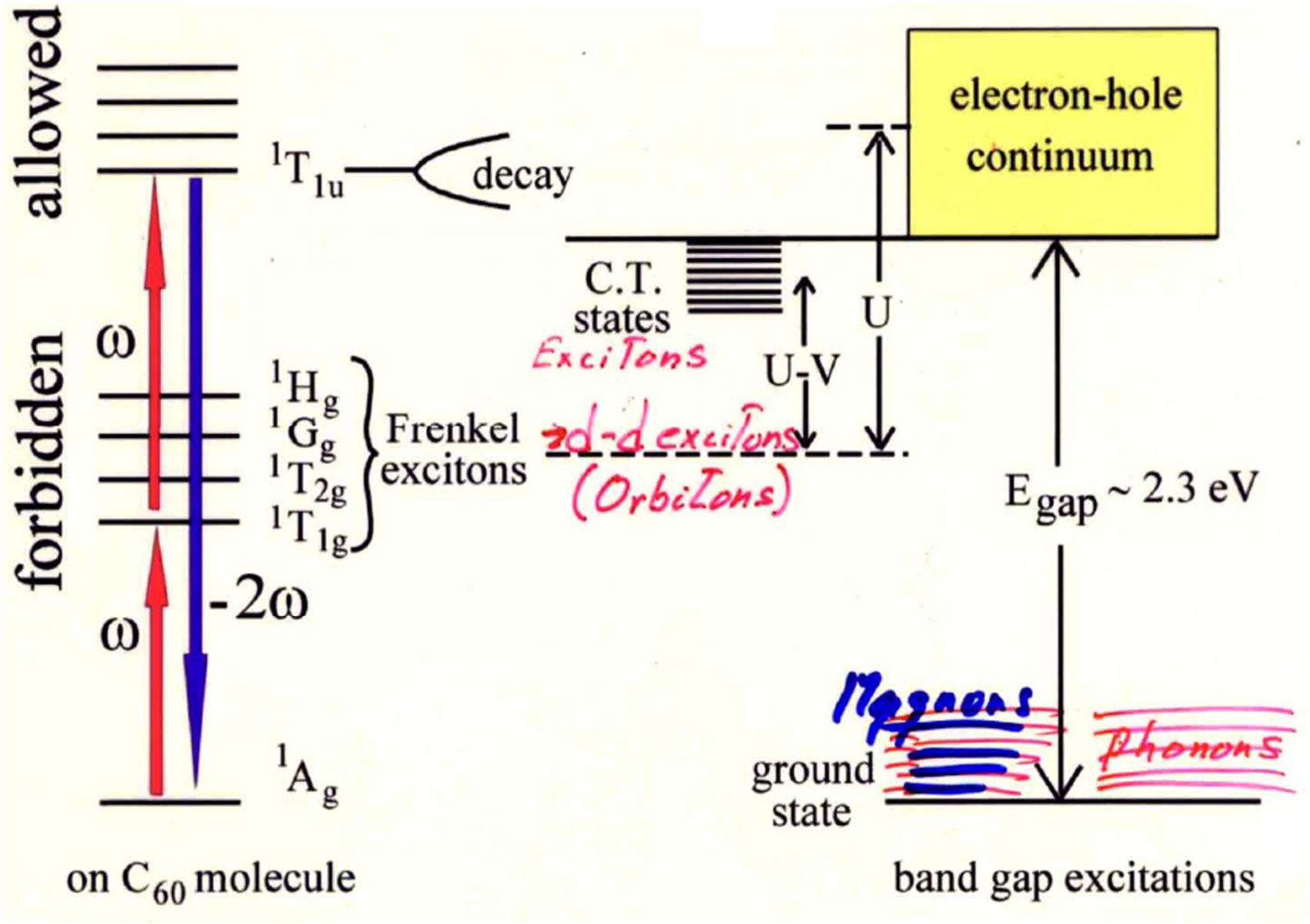

Courtesy of George Sawatzky

Absorption Coefficient in a Semiconductor

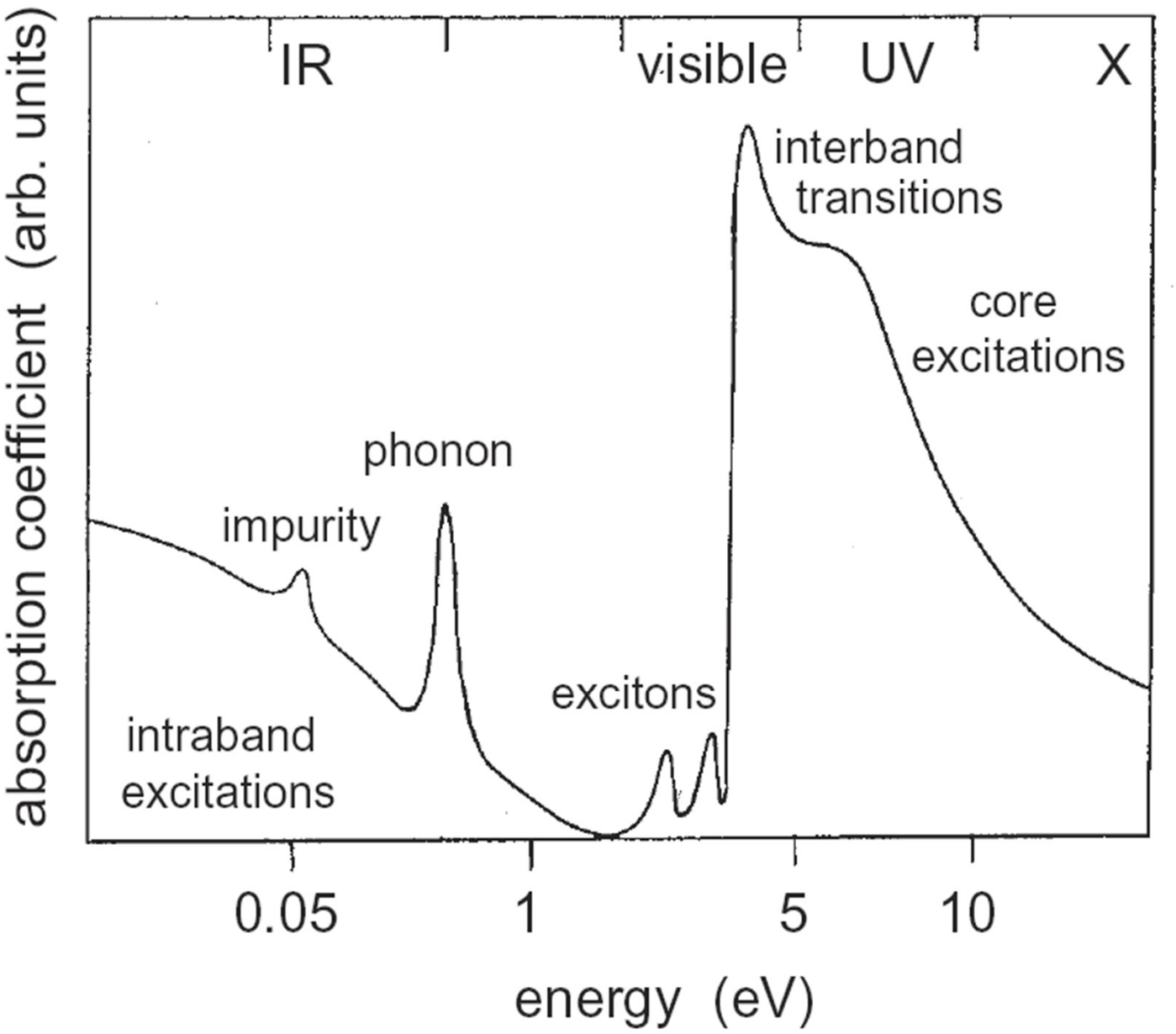

Excitons versus Band Gap

The 1.55 eV excitations which agrees with the DFT band gap was thought to be the conductivity gap

Electron Energy Loss Spectroscopy

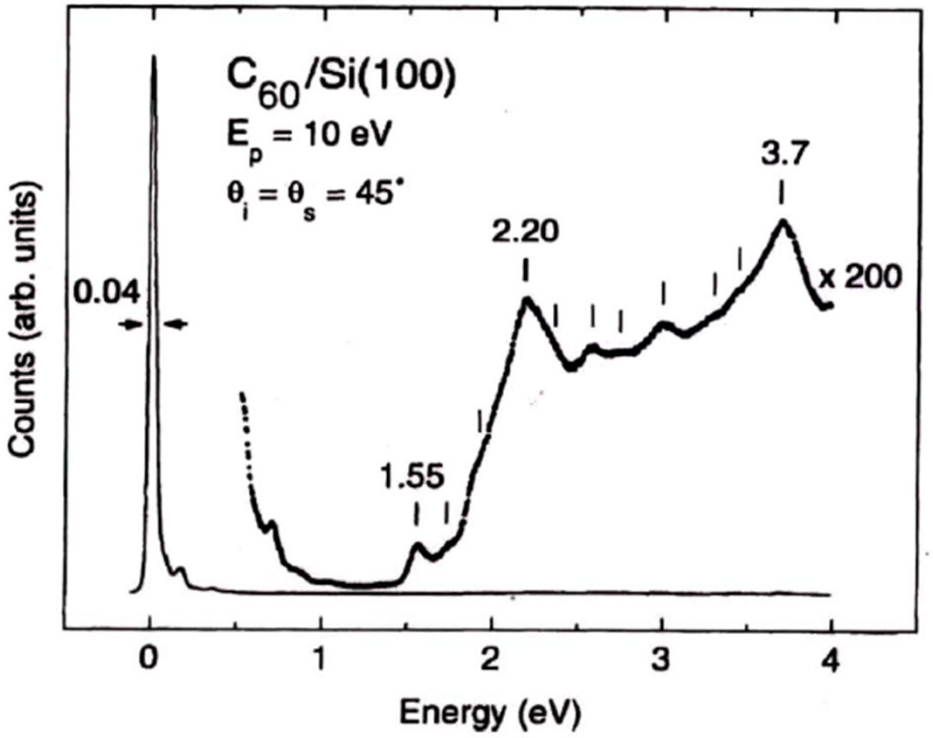

G. Gensterblum *et al*, PRL **67**, 2171 (1991); A. Lucas *et al*, PRB **45**, 13694 (1992)

R.W. Loft *et al*, PRL **68**, 3924 (1992)

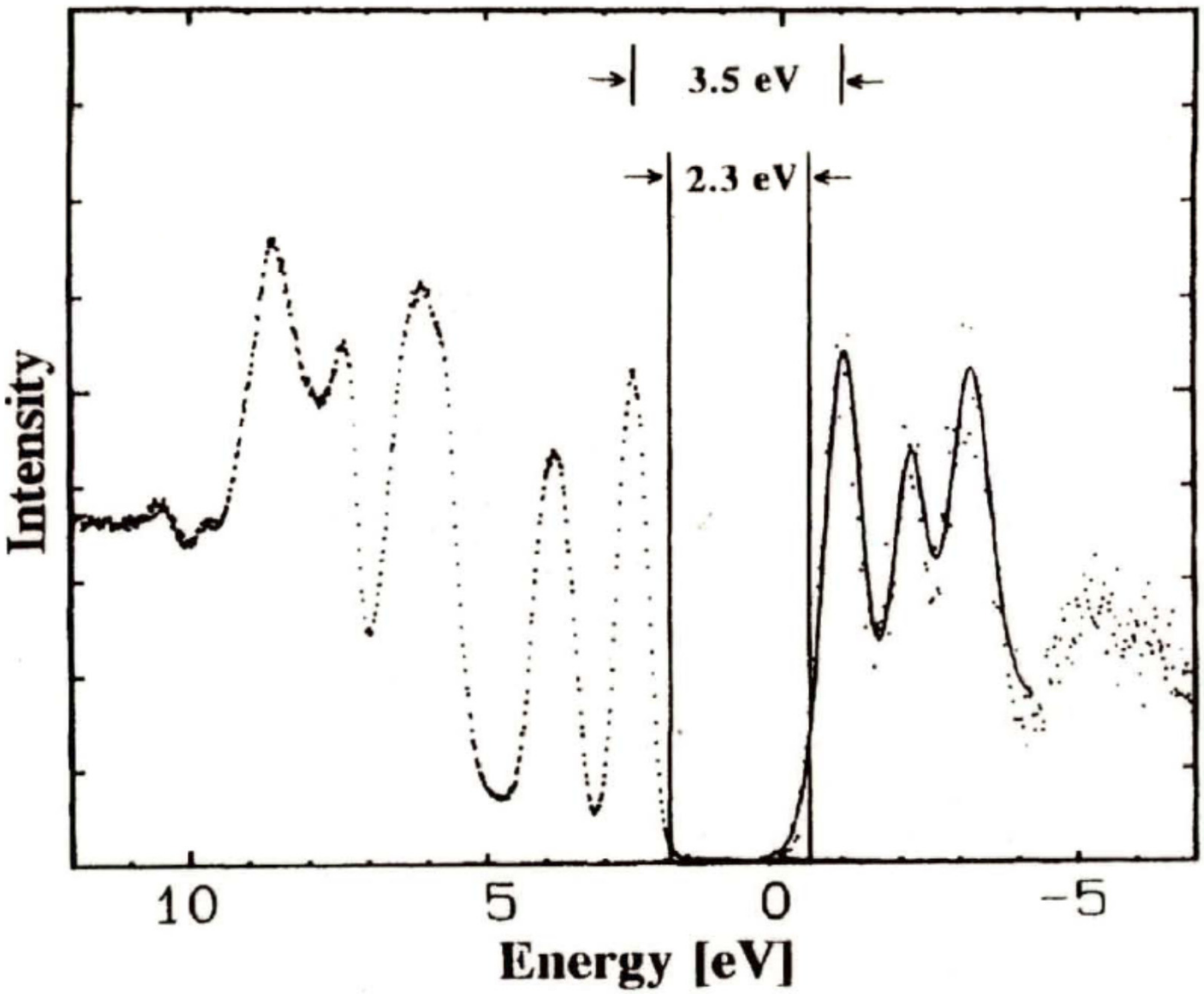

NiO - Bunsenite

Courtesy of
Jan Kuneš

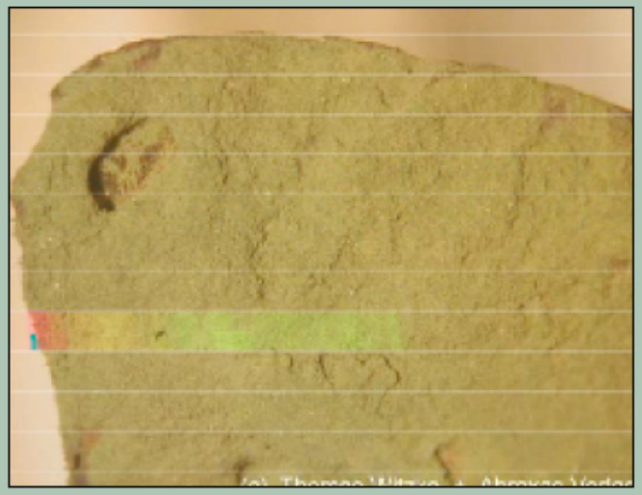

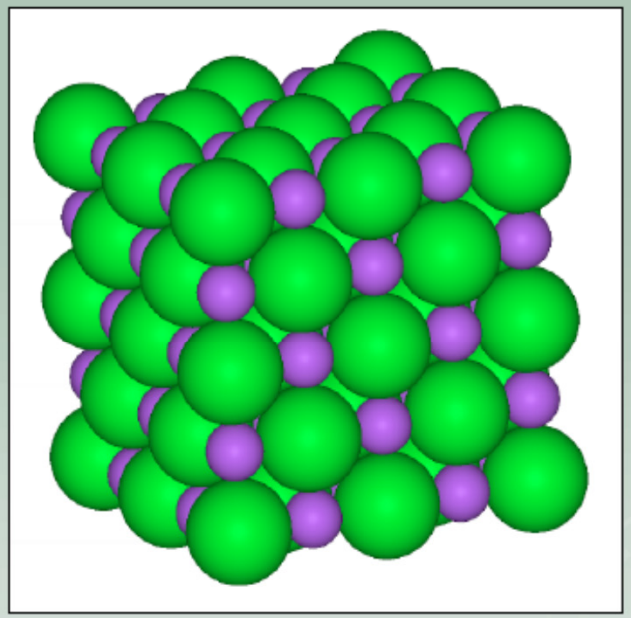

- rock-salt structure (T_m= 2261 K)
  bulk modulus: 209 GPa
  (CoO 194, MnO 148, diamond 462, Li 11)
- type II AFM (T_N= 532 K)
- charge gap: 3.7 eV
- Formal valency: Ni^{2+}: d^8s^0 O^{2-}: p^6
- U ~ 9 eV

Transition-Metal Monoxides: Band or Mott Insulators

K. Terakura[a] and A. R. Williams
IBM Thomas J. Watson Research Center, Yorktown Heights, New York 10598

and

T. Oguchi
Institute for Solid State Physics, The University of Tokyo, Roppongi, Minato-ku, Tokyo, Japan

and

J. Kübler
Fachgebiet Theoretische Physik, Institut für Festkörperphysik, D-6100 Darmstadt, West Germany
(Received 24 February 1984)

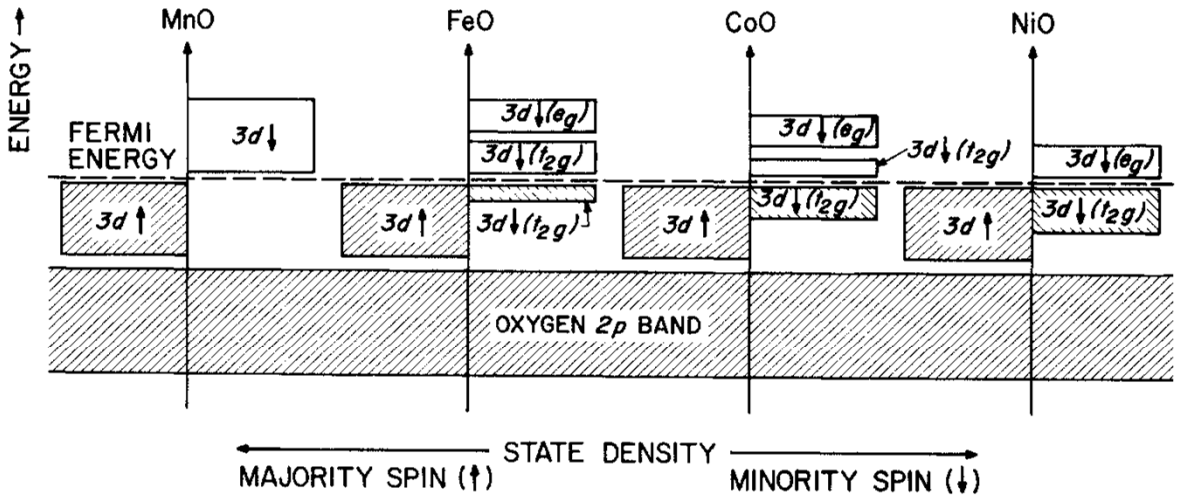

FIG. 1. Band picture of the monoxides. The qualitative difference between this picture and the commonly accepted one is the energy position of the empty d states. To quantify the state-density information, we find the width of the Mn $3d$ and the O $2p$ bands to be 3 eV and 5 eV, respectively. The band centers are separated by ~ 5 eV. The gaps in MnO and NiO are 0.4 and 0.3 eV, respectively.

Optical Properties of Nickel Oxide*

R. NEWMAN† AND R. M. CHRENKO
General Electric Research Laboratory, Schenectady, New York

(Received January 28, 1959)

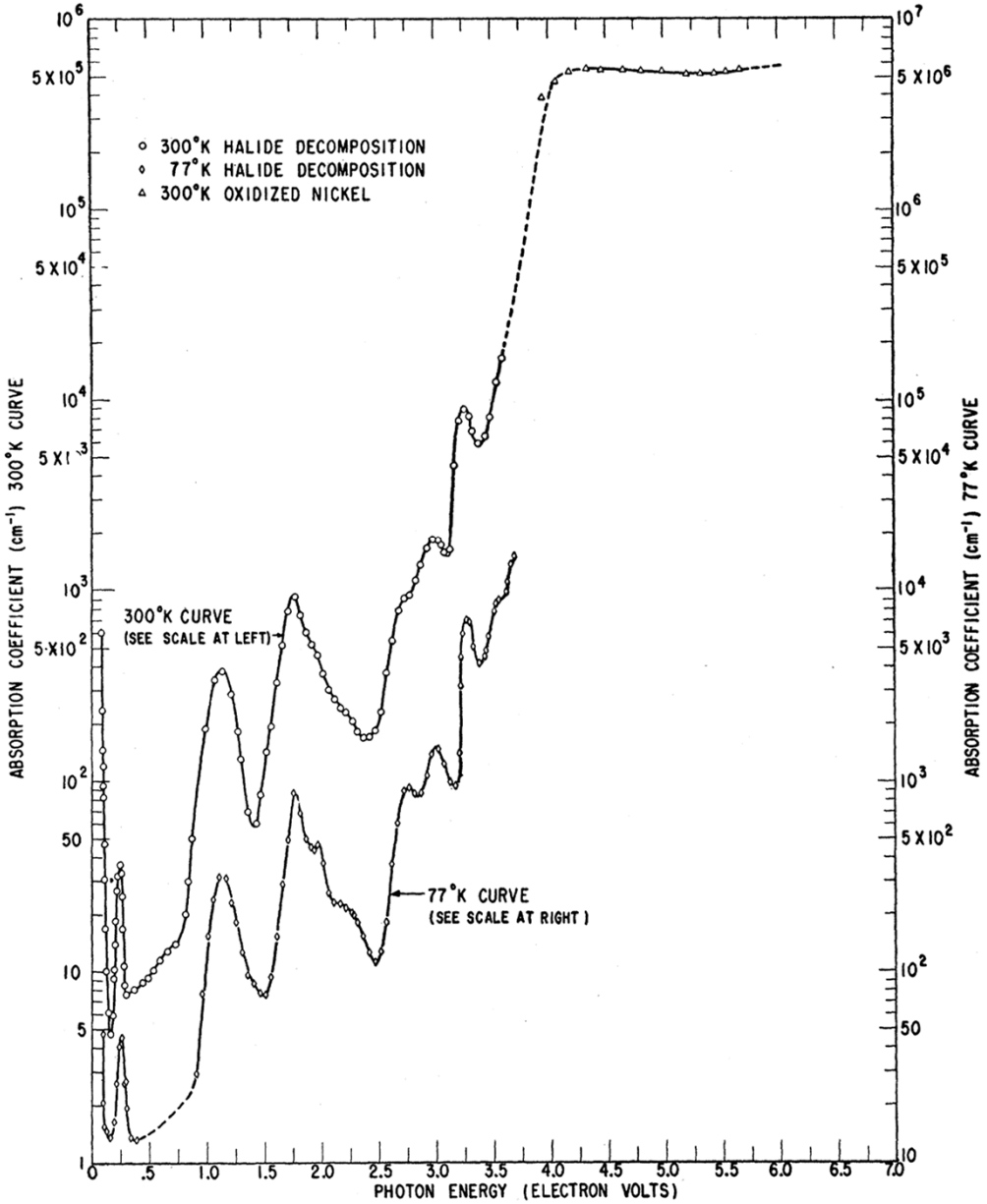

FIG. 2. Absorption spectrum of NiO at 300°K, 77°K. Dashed lines are interpolations.

Magnitude and Origin of the Band Gap in NiO

G. A. Sawatzky[(a)] and J. W. Allen
Xerox Palo Alto Research Center, Palo Alto, California 94304
(Received 5 July 1984)

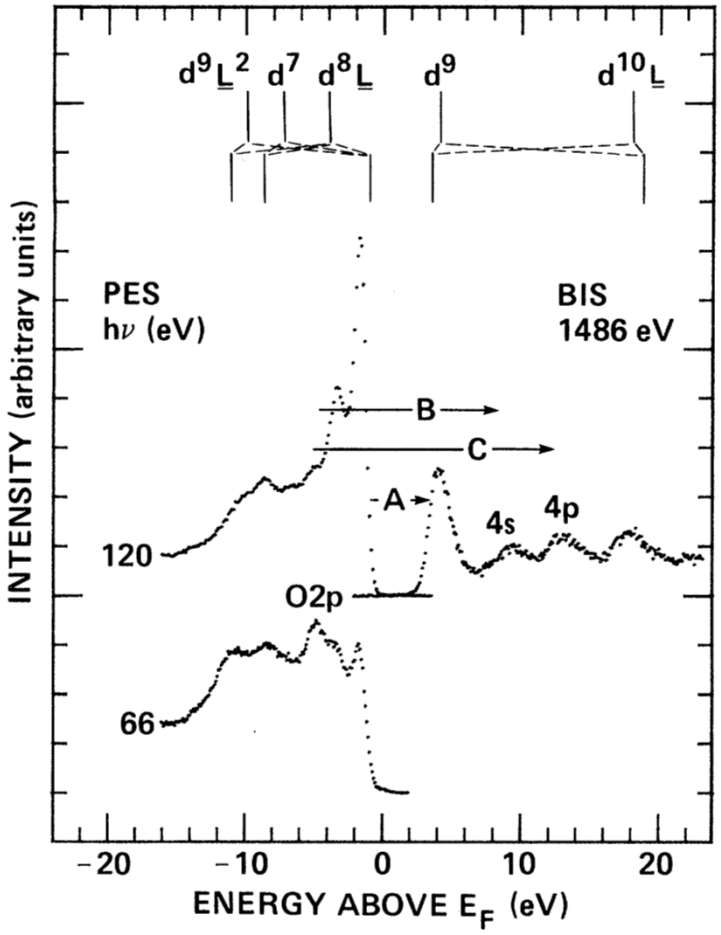

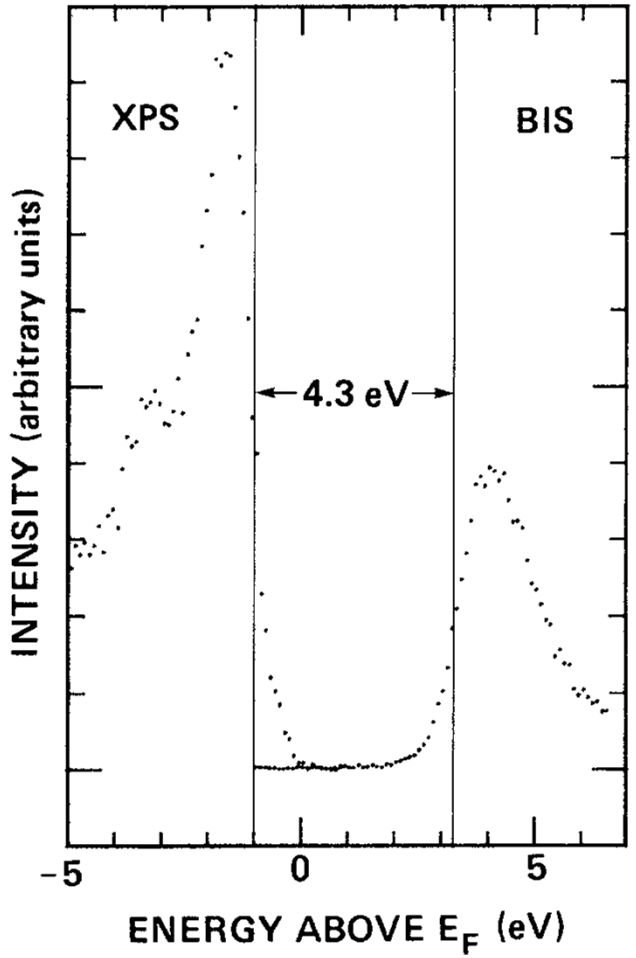

NiO is a charge transfer insulator

Transition metal oxides: ZSA scheme

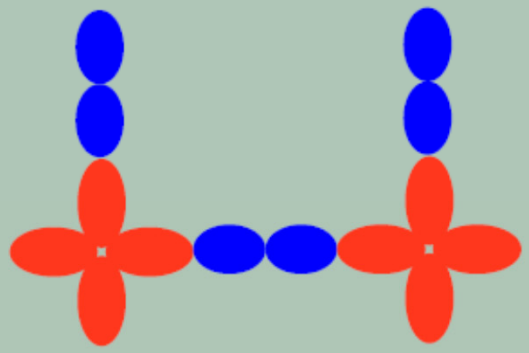

O - 2p

Transition metal - 3d

Courtesy of
Jan Kuneš

Mott-Hubbard type (Ti-O, V-O)

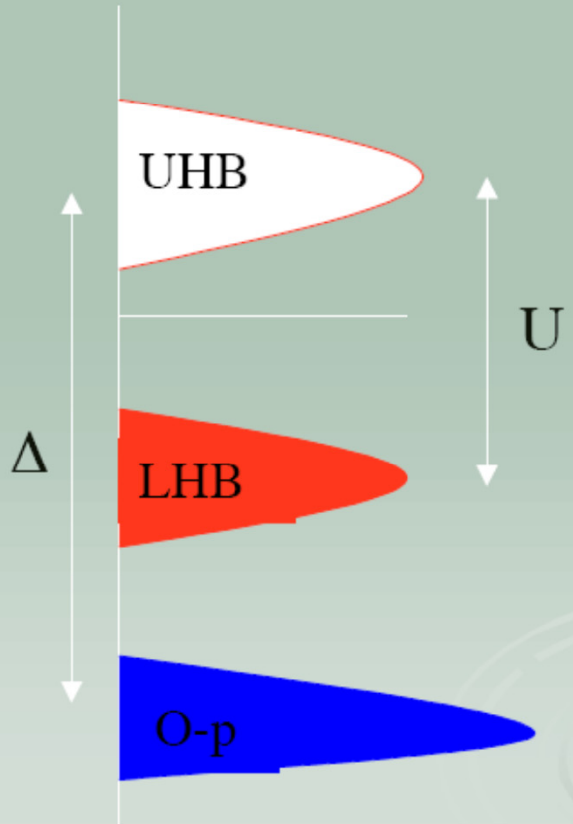

charge-transfer type (Ni-O,Cu-O)

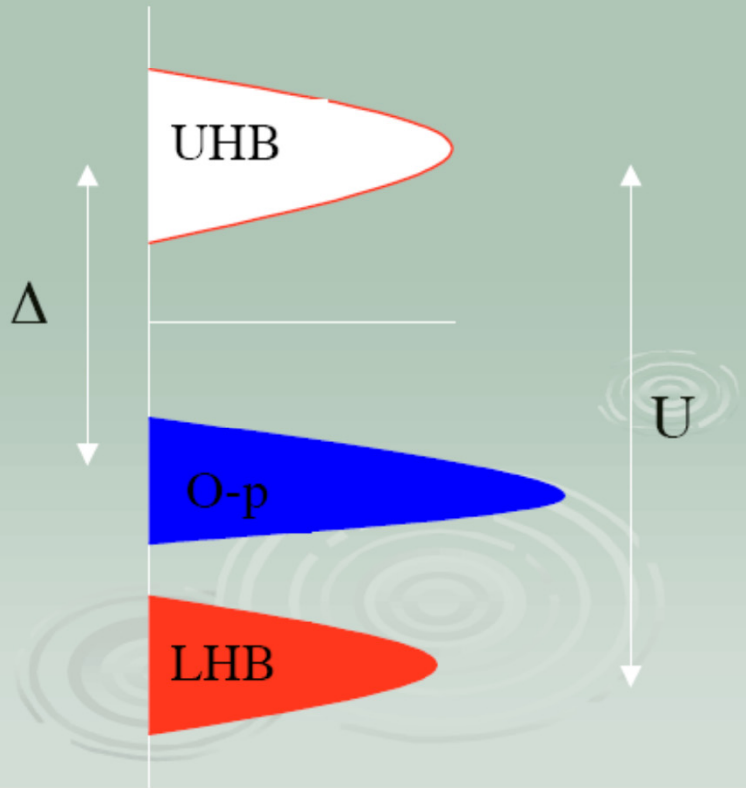

PHYSICAL REVIEW B VOLUME 44, NUMBER 8 15 AUGUST 1991-II

Electronic structure of NiO: Correlation and band effects

Z.-X. Shen
Stanford Electronics Laboratory, Stanford University, Stanford, California 94305

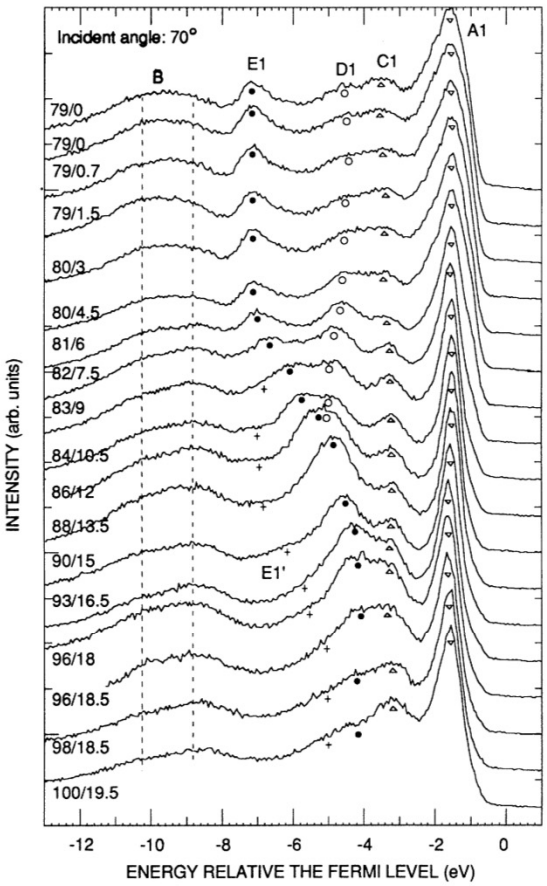

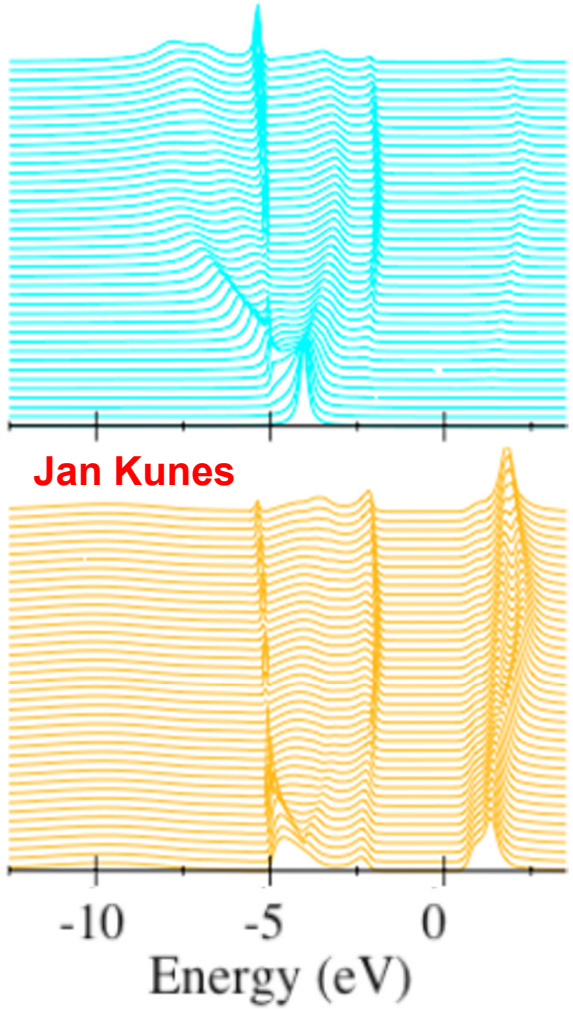

O – 2p

Jan Kunes

Ni – 3d(e_g)

NiO is a charge transfer insulator

Electronic Structure of a Mott Insulator: LDA+U

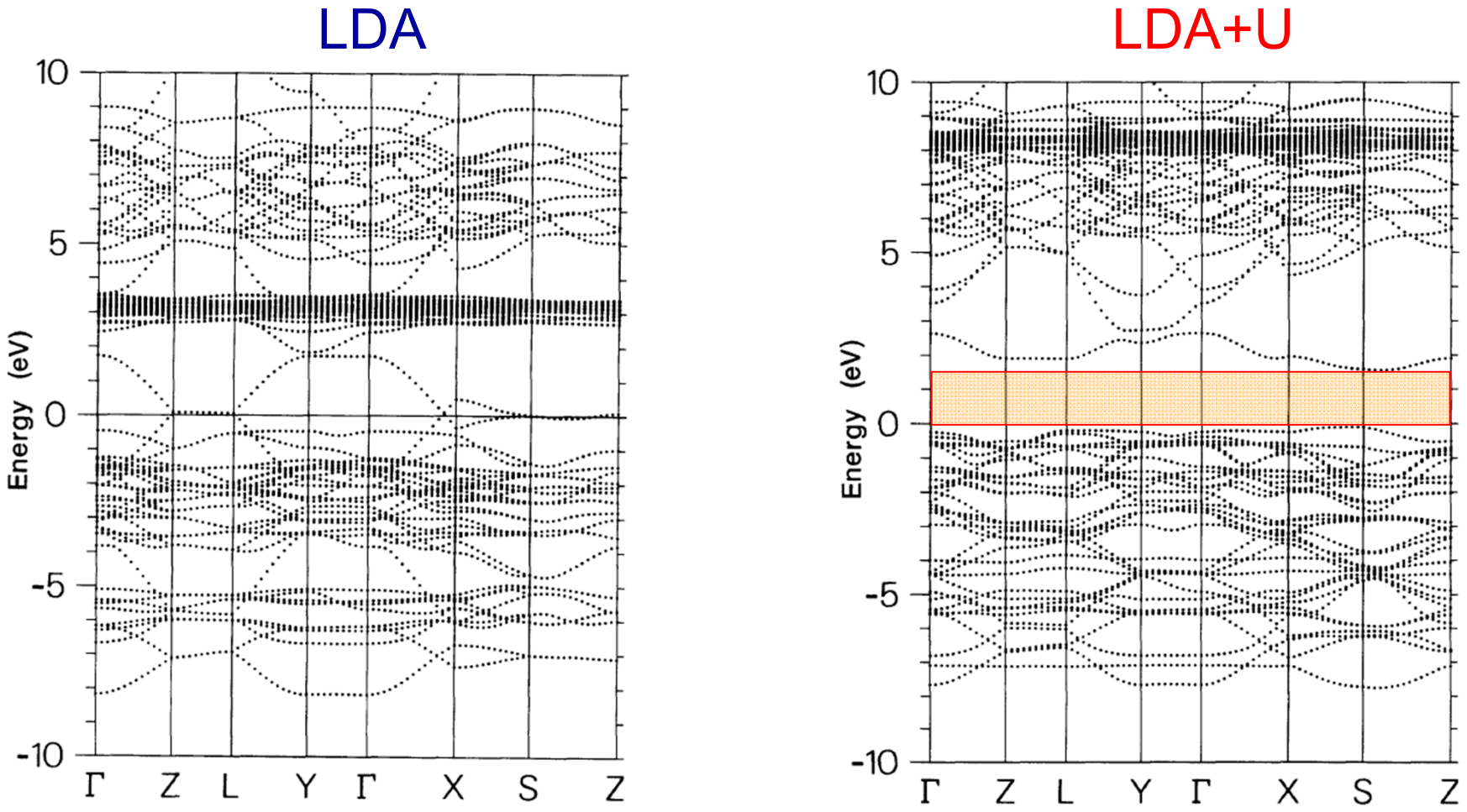

LDA+U can describe the Mott insulator with a gap, BUT:

- It works only for truly insulating systems with no open shells (1/2-filled)
- It does not include many body states such as the Zhang-Rice singlet

Czyżyk and Sawatzky, Phys. Rev. B 49, 14211 (1994)

Electronic Structure of a Mott Insulator: LDA+U

Zhang-Rice Singlet

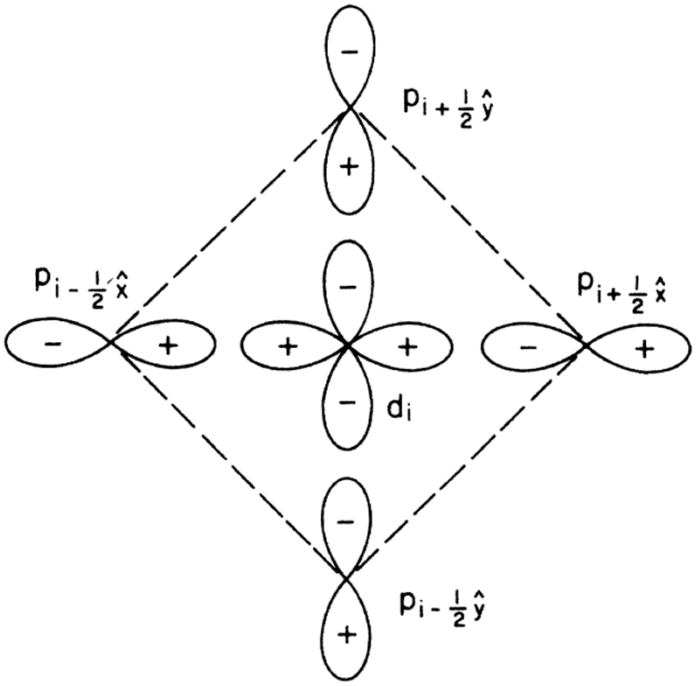

FIG. 1. Schematic diagram of the hybridization of the O hole ($2p^5$) and Cu hole ($3d^9$). The signs + and − represent the phase of the wave functions.

Zhang and Rice, Phys. Rev. B 37, 3759 (1988)

LDA+U

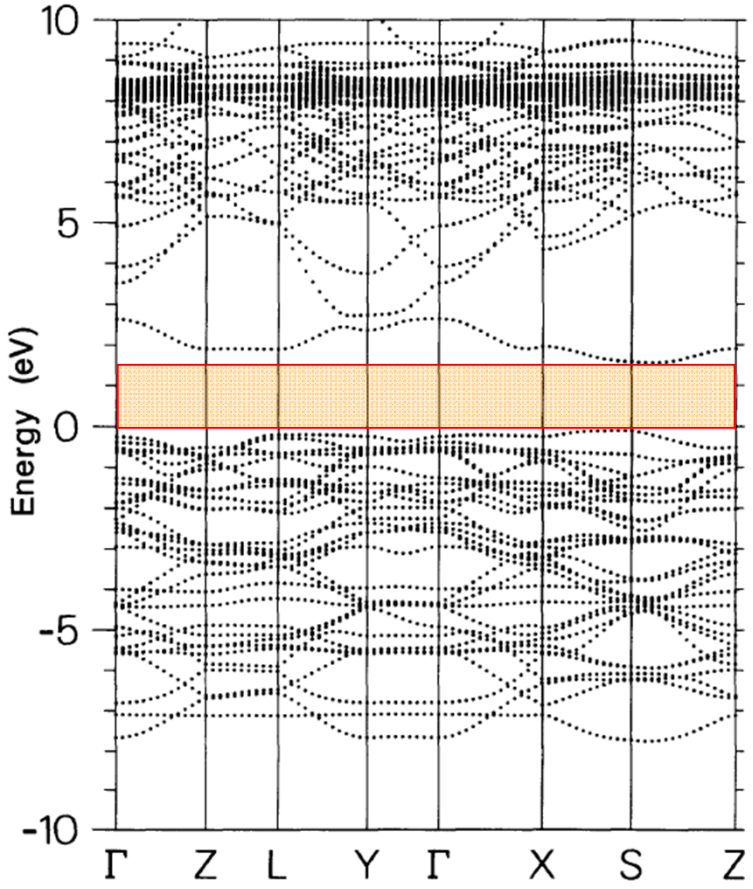

- ZR singlets are truly many body states (1 Cu hole + 1 hole in ligand orbitals)
- They can be probed by photoemission because they can be reached by a one-particle excitation from the ground state with 1 hole per Cu site

Doping a Mott Insulator: Spectral Weight Transfer

PHYSICAL REVIEW B VOLUME 48, NUMBER 6 1 AUGUST 1993-II

Spectral-weight transfer: Breakdown of low-energy-scale sum rules in correlated systems

M. B. J. Meinders
Materials Science Centre, Department of Solid State and Applied Physics, University of Groningen, Nijenborgh 4, 9747 AG Groningen, The Netherlands

H. Eskes
Max-Planck-Institut für Festkörperforschung, Heisenbergstrasse 1, D-7000 Stuttgart 80, Federal Republic of Germany

G. A. Sawatzky
Materials Science Centre, Department of Solid State and Applied Physics, University of Groningen, Nijenborgh 4, 9747 AG Groningen, The Netherlands

(Received 4 March 1993)

In this paper we study the spectral-weight transfer from the high- to the low-energy scale by means of exact diagonalization of finite clusters for the Mott-Hubbard and charge-transfer model. We find that the spectral-weight transfer is very sensitive to the hybridization strength as well as to the amount of doping. This implies that the effective number of low-energy degrees of freedom is a function of the hybridization and therefore of the volume and temperature. In this sense it is not possible to define a Hamiltonian which describes the low-energy-scale physics unless one accepts an effective nonparticle conservation.

It is the connection between low and high energy scales that distinguishes the Mott gap from a more conventional gap (i.e., semiconductor, CDW, etc.)

Doping a Mott Insulator: Spectral Weight Transfer

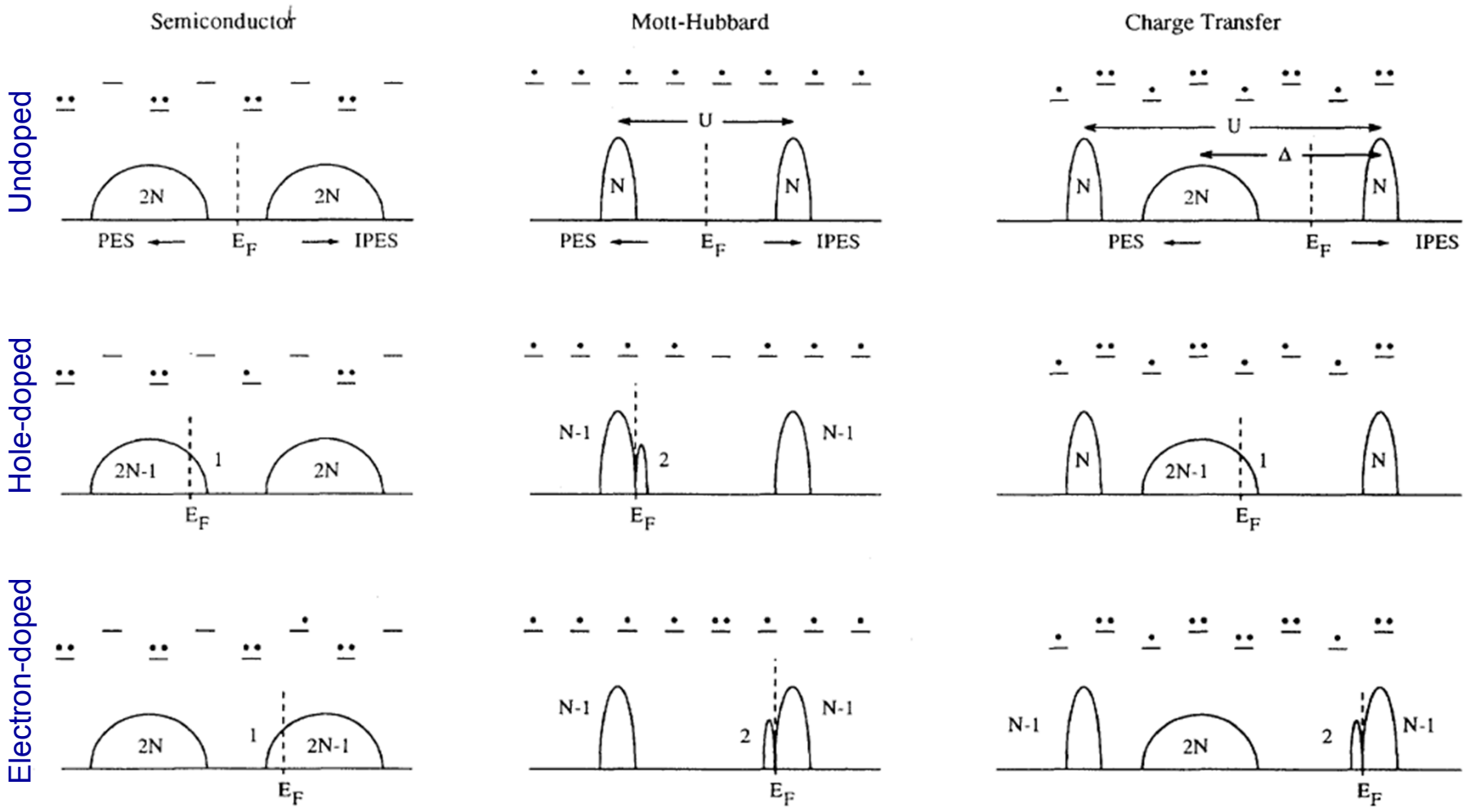

It is the connection between low and high energy scales that distinguishes the Mott gap from a more conventional gap (i.e., semiconductor, CDW, etc.)

Doping a Mott Insulator: Spectral Weight Transfer

Meinders, Eskes, Sawatzky , PRB 48, 3916 (1993)

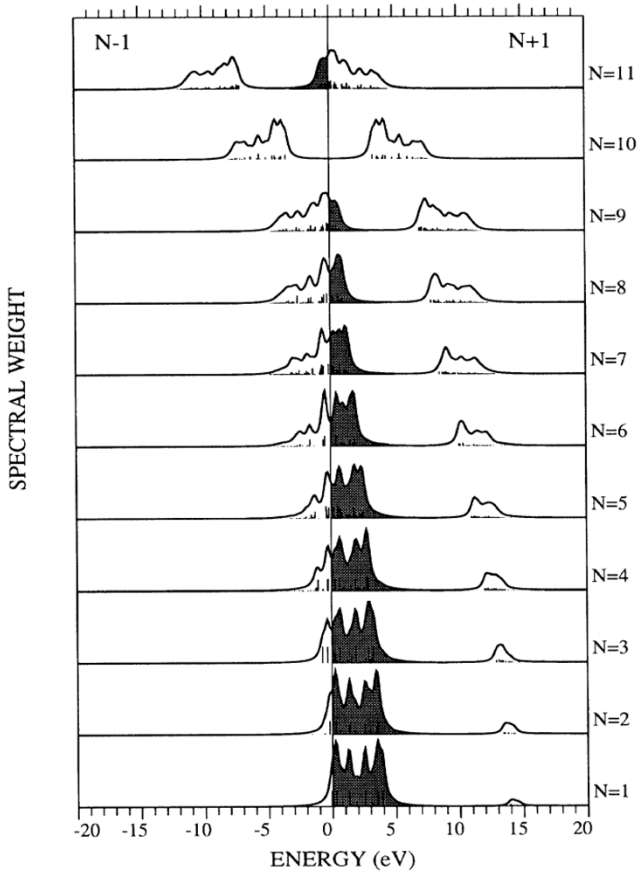

FIG. 2. One-particle Green's function for a one-dimensional Hubbard-ring of $N=10$ sites for $U=10$ eV and $t=1$ eV. The number of electrons in the ground state N are indicated. The low-energy electron-addition spectral weight is obtained by integration over the shaded area.

C.T. Chen et al., PRL 66, 104 (1991)

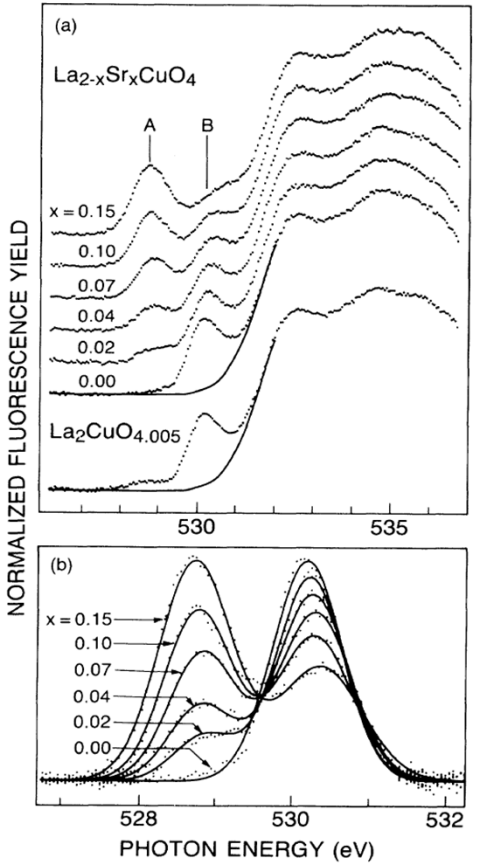

FIG. 1. (a) Normalized fluorescence yield at the O K edge of $La_{2-x}Sr_xCuO_{4+\delta}$. The solid curves are the common background described in the text. (b) The difference between the data of $La_{2-x}Sr_xCuO_4$ and the common background. The solid lines are the fitted curves using two Gaussian line shapes.

It is the connection between low and high energy scales that distinguishes the Mott gap from a more conventional gap (i.e., semiconductor, CDW, etc.)

Outline Part II

Sudden approximation and quasiparticle renormalization

CUSO Lecture – Lausanne 02/2011

ARPES: Interacting Systems

A. Damascelli, Z. Hussain, Z.-X Shen, Rev. Mod. Phys. **75**, 473 (2003)

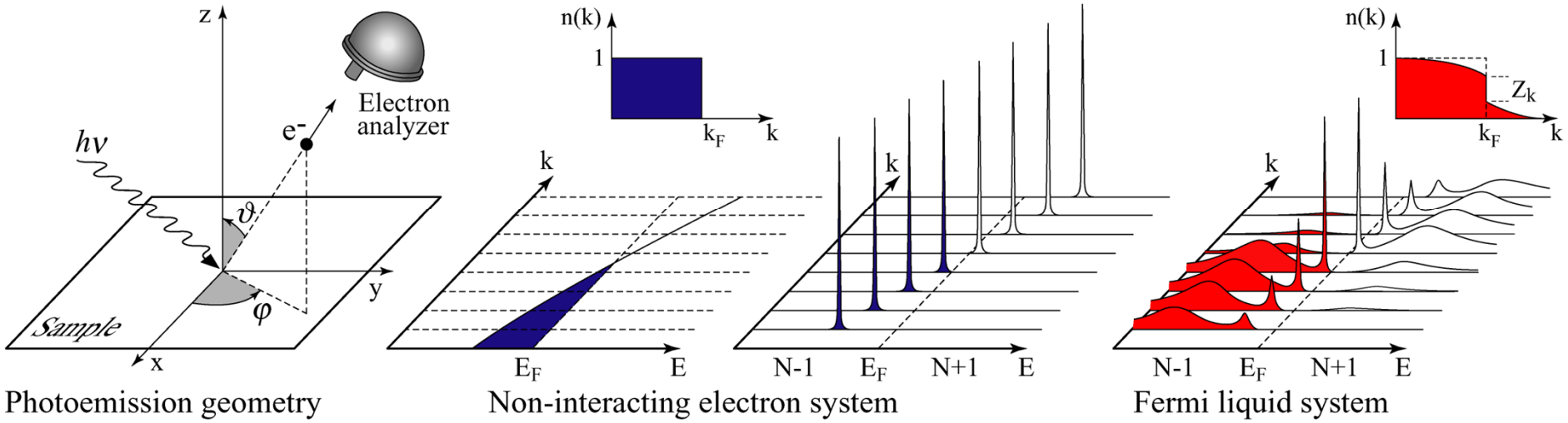

Photoemission geometry | Non-interacting electron system | Fermi liquid system

Photoemission intensity: $I(\mathbf{k}, E_{kin}) = \sum_{f,i} w_{f,i}$

$$I(\mathbf{k}, E_{kin}) \propto \sum_{f,i} |M^{\mathbf{k}}_{f,i}|^2 \sum_{m} |c_{m,i}|^2 \delta(E_{kin} + E^{N-1}_m - E^N_i - h\nu)$$

$$|M^{\mathbf{k}}_{f,i}|^2 \equiv |\langle \phi^{\mathbf{k}}_f | \mathbf{A}\cdot\mathbf{p} | \phi^{\mathbf{k}}_i \rangle|^2 \qquad |c_{m,i}|^2 = |\langle \Psi^{N-1}_m | \Psi^{N-1}_i \rangle|^2$$

In general $\Psi^{N-1}_i = c_{\mathbf{k}} \Psi^N_i$ **NOT orthogonal** Ψ^{N-1}_m

ARPES: Interacting Systems

A. Damascelli, Z. Hussain, Z.-X Shen, Rev. Mod. Phys. **75**, 473 (2003)

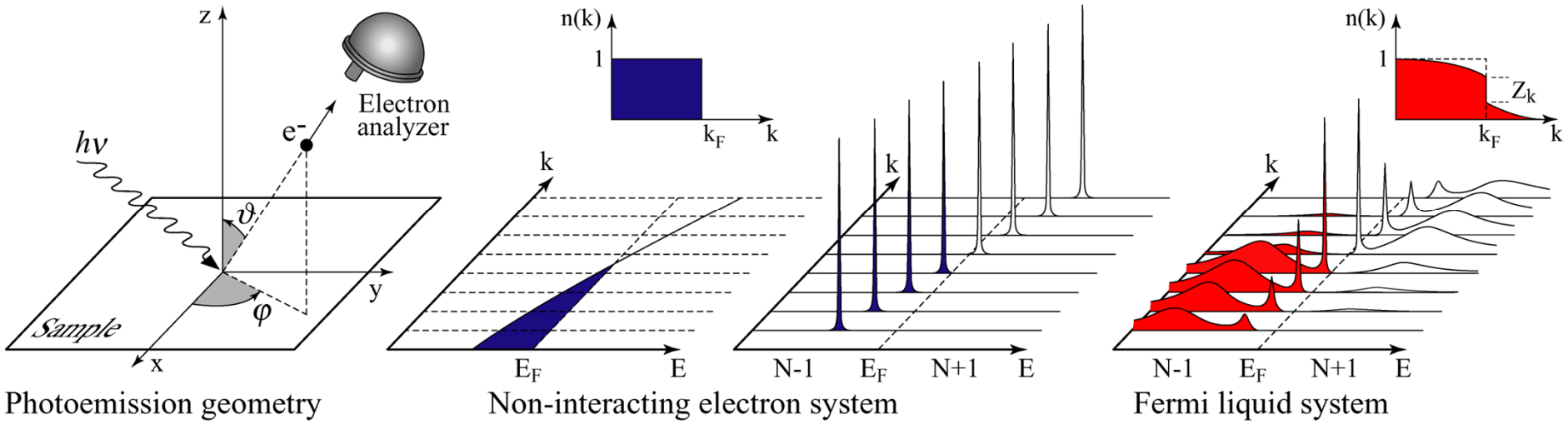

Photoemission intensity: $I(\mathbf{k}, E_{kin}) = \sum_{f,i} w_{f,i}$

$$I(\mathbf{k}, E_{kin}) \propto \sum_{f,i} |M^{\mathbf{k}}_{f,i}|^2 \sum_{m} |c_{m,i}|^2 \delta(E_{kin} + E^{N-1}_m - E^N_i - h\nu)$$

$$|M^{\mathbf{k}}_{f,i}|^2 \equiv |\langle \phi^{\mathbf{k}}_f | \mathbf{A}\cdot\mathbf{p} | \phi^{\mathbf{k}}_i \rangle|^2 \qquad |c_{m,i}|^2 = |\langle \Psi^{N-1}_m | \Psi^{N-1}_i \rangle|^2$$

“Like removing a stone from a water bucket”

ARPES: Fermi Liquid Description

A. Damascelli, Z. Hussain, Z.-X Shen, Rev. Mod. Phys. **75**, 473 (2003)

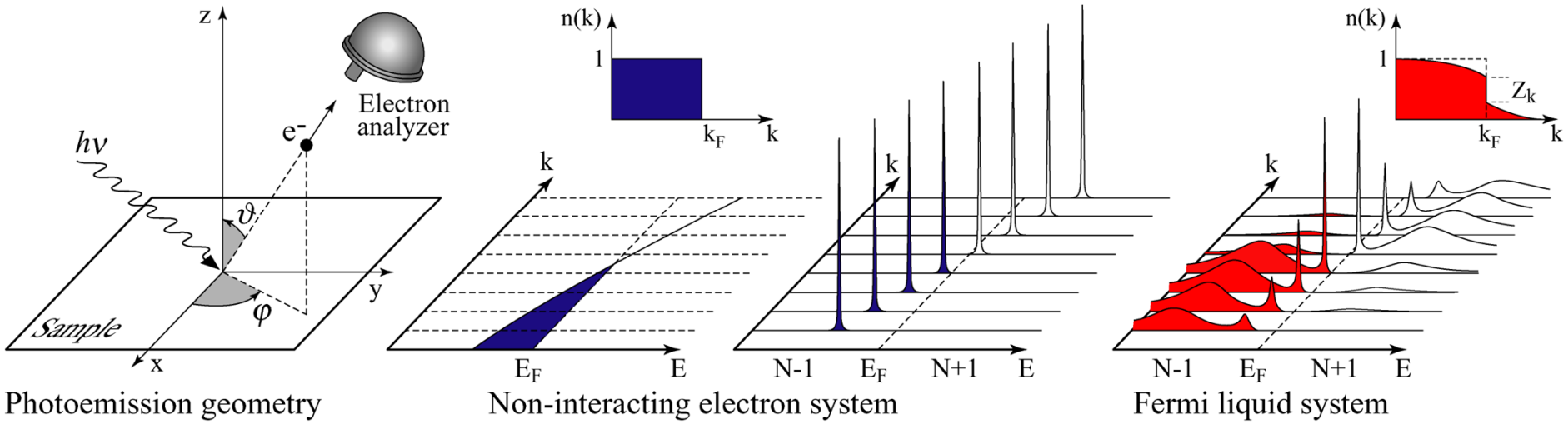

Photoemission geometry | Non-interacting electron system | Fermi liquid system

Photoemission intensity: $I(k,\omega)=I_0\,|M(k,\omega)|^2 f(\omega)\,A(k,\omega)$

Non-interacting

$$A(\mathbf{k},\omega)=\delta(\omega-\epsilon_k)$$

No Renormalization
Infinite lifetime

Fermi Liquid

$$A(\mathbf{k},\omega)=Z_{\mathbf{k}}\frac{\Gamma_{\mathbf{k}}/\pi}{(\omega-\varepsilon_{\mathbf{k}})^2+\Gamma_{\mathbf{k}}^2}+A_{inc}$$

$$m^*>m \qquad |\varepsilon_{\mathbf{k}}|<|\epsilon_{\mathbf{k}}|$$

$$\tau_{\mathbf{k}}=1/\Gamma_{\mathbf{k}}$$

$\Sigma(\mathbf{k},\omega)$: the "self-energy" captures the effects of interactions

NEWS AND VIEWS

Nature **342**, 480 (1989)

HIGH-TEMPERATURE SUPERCONDUCTIVITY

Testing Fermi-liquid models

G.A. Sawatzky

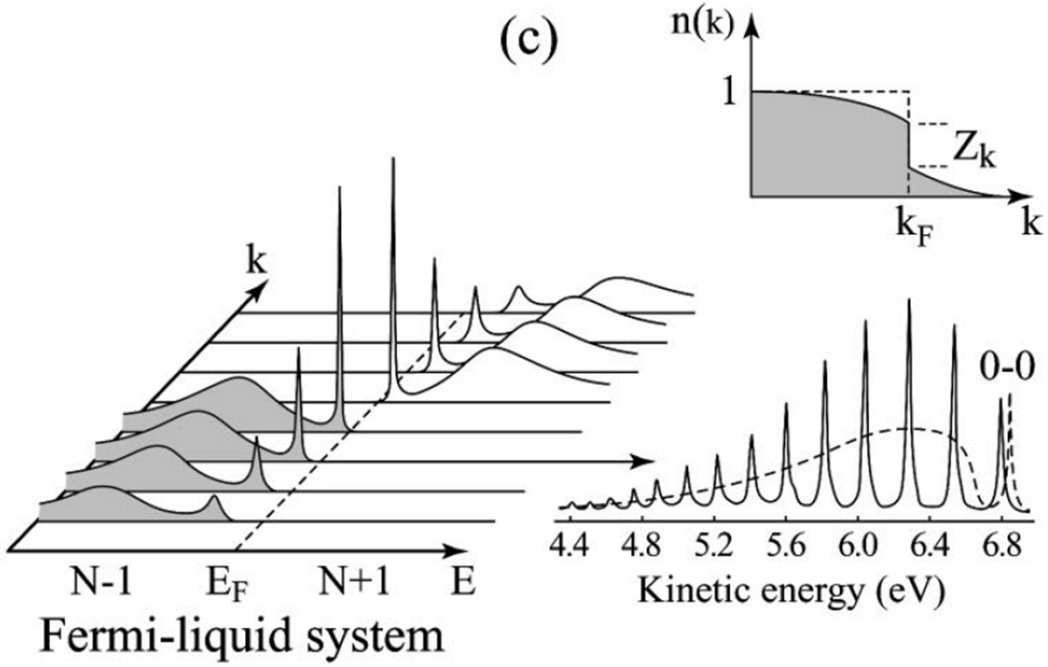

Franck-Condon

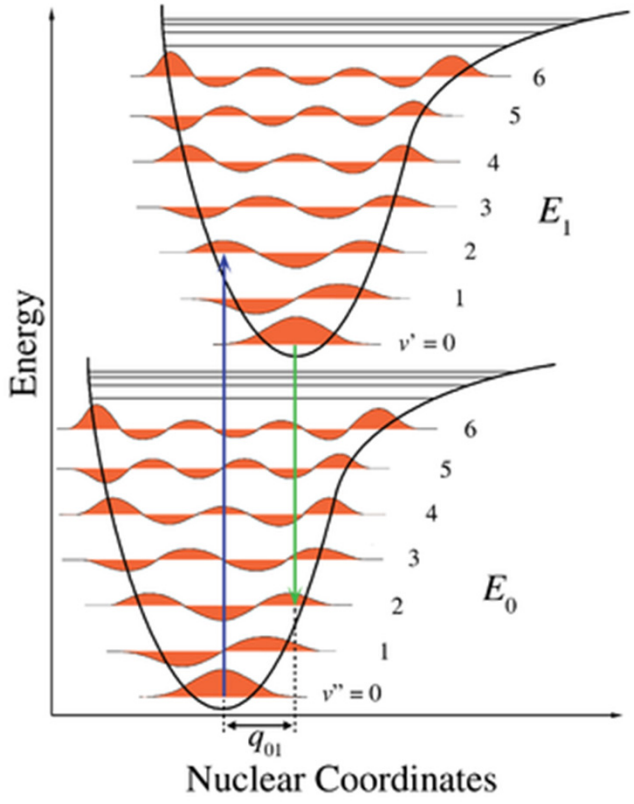

"In gaseous hydrogen, the equilibrium bond length is dependent on the degree of occupation of that level. The electrons are dressed by interatomic displacements. The intensities are given by the Franck-Condon factors, the molecular equivalent of the sudden approximation. The ARPES spectrum of solid hydrogen, developed from the molecular spectrum, will be angle dependent but for some angle will resemble the broken line. The fundamental transition (0-0) becomes the solid state quasiparticle peak. The phonon excitations develop into a broad, incoherent quasicontinuum."

Development of Low-Energy LASER-ARPES

PRL 94, 057001 (2005) PHYSICAL REVIEW LETTERS week ending 11 FEBRUARY 2005

Photoemission Spectroscopic Evidence of Gap Anisotropy in an *f*-Electron Superconductor

T. Kiss,[1,*] F. Kanetaka,[1] T. Yokoya,[1,†] T. Shimojima,[1] K. Kanai,[1] S. Shin,[1,2] Y. Onuki,[3,4] T. Togashi,[2] C. Zhang,[5] C. T. Chen,[5] and S. Watanabe[1]

[1]*Institute for Solid State Physics (ISSP), University of Tokyo, Kashiwa, Chiba 277-8581, Japan*
[2]*The Institute of Physical and Chemical Research (RIKEN), Sayo-gun, Hyogo 679-5143, Japan*
[3]*Graduate School of Science, Osaka University, Toyonaka, Osaka 560-0043, Japan*
[4]*Advanced Science Research Center, JAERI, Tokai Ibaraki 319-1195, Japan*
[5]*Beijing Center for Crystal R&D, Chinese Academy of Science, Zhongguancun, Beijing 100080, China*

(Received 5 June 2004; published 7 February 2005)

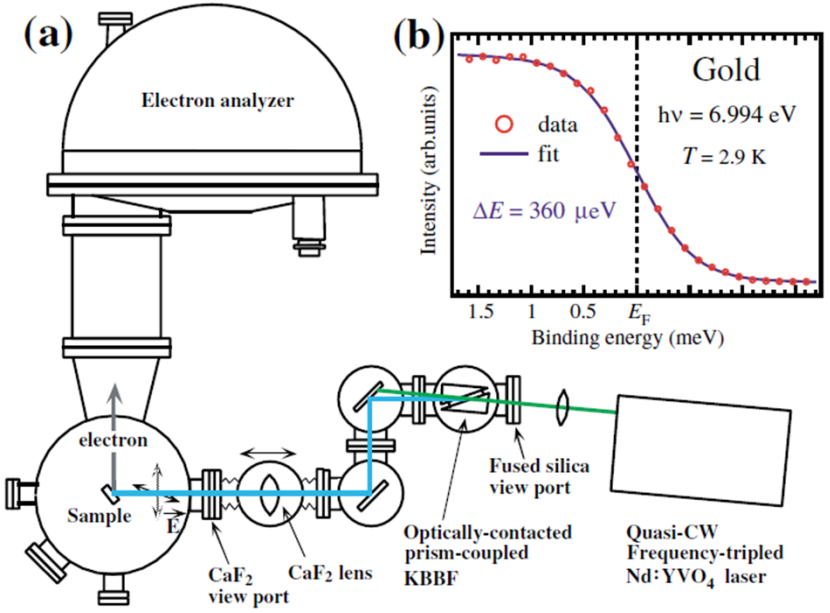

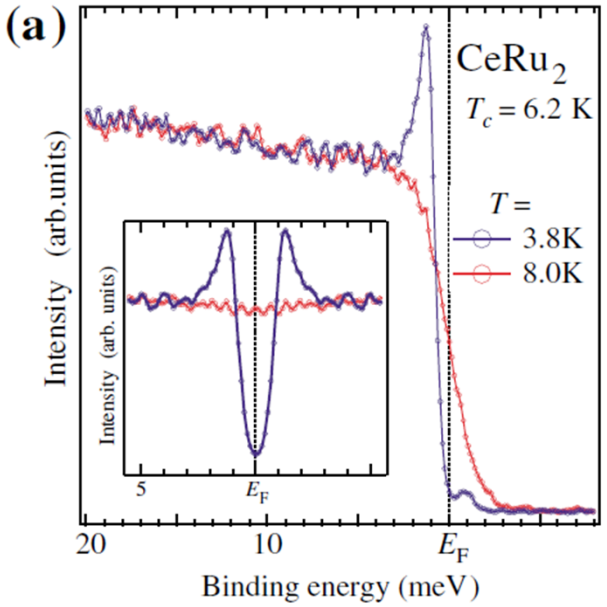

Development of Low-Energy LASER-ARPES

PRL 94, 057001 (2005) PHYSICAL REVIEW LETTERS week ending 11 FEBRUARY 2005

Photoemission Spectroscopic Evidence of Gap Anisotropy in an *f*-Electron Superconductor

T. Kiss,[1,*] F. Kanetaka,[1] T. Yokoya,[1,†] T. Shimojima,[1] K. Kanai,[1] S. Shin,[1,2] Y. Onuki,[3,4] T. Togashi,[2] C. Zhang,[5] C. T. Chen,[5] and S. Watanabe[1]

[1]*Institute for Solid State Physics (ISSP), University of Tokyo, Kashiwa, Chiba 277-8581, Japan*
[2]*The Institute of Physical and Chemical Research (RIKEN), Sayo-gun, Hyogo 679-5143, Japan*
[3]*Graduate School of Science, Osaka University, Toyonaka, Osaka 560-0043, Japan*
[4]*Advanced Science Research Center, JAERI, Tokai Ibaraki 319-1195, Japan*
[5]*Beijing Center for Crystal R&D, Chinese Academy of Science, Zhongguancun, Beijing 100080, China*
(Received 5 June 2004; published 7 February 2005)

Low energy ARPES is now becoming popular as a new tool for spectroscopy

Advantages:
- Higher bulk sensitivity: material specific, depending on relaxations
- Narrow excitation linewidth: higher energy resolution
- Smaller light spot: higher angular resolution

Drawbacks:
- Breakdown of sudden approximation?
- Higher sensitivity to final state effects
- Smaller amount of k-space accessible

Sudden approximation

$$w_{fi} \propto \left|\left\langle \phi_f^{\mathbf{k}} \middle| \mathbf{A}\cdot\mathbf{p} \middle| \phi_i^{\mathbf{k}} \right\rangle \left\langle \Psi_m^{N-1} \middle| \Psi_i^{N-1} \right\rangle\right|^2 \delta(\omega - h\nu)$$

The N-1 system eigenstates don't change

But the projection of final on initial states does!

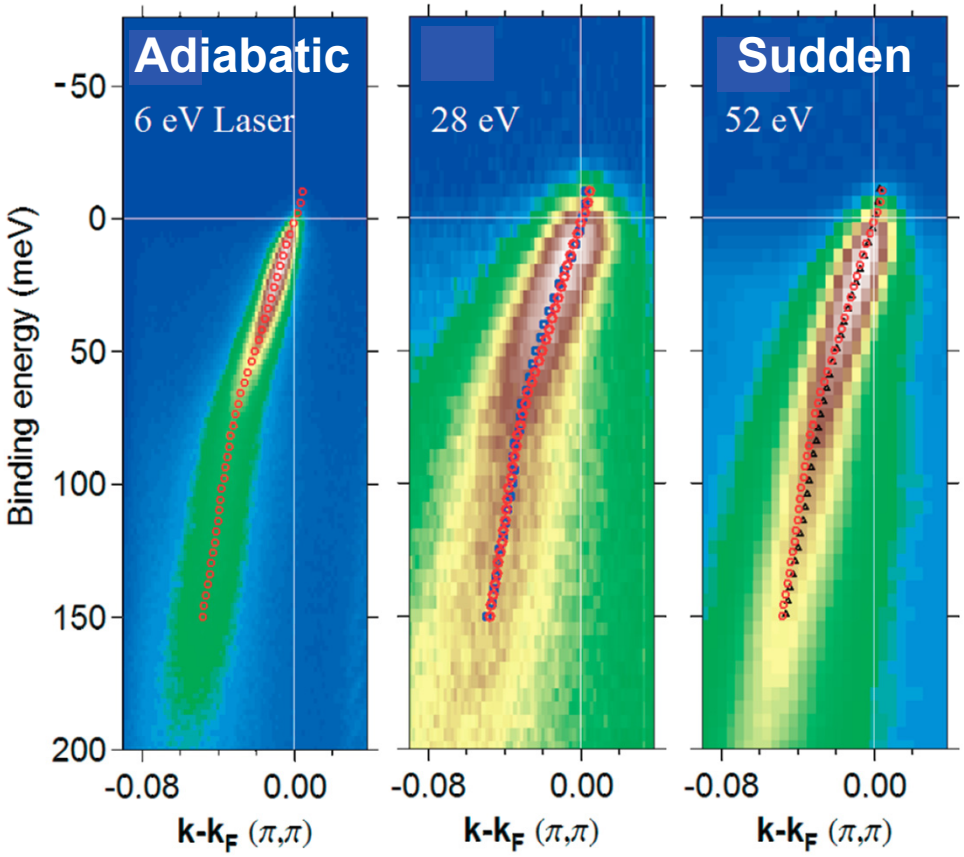

Koralek et al.,PRL **96,** 017005 (2006)

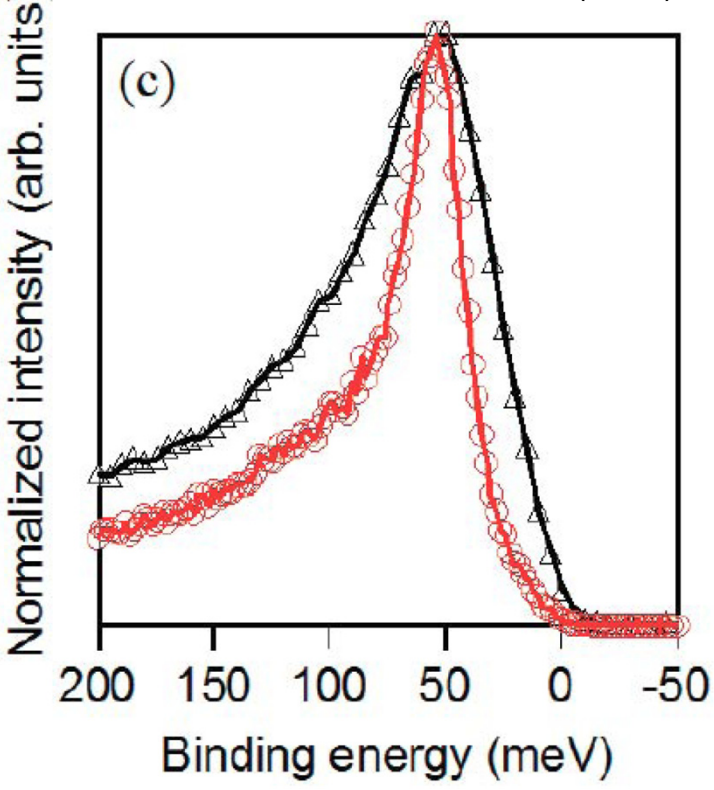

The intensity changes but not the dispersion!

Sudden approximation

$$w_{fi} \propto \left|\langle \phi_f^{\mathbf{k}} | \mathbf{A}\cdot\mathbf{p} | \phi_i^{\mathbf{k}} \rangle \langle \Psi_m^{N-1} | \Psi_i^{N-1} \rangle\right|^2 \delta(\omega - h\nu)$$

The N-1 system eigenstates don't change

But the projection of final on initial states does!

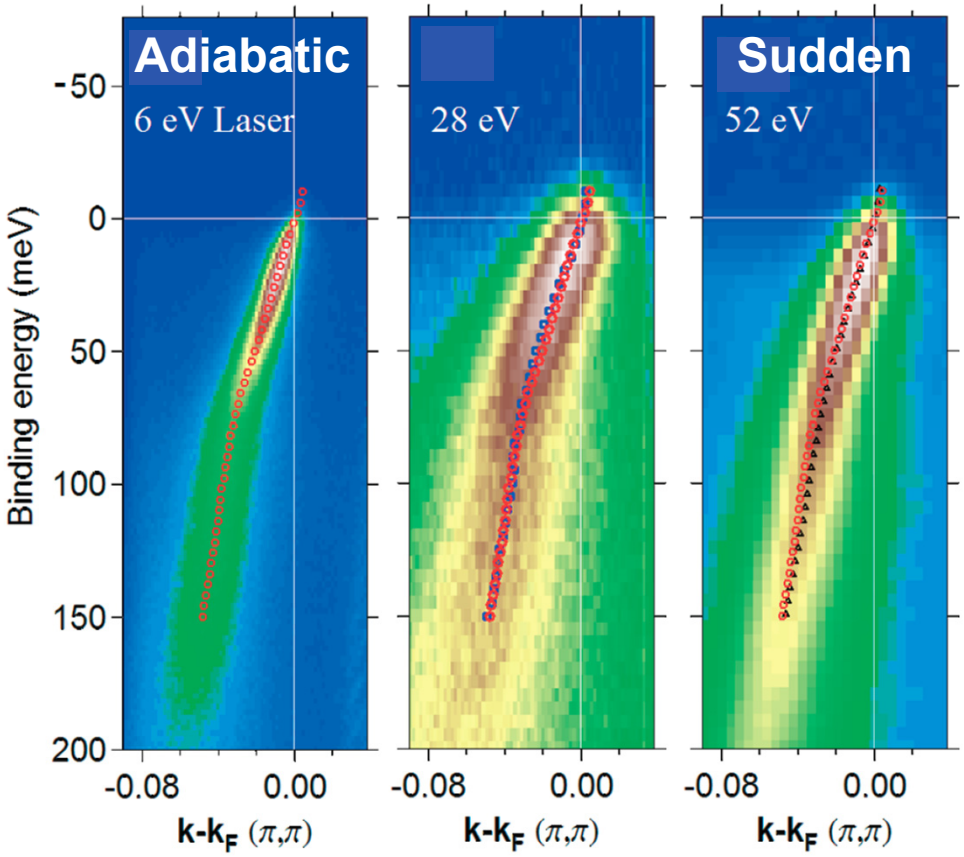

If the sudden approximation breaks down, the electron will be emitted with the highest possible kinetic energy and most of its spectral weight will be in a sharp line since the incoherent continuum is suppressed).

This does NOT prevent detecting features in the experiments due to correlation effects, because the (many-body) eigenstates of the N-1 particle system remain the same.

However, the ratio of intensity between coherent and incoherent parts of the spectral function will change, which WILL prevent a determination of Z from the evolution of the spectral weight detected by ARPES.

The intensity changes but not the dispersion!

Low-Energy ARPES and Final State Effects

Photoemission Intensity $I(k,\omega)$

$$w_{fi} \propto |\langle \phi_f^{\mathbf{k}} | \mathbf{A}\cdot\mathbf{p} | \phi_i^{\mathbf{k}} \rangle \langle \Psi_m^{N-1} | \Psi_i^{N-1} \rangle|^2 \delta(\omega - h\nu)$$

Excitation in the solid

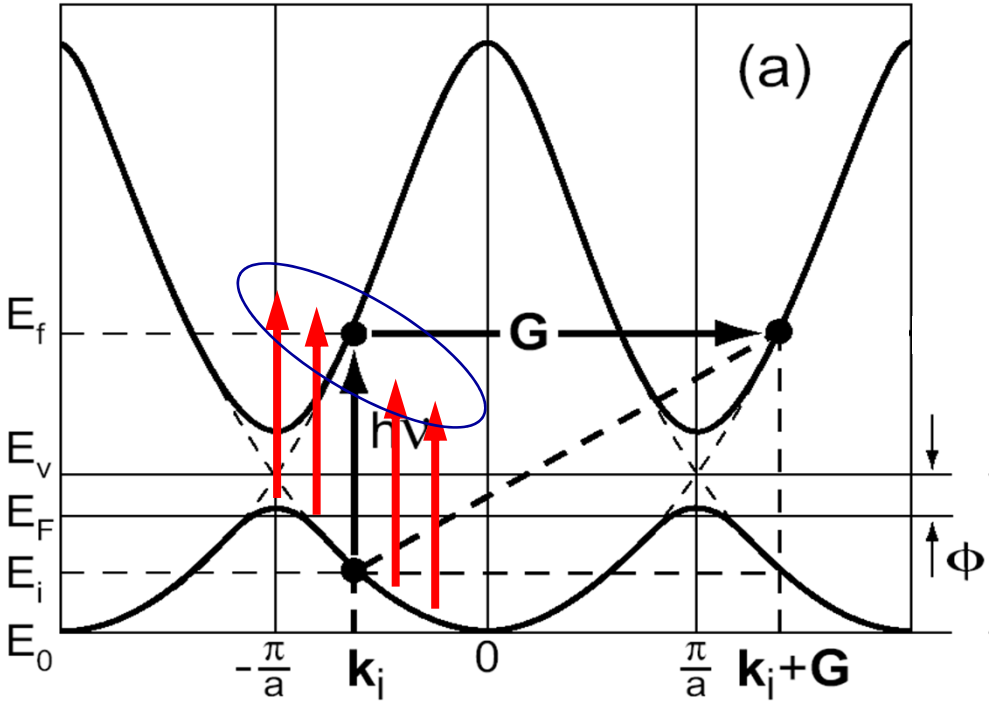

Working at high photon energies the electron is excited in a continuum of high-energy states; a final state is always available and the photoemission process can take place (with intensity still dependent on matrix elements).

At low photon energy photoemission is affected by the kinematic constrain deriving from energy and momentum conservation, and the k-dependent structure of the final states. For some initial state there is no final state that can be reached at a given photon energy and the intensity vanishes.

Many-Body Correlation Effects in Sr_2RuO_4

Single-particle spectral function

$$A(\mathbf{k},\omega) = -\frac{1}{\pi}\frac{\Sigma''(\mathbf{k},\omega)}{[\omega - \epsilon_{\mathbf{k}} - \Sigma'(\mathbf{k},\omega)]^2 + [\Sigma''(\mathbf{k},\omega)]^2}$$

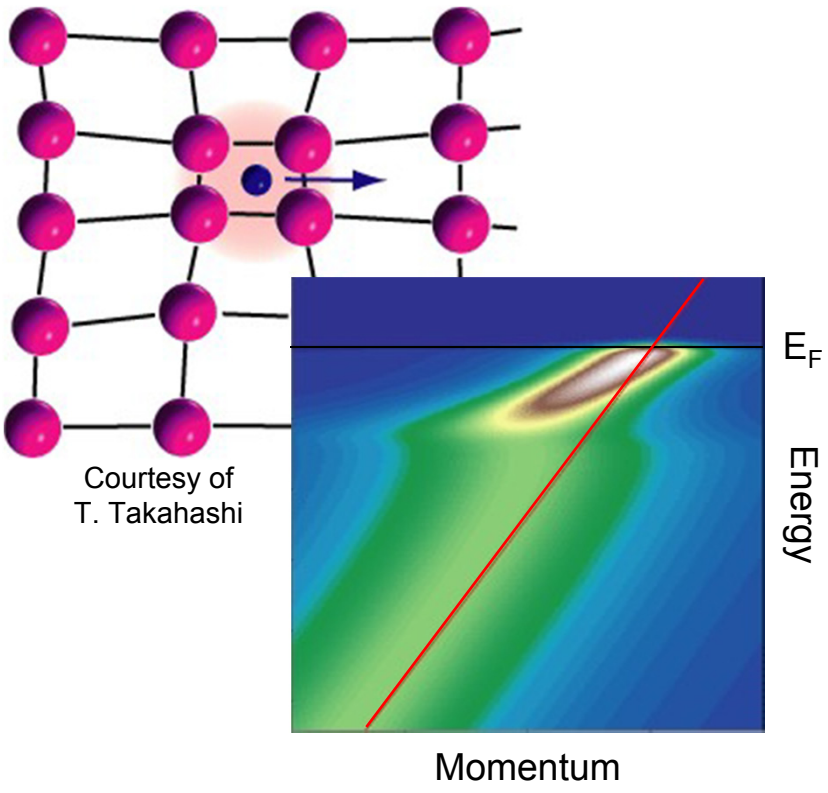

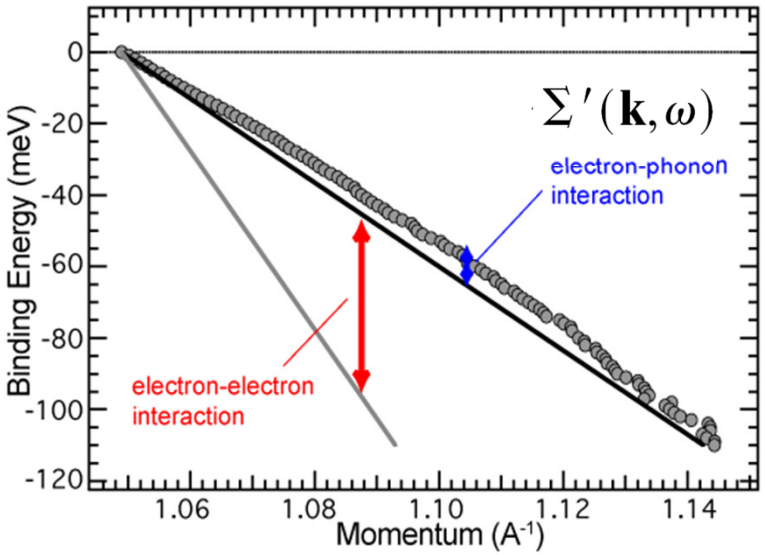

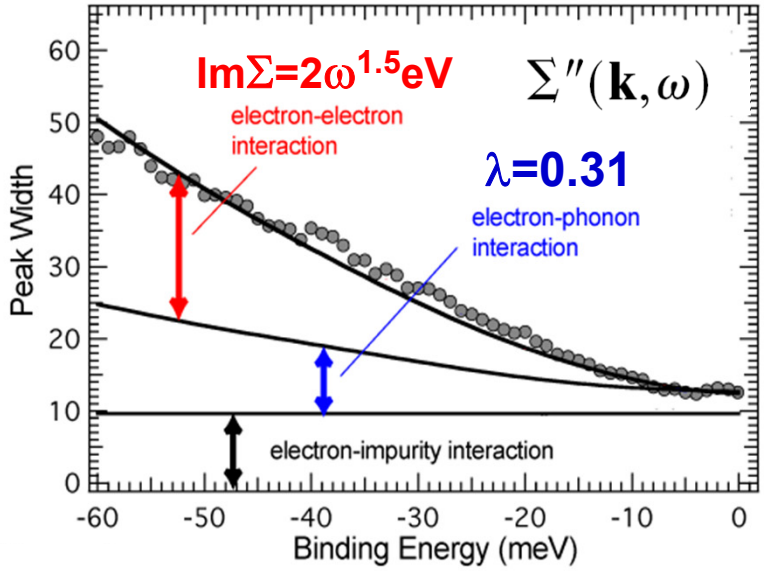

N.J.C. Ingle, K.M. Shen, A. Damascelli *et al.*, PRB **72**, 205114 (2005)

Many-Body Effects: Electron-Boson Coupling

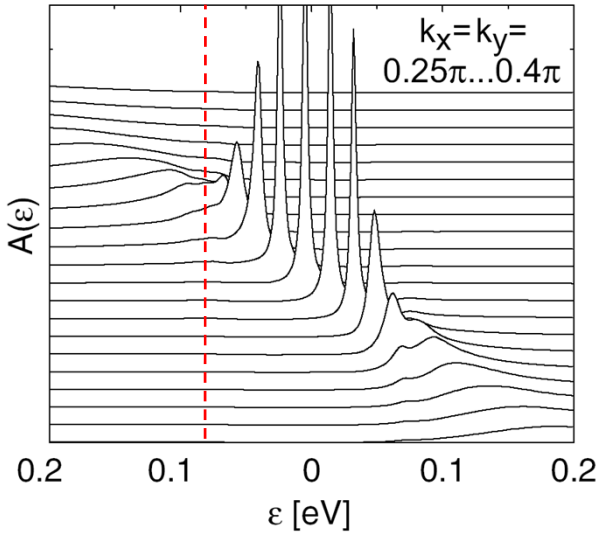

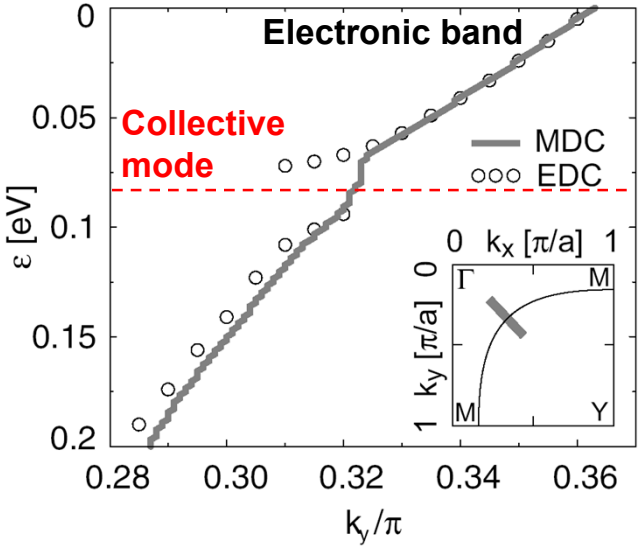

Eschrig, Norman, PRB **67**, 144503 (2003)

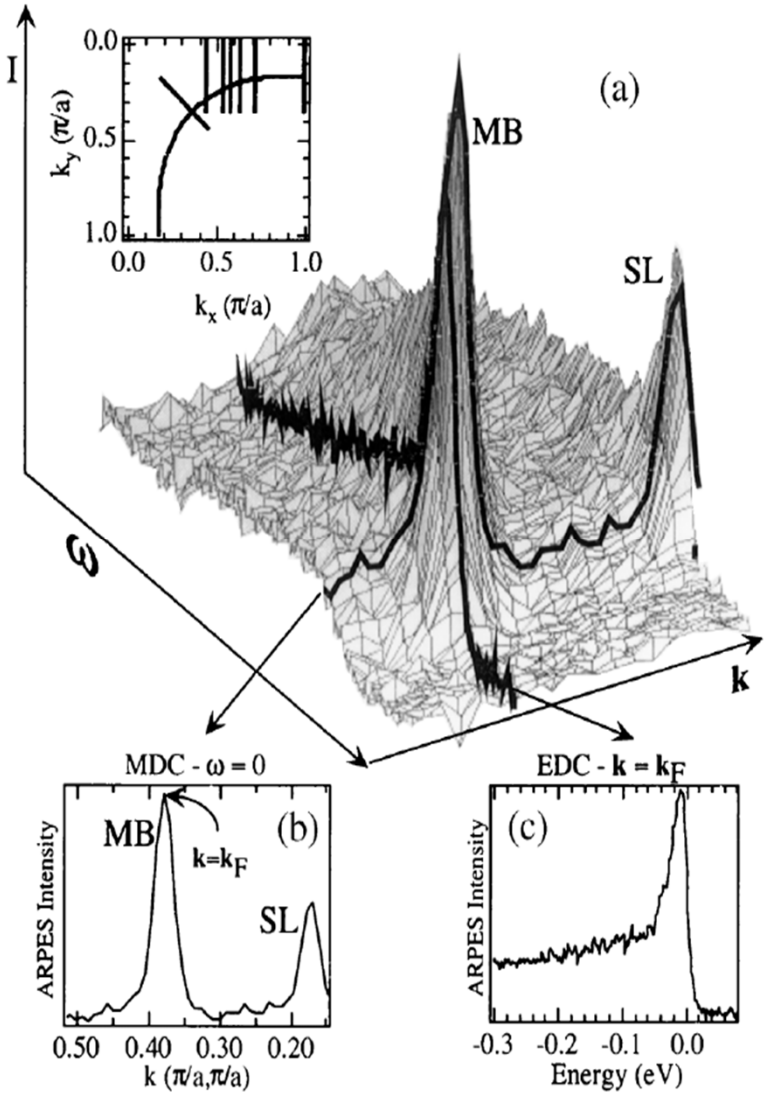

Kaminski et al., Phys. Rev. Lett. 86**, 1070 (2001)**

Many-Body Effects: Electron-Phonon Coupling

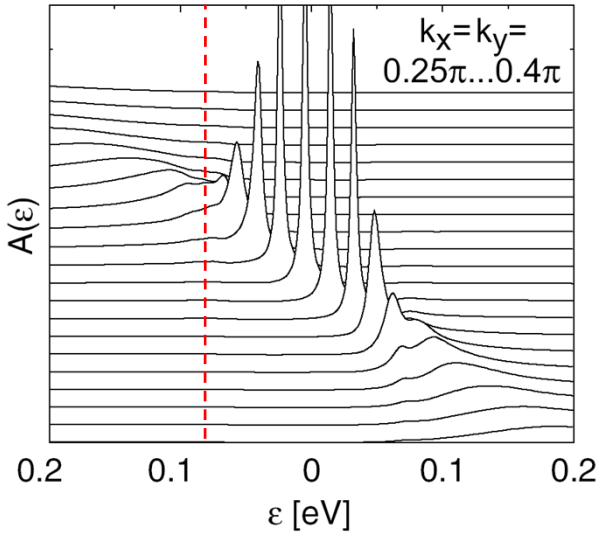

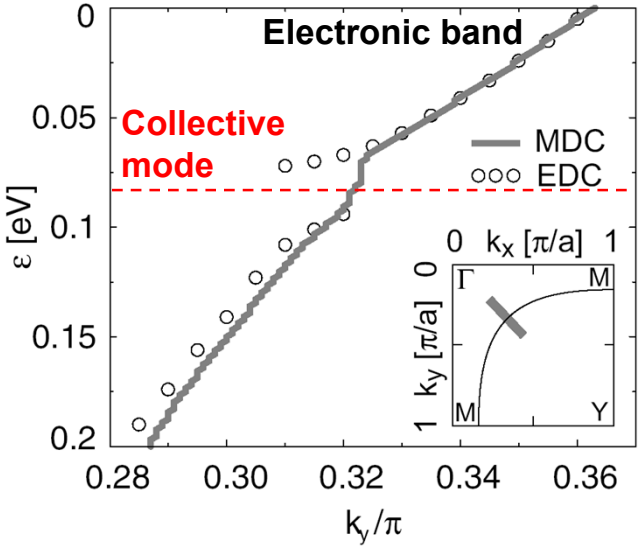

Eschrig, Norman, PRB **67**, 144503 (2003)

Single-particle spectral function

$$A(\mathbf{k},\omega) = -\frac{1}{\pi}\frac{\Sigma''(\mathbf{k},\omega)}{[\omega-\epsilon_{\mathbf{k}}-\Sigma'(\mathbf{k},\omega)]^2+[\Sigma''(\mathbf{k},\omega)]^2}$$

Be(0001)

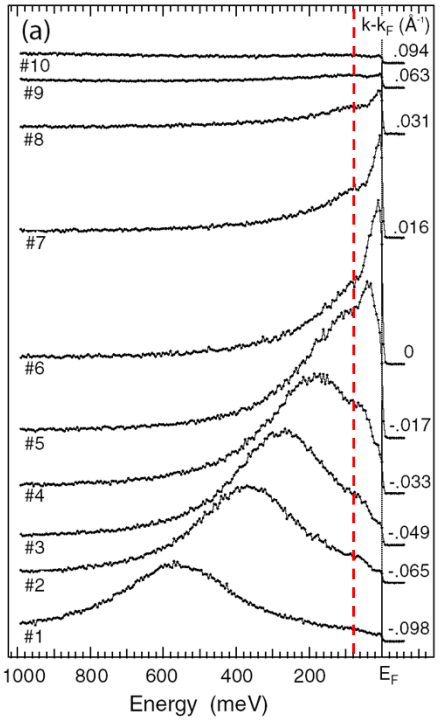

Hengsberger *et al.*, PRL **83**, 592 (1999)

Mo(110)

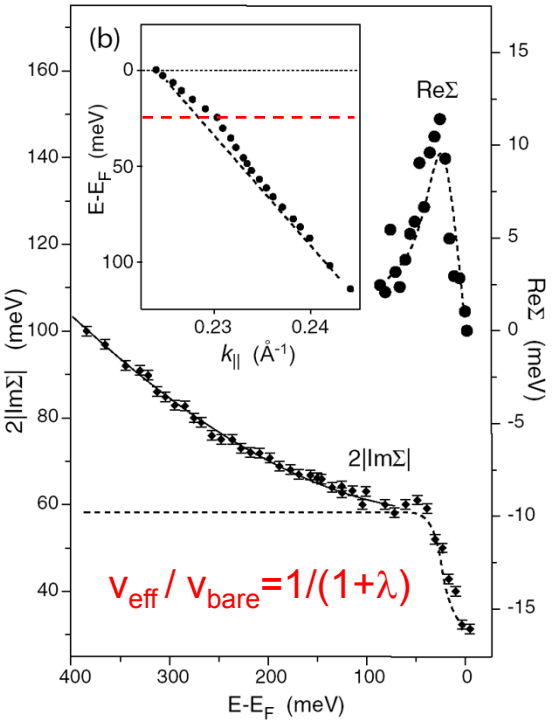

Valla *et al.*, PRL **83**, 2085 (1999)

Many-Body effects in the High-T_C Cuprates

Valla *et al.*, Science **285**, 2110 (1999)

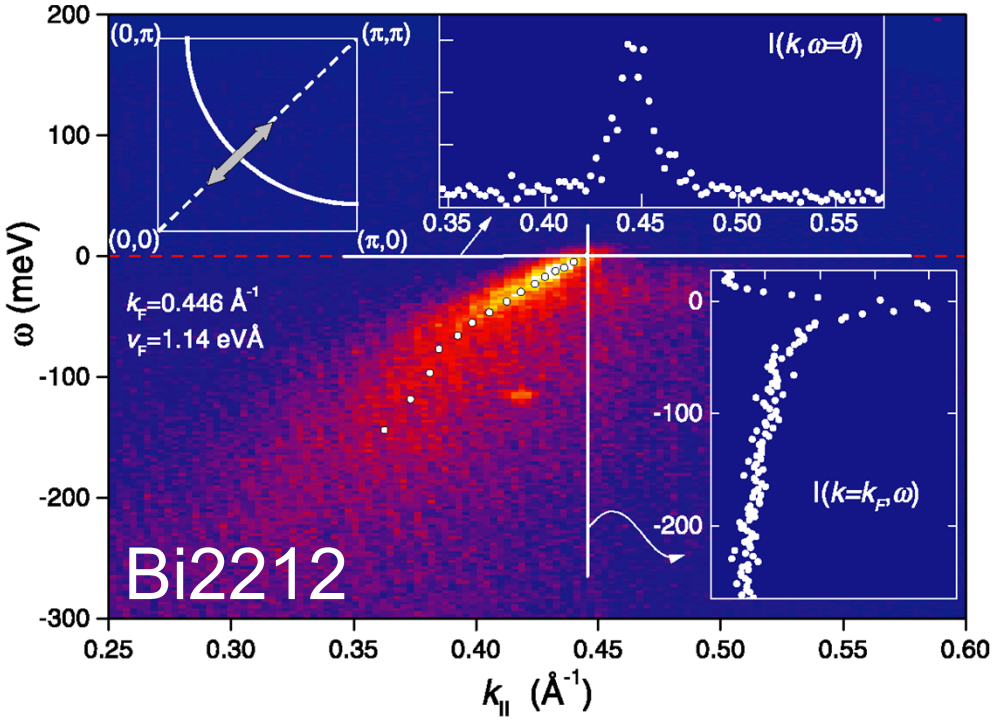

Mechanism for High-T_C { **Magnetic fluctuations ?**
Electron-phonon coupling ?

Many-Body effects in the High-T_C Cuprates

Lanzara *et al.*, Nature **412**, 510 (2001)

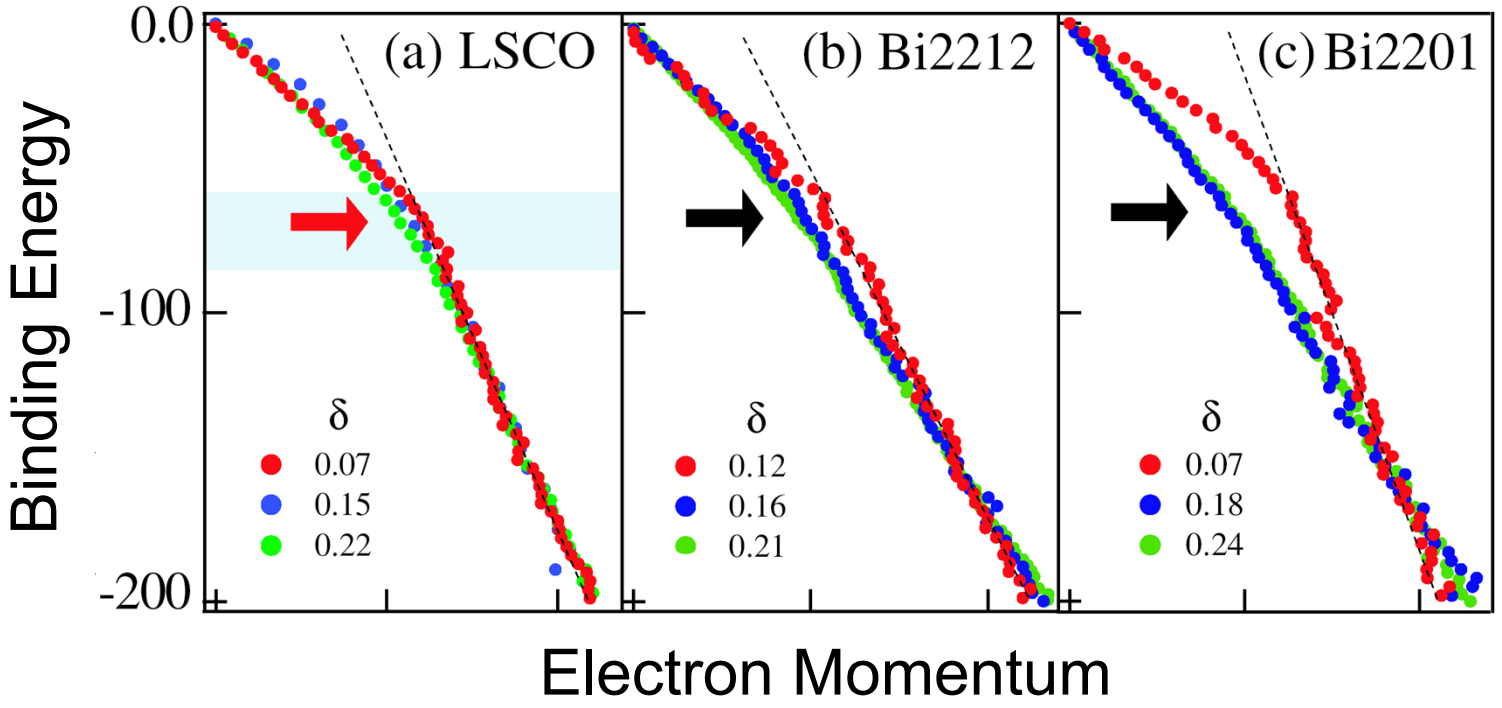

Mechanism for High-T_C { **Magnetic fluctuations ?** / **Electron-phonon coupling ?**

Many-Body effects in the High-T_C Cuprates

Devereaux et al., Phys. Rev. Lett. **93**, 117004 (2004)

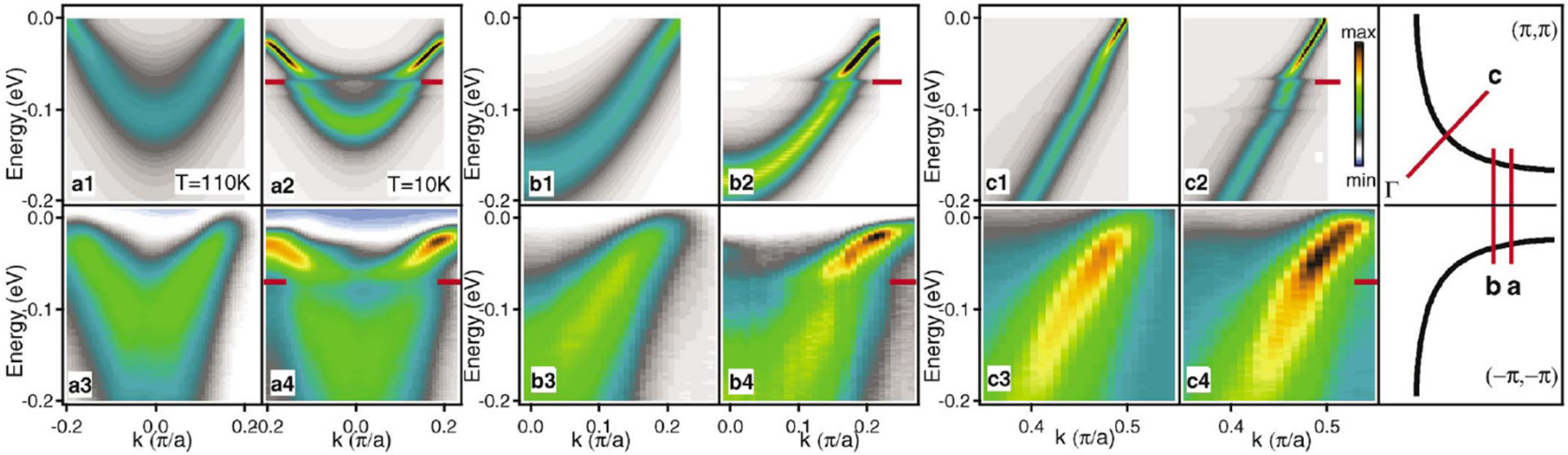

FIG. 3 (color). Image plots of the calculated spectral functions in the normal (a1,b1,c1) and superconducting (a2,b2,c2) states compared to the spectral functions in the normal (a3,b3,c3) and superconducting (a4,b4,c4) states measured in $Bi_2Sr_2Ca_{0.92}Y_{0.08}Cu_2O_{8+\delta}$ (Bi-2212) [6] for momentum cuts *a*, *b*, *c* shown in the rightmost panel and in Fig. 2. The same color scale is used for the normal or superconducting pairs within each cut, but the scaling for the data and the calculation are separate. The red markers indicate 70 meV in the superconducting state.

Mechanism for High-T_C { **Magnetic fluctuations ?**
Electron-phonon coupling ?

Many-body signatures in $Bi_2Sr_2CaCu_2O_{8+\delta}$

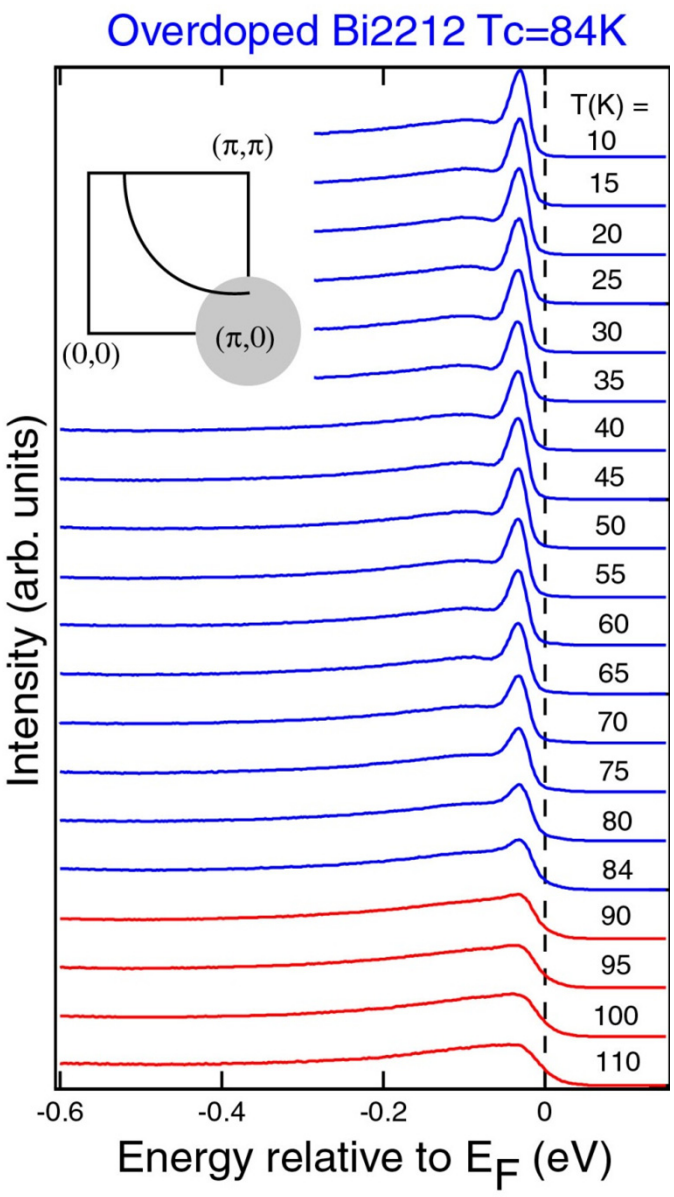

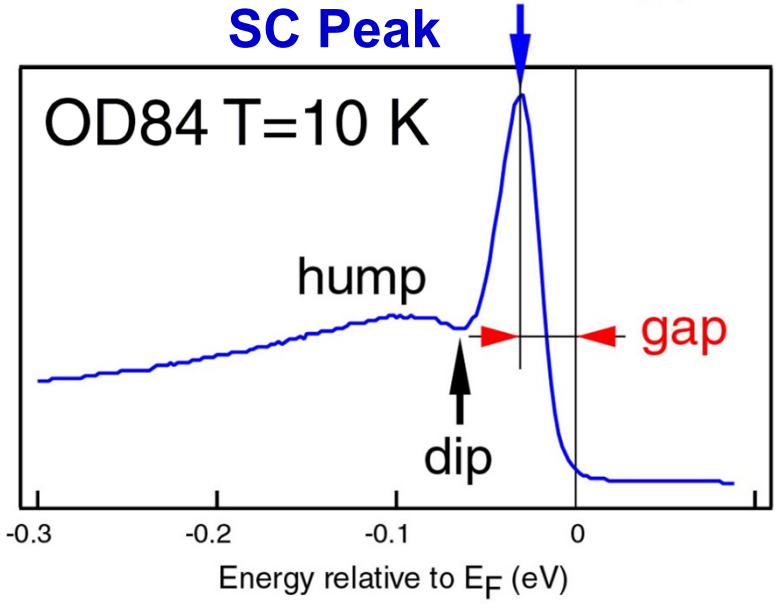

Pairing
d-wave SC Gap

Phase coherence
Coherent QP weight

Feng *et al.*, Science **289**, 277 (2000)

Many-body signatures in $Bi_2Sr_2CaCu_2O_{8+\delta}$

Electron-boson coupling?
With a (π,π) collective mode?

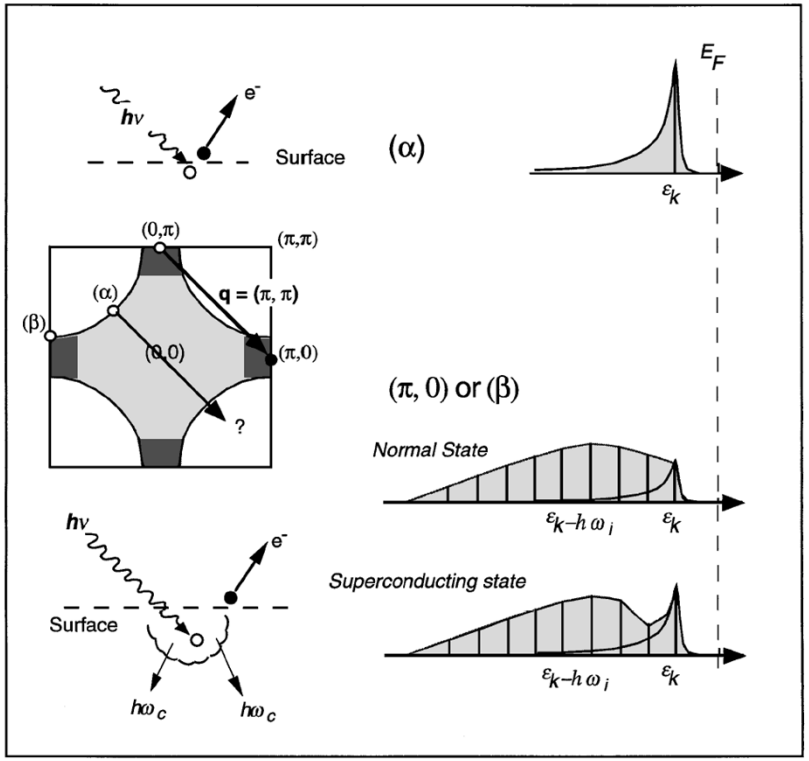

Shen and Schrieffer, Phys. Rev. Lett. **78**, 1771 (1997).

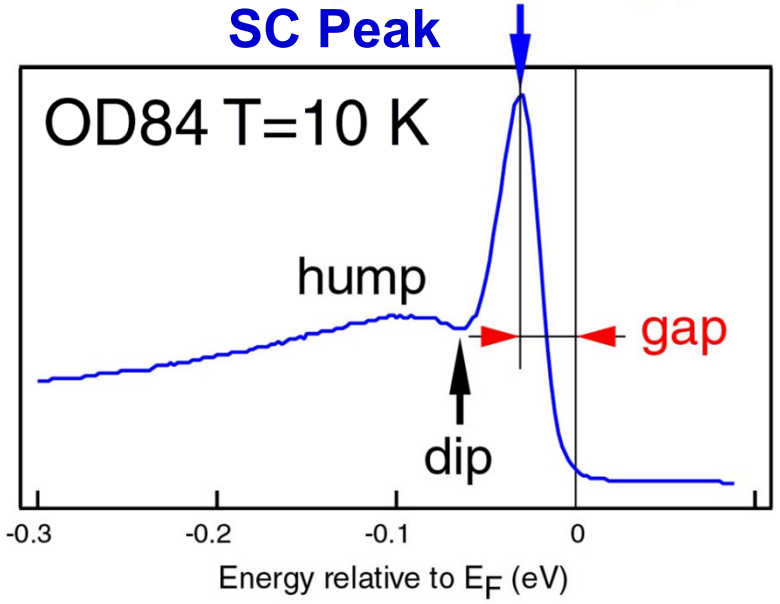

Pairing
d-wave SC Gap

Phase coherence
Coherent QP weight

Feng *et al.*, Science **289**, 277 (2000)

Renormalization of Polaronic Quasiparticles

$$\mathcal{H} = \sum_k \varepsilon_k^b c_k^\dagger c_k + \Omega \sum_Q b_Q^\dagger b_Q + \frac{g}{\sqrt{N}} \sum_{k,Q} c_{k-Q}^\dagger c_k (b_Q^\dagger + b_{-Q})$$

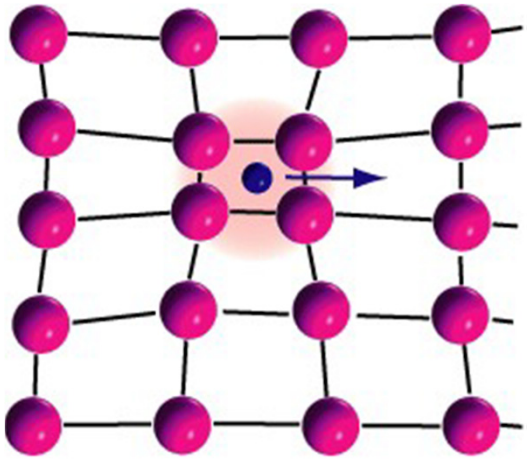

$$A(\mathbf{k},\omega) = Z_{\mathbf{k}} \frac{\Gamma_{\mathbf{k}}/\pi}{(\omega - \varepsilon_{\mathbf{k}})^2 + \Gamma_{\mathbf{k}}^2} + A_{inc}$$

$$m^* > m \qquad |\varepsilon_{\mathbf{k}}| < |\epsilon_{\mathbf{k}}|$$

$$\tau_{\mathbf{k}} = 1/\Gamma_{\mathbf{k}}$$

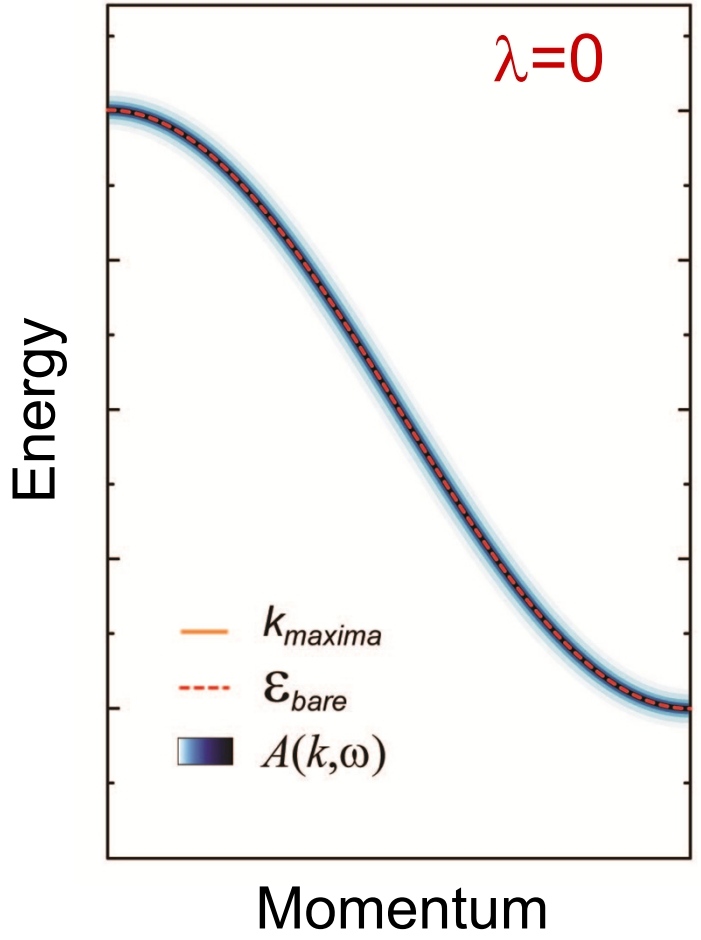

Veenstra, Goodvin, Berciu, Damascelli, PRB **82**, 012504 (2010)

Renormalization of Polaronic Quasiparticles

$$\mathcal{H} = \sum_k \varepsilon_k^b c_k^\dagger c_k + \Omega \sum_Q b_Q^\dagger b_Q + \frac{g}{\sqrt{N}} \sum_{k,Q} c_{k-Q}^\dagger c_k (b_Q^\dagger + b_{-Q})$$

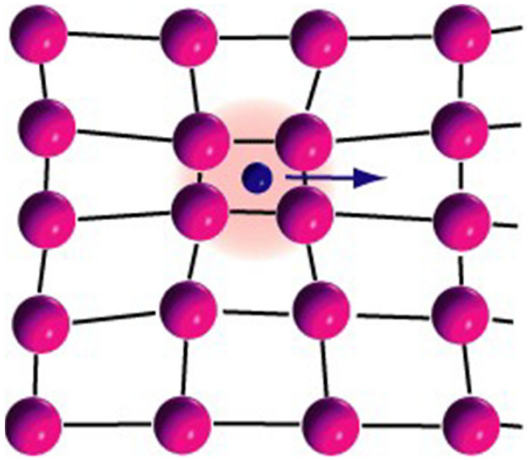

$$A(\mathbf{k},\omega) = Z_\mathbf{k} \frac{\Gamma_\mathbf{k}/\pi}{(\omega - \varepsilon_\mathbf{k})^2 + \Gamma_\mathbf{k}^2} + A_{inc}$$

$$m^* > m \qquad |\varepsilon_\mathbf{k}| < |\epsilon_\mathbf{k}|$$

$$\tau_\mathbf{k} = 1/\Gamma_\mathbf{k}$$

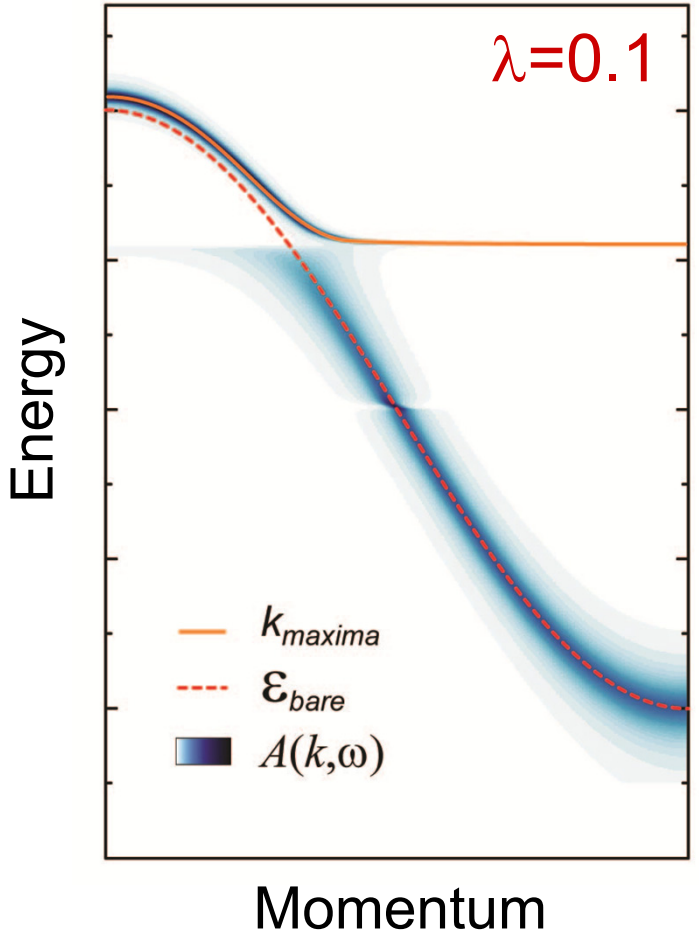

Veenstra, Goodvin, Berciu, Damascelli, PRB **82**, 012504 (2010)

Renormalization of Polaronic Quasiparticles

$$\mathcal{H} = \sum_k \varepsilon_k^b c_k^\dagger c_k + \Omega \sum_Q b_Q^\dagger b_Q + \frac{g}{\sqrt{N}} \sum_{k,Q} c_{k-Q}^\dagger c_k (b_Q^\dagger + b_{-Q})$$

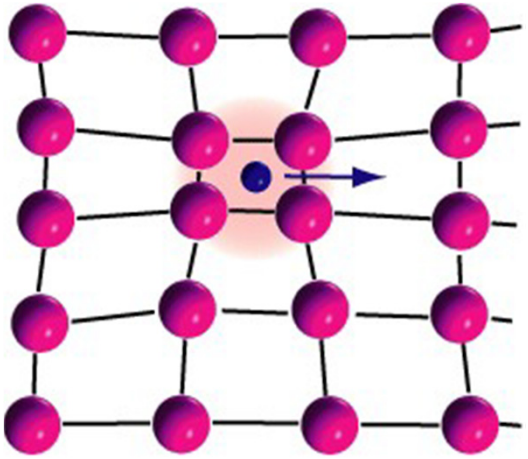

$$A(\mathbf{k},\omega) = Z_\mathbf{k} \frac{\Gamma_\mathbf{k}/\pi}{(\omega - \varepsilon_\mathbf{k})^2 + \Gamma_\mathbf{k}^2} + A_{inc}$$

$$m^* > m \qquad |\varepsilon_\mathbf{k}| < |\epsilon_\mathbf{k}|$$

$$\tau_\mathbf{k} = 1/\Gamma_\mathbf{k}$$

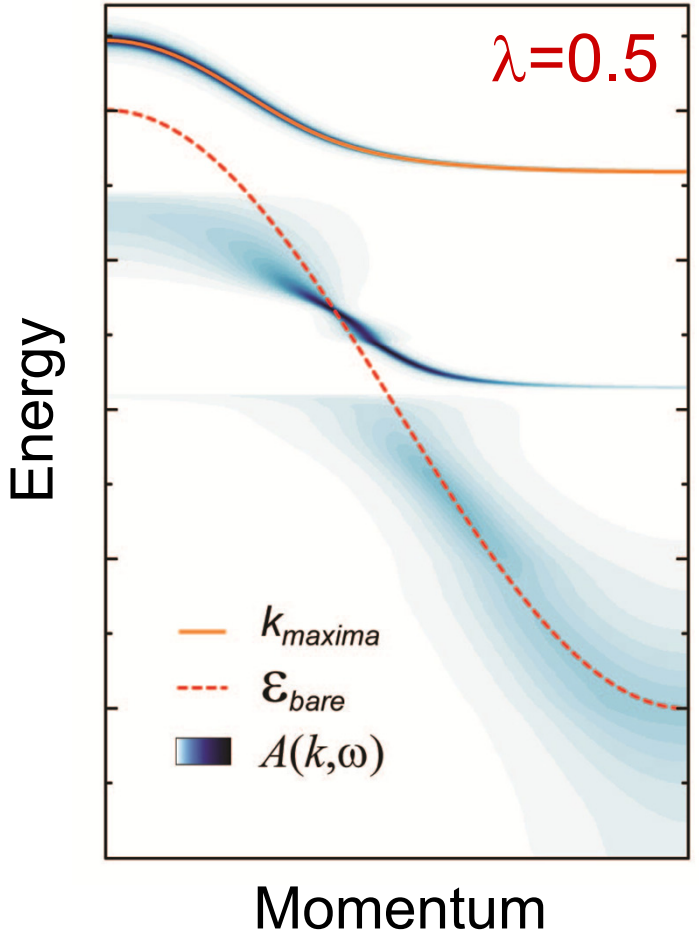

Veenstra, Goodvin, Berciu, Damascelli, PRB **82**, 012504 (2010)

Renormalization of Polaronic Quasiparticles

$$\mathcal{H} = \sum_k \varepsilon_k^b c_k^\dagger c_k + \Omega \sum_Q b_Q^\dagger b_Q + \frac{g}{\sqrt{N}} \sum_{k,Q} c_{k-Q}^\dagger c_k (b_Q^\dagger + b_{-Q})$$

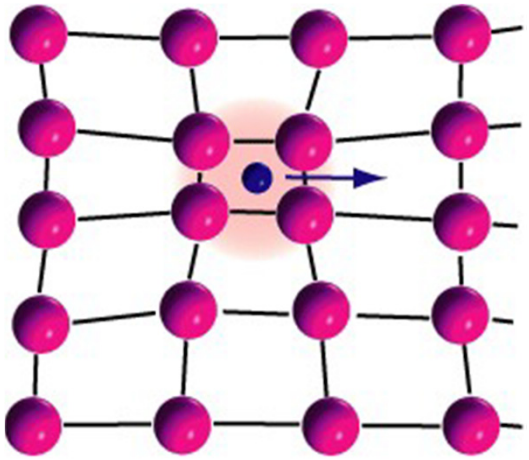

$$A(\mathbf{k},\omega) = Z_\mathbf{k} \frac{\Gamma_\mathbf{k}/\pi}{(\omega - \varepsilon_\mathbf{k})^2 + \Gamma_\mathbf{k}^2} + A_{inc}$$

$$m^* > m \qquad |\varepsilon_\mathbf{k}| < |\epsilon_\mathbf{k}|$$

$$\tau_\mathbf{k} = 1/\Gamma_\mathbf{k}$$

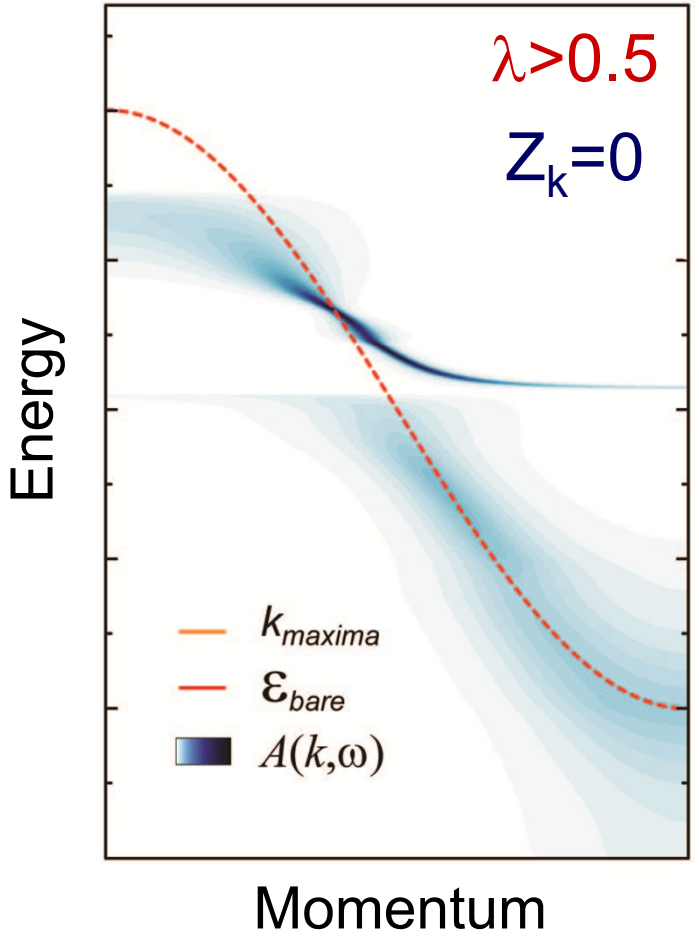

Veenstra, Goodvin, Berciu, Damascelli, PRB **82**, 012504 (2010)

$$\mathcal{H} = \sum_k \varepsilon_k^b c_k^\dagger c_k + \Omega \sum_Q b_Q^\dagger b_Q + \frac{g}{\sqrt{N}} \sum_{k,Q} c_{k-Q}^\dagger c_k (b_Q^\dagger + b_{-Q})$$

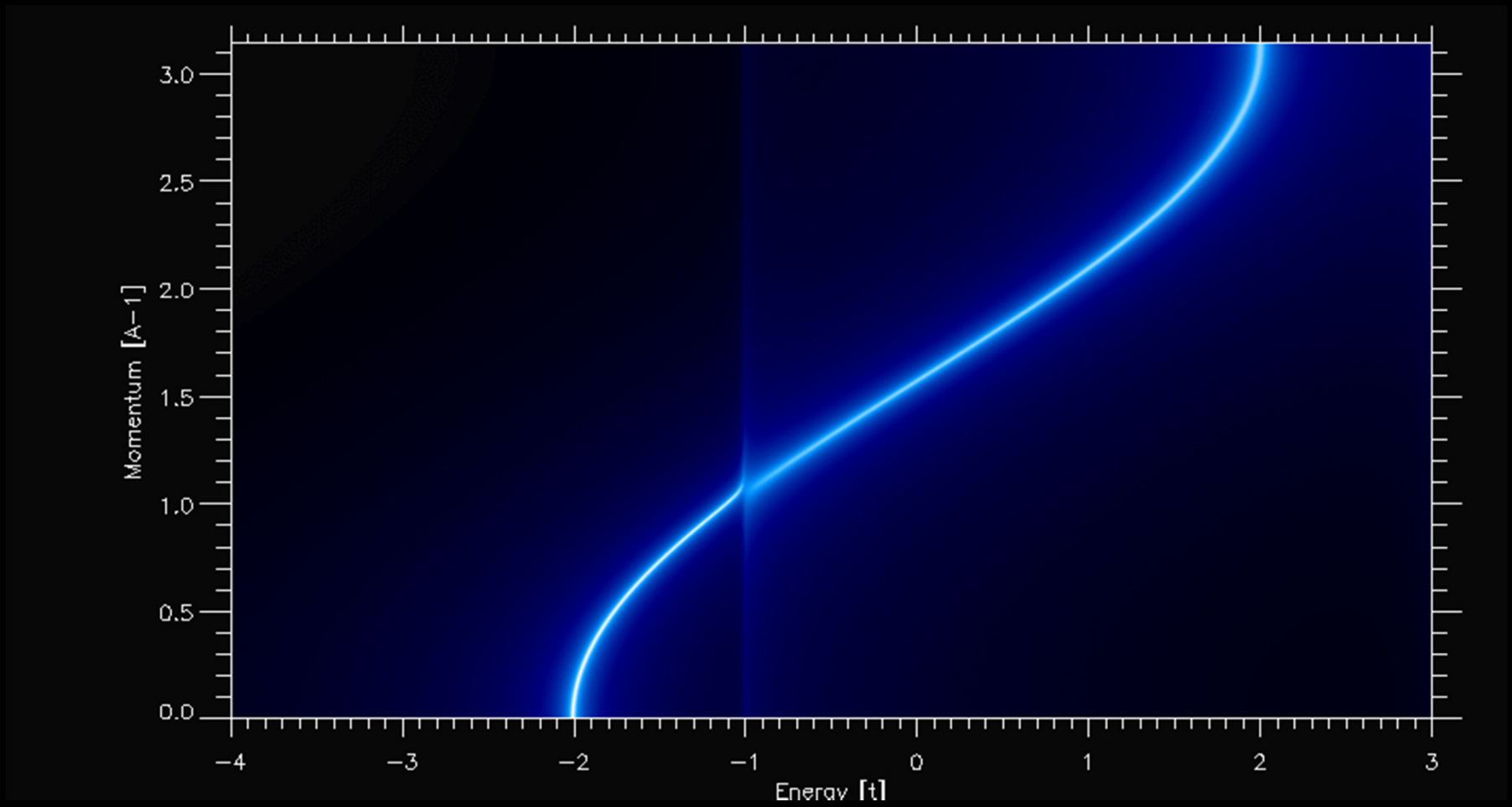

Veenstra, Goodvin, Berciu, Damascelli, PRB **82**, 012504 (2010)

Renormalization of Polaronic Quasiparticles

$$\mathcal{H} = \sum_k \varepsilon_k^b c_k^\dagger c_k + \Omega \sum_Q b_Q^\dagger b_Q + \frac{g}{\sqrt{N}} \sum_{k,Q} c_{k-Q}^\dagger c_k (b_Q^\dagger + b_{-Q})$$

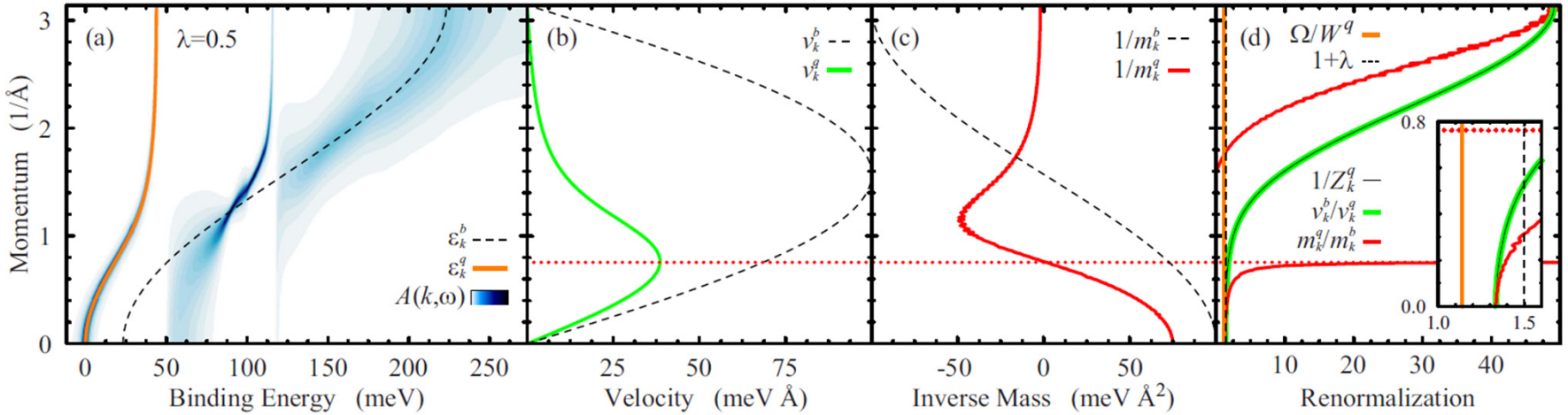

FIG. 1. (Color online) (a) $A(k,\omega)$ calculated within MA$^{(1)}$ for $\Omega=50$ meV and $\lambda=0.5$; the quasiparticle dispersion ε_k^q and the bare band ε_k^b are also shown. (b) Quasiparticle and bare-band velocities, v_k^q and v_k^b, and (c) corresponding inverse masses, $1/m_k^q$ and $1/m_k^b$, according to the definitions $v_k=\partial\varepsilon_k/\partial k$ and $1/m_k=\partial^2\varepsilon_k/\partial k^2$. (d) Momentum-dependent quasiparticle renormalization as obtained from v_k^b/v_k^q, m_k^q/m_k^b, and the inverse quasiparticle coherence $1/Z_k^q$, where $Z_k^q=\int^q A(k,\omega)d\omega$ is the quasiparticle-only integrated spectral weight; in the inset, these quantities are compared near $k=0$ to the renormalization factors Ω/W^q and $(1+\lambda)$, obtained from quasiparticle bandwidth W^q and dimensionless coupling $\lambda=g^2/2t\Omega$ in our model.

Far from the Migdal limit ($\Omega << E_F$ for a parabolic band), the effective coupling parameters deduced from the renormalization of quasiparticle mass, velocity, and spectral weight are momentum dependent and, in general, distinct from the true microscopic coupling; the latter is thus not readily accessible in the quasiparticle dispersion revealed by ARPES through the mass enhancement factor $1/(1+\lambda)$.

Veenstra, Goodvin, Berciu, Damascelli, PRB **82**, 012504 (2010)

Renormalization of Polaronic Quasiparticles

$$\mathcal{H} = \sum_k \varepsilon_k^b c_k^\dagger c_k + \Omega \sum_Q b_Q^\dagger b_Q + \frac{g}{\sqrt{N}} \sum_{k,Q} c_{k-Q}^\dagger c_k (b_Q^\dagger + b_{-Q})$$

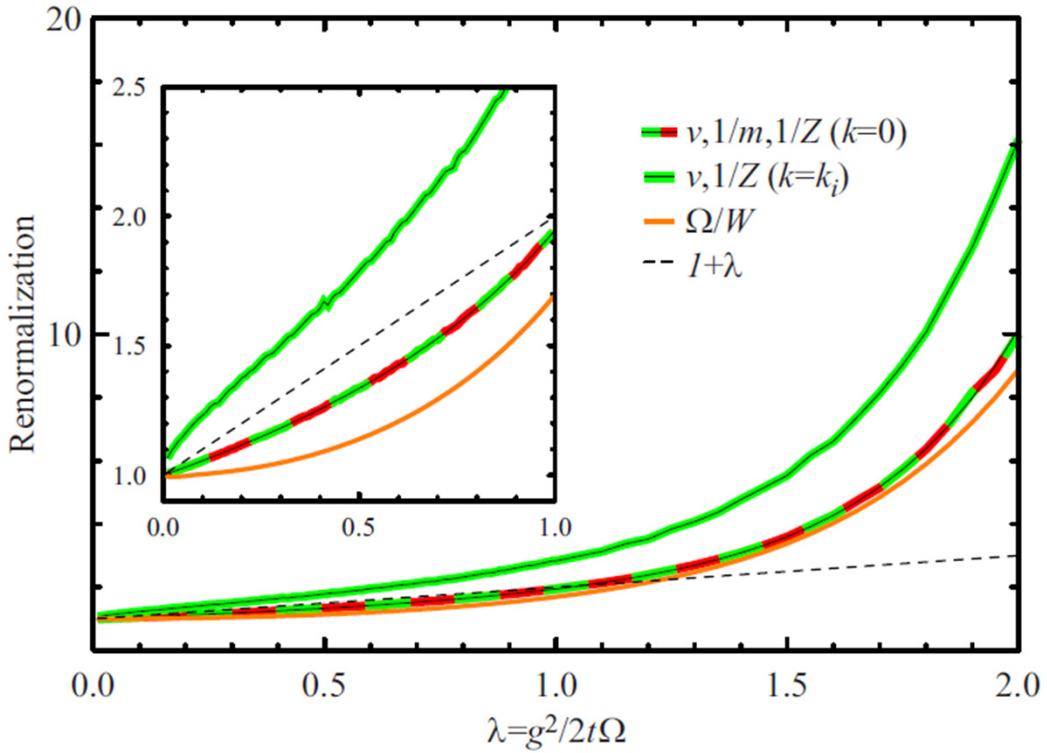

Based on the renormalization parameters and the mass enhancement factor 1/(1+λ), one can overestimate the true electron phonon microscopic coupling even by a factor of 10.

Veenstra, Goodvin, Berciu, Damascelli, PRB **82**, 012504 (2010)

Renormalization of Polaronic Quasiparticles

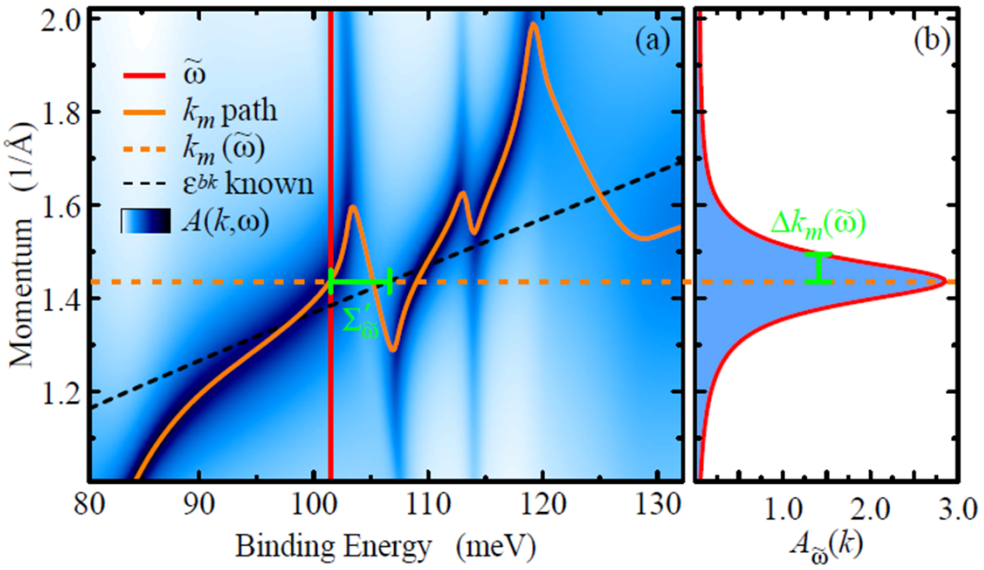

Instead of extracting directly λ, one can estimate real and imaginary part of the self energy through bare -band fitting and Kramers-Kronig analysis.

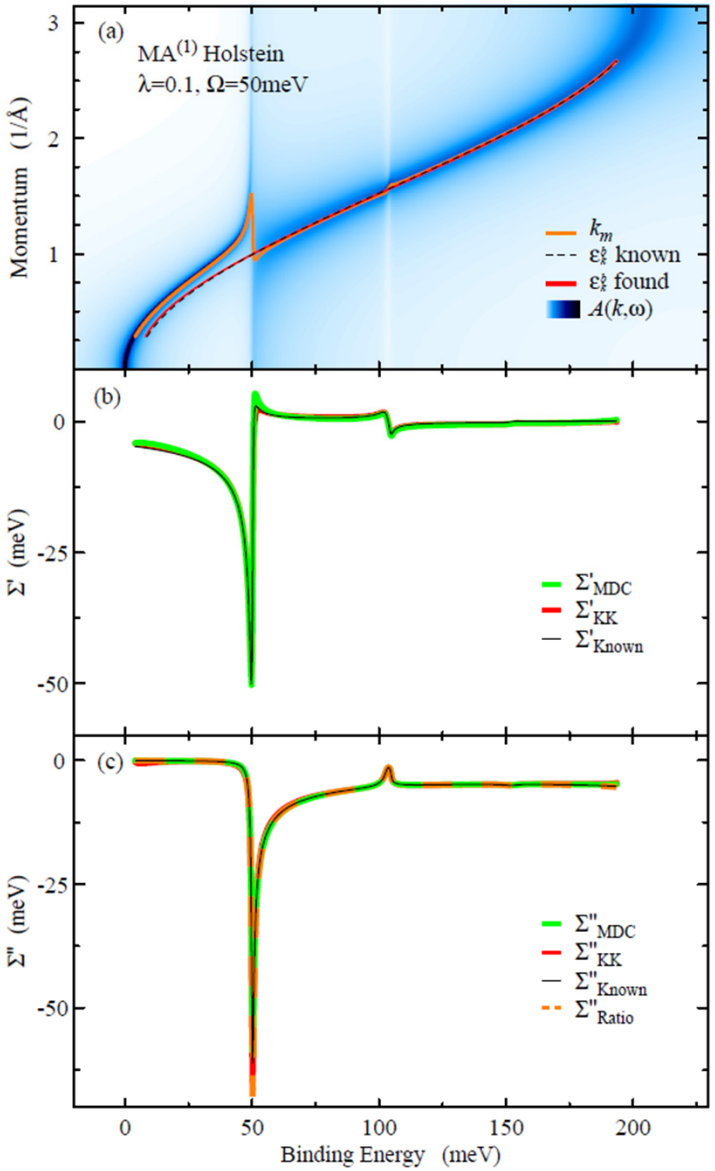

Veenstra, Goodvin, Berciu, Damascelli, PRB **82**, 012504 (2010)

Outline Part II

HTSC: The fate of quasiparticle strength

CUSO Lecture – Lausanne 02/2011

From Fermi Liquid to Mott Insulator

Correlations suppress Z_k

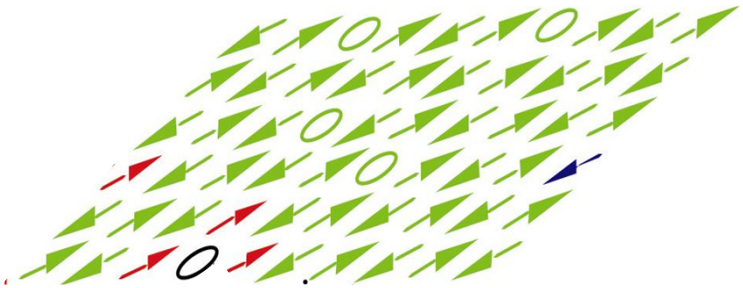

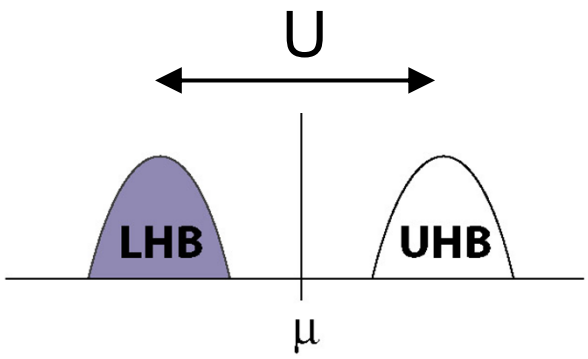

$$Z \simeq 2p/(p+1)$$

Sawatzky, Anderson, Randeria,
Paramekanti, Yang, Rice, et al.

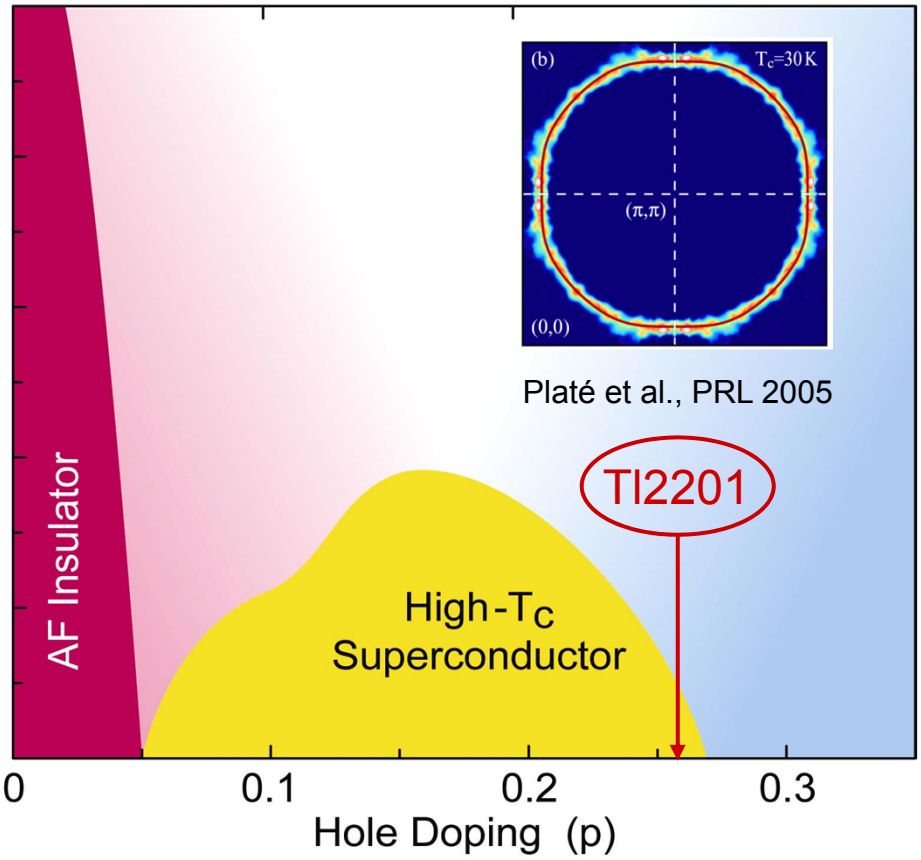

Normal state properties

Fermiology across the Cuprate Phase Diagram

CCOC - x=0.12

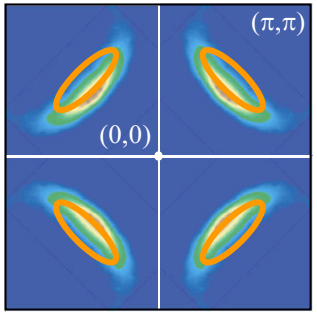

ARPES – Shen (05)

YBCO - x=0.10

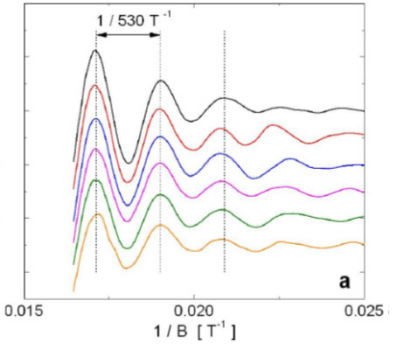

QO – Doiron-Leyraud (07)

ARPES on YBCO6.5

Overdoped Tl2201

Quantitative agreement between single-particle and transport probes

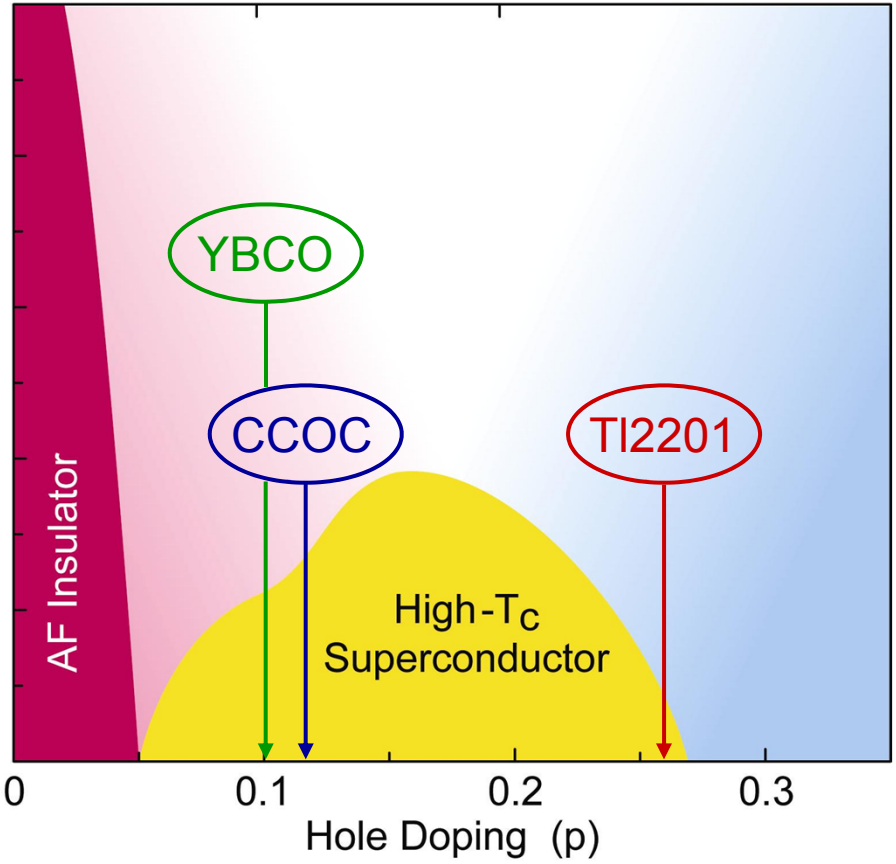

Can this be the gateway to a unified picture for underdoped cuprates?

Tl2201 - x=0.26

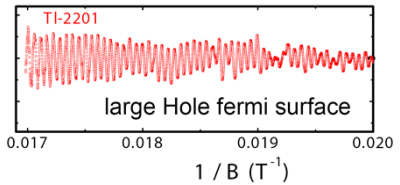

dHvA – Vignolle (08)

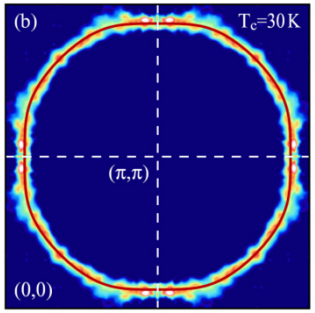

ARPES – Platé (05)

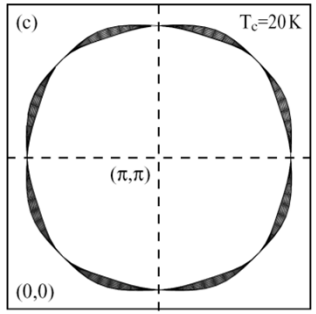

AMRO – Hussey (03)

Electronic Structure of YBCO: Hole Pockets

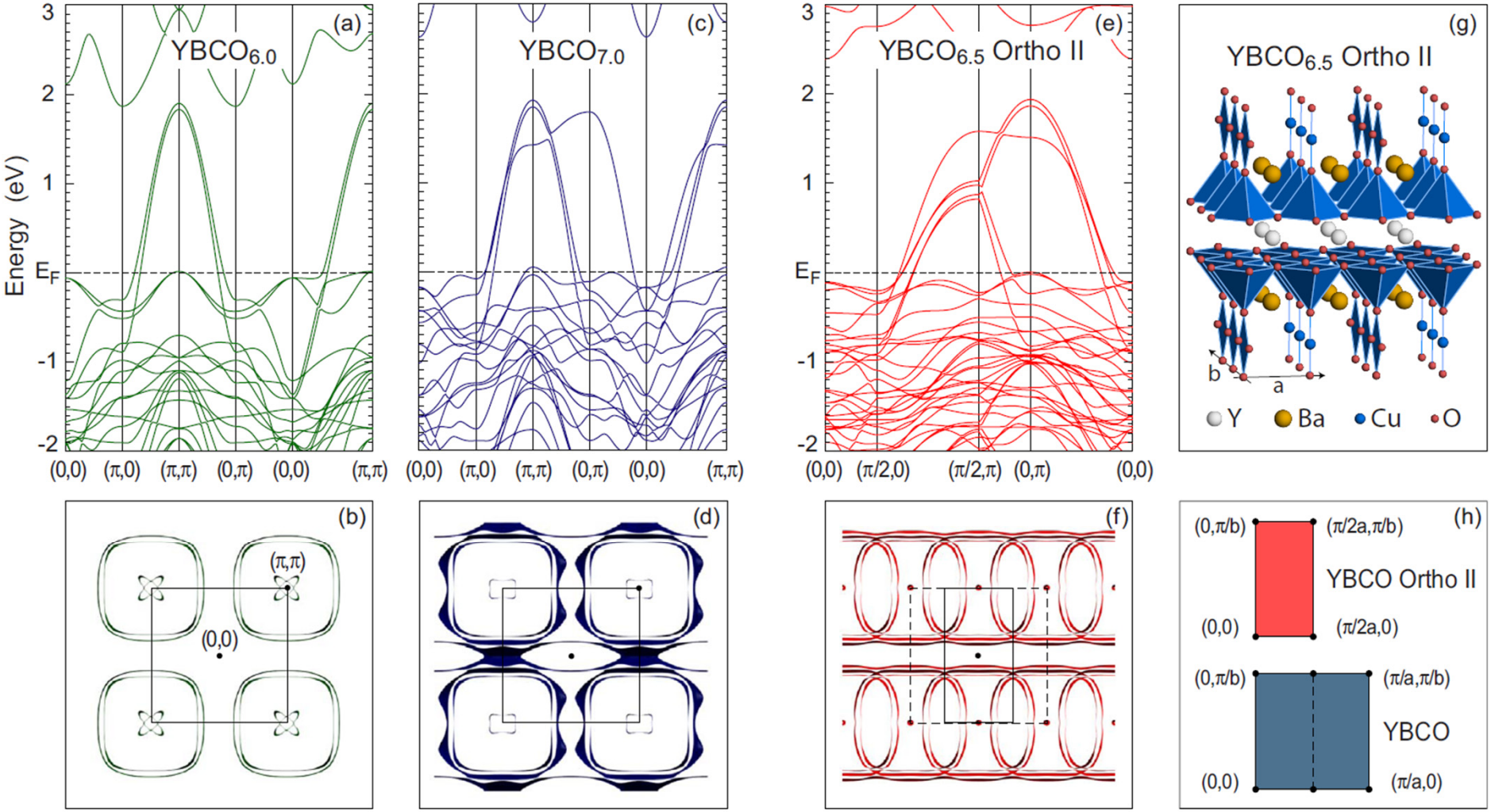

Elfimov, Sawatzky, Damascelli, PRB **77**, 060504(R) (2008)

Electronic Structure of YBCO: Hole Pockets

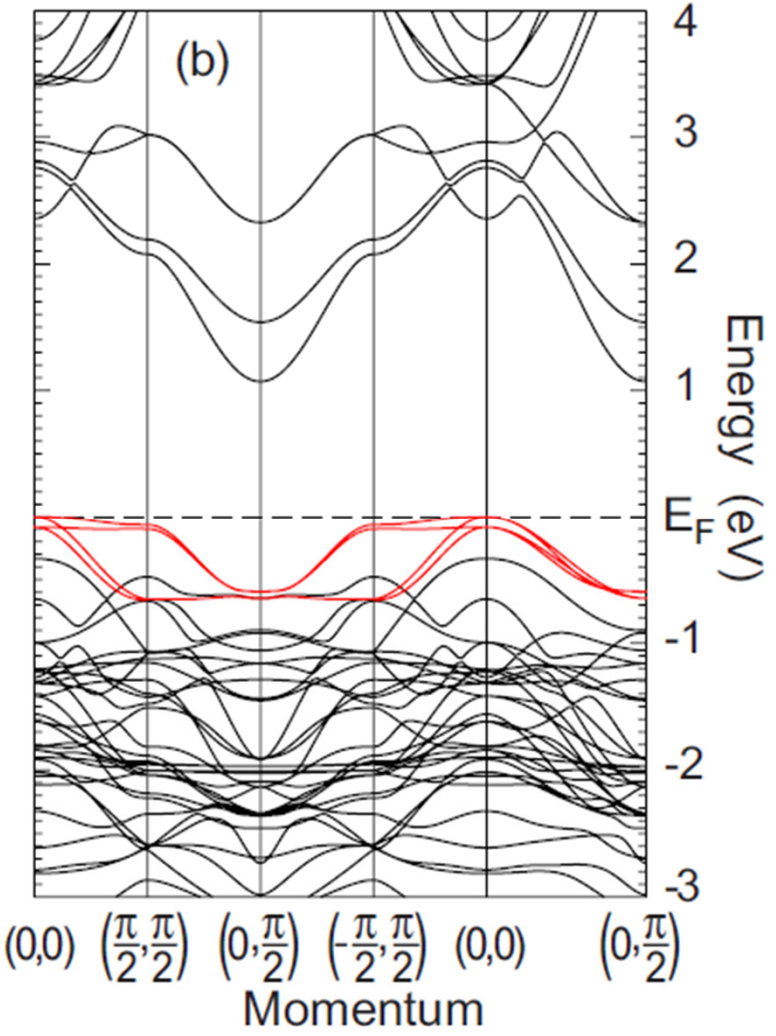

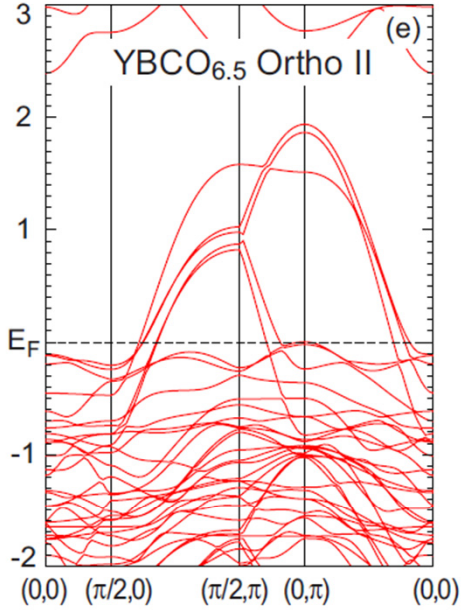

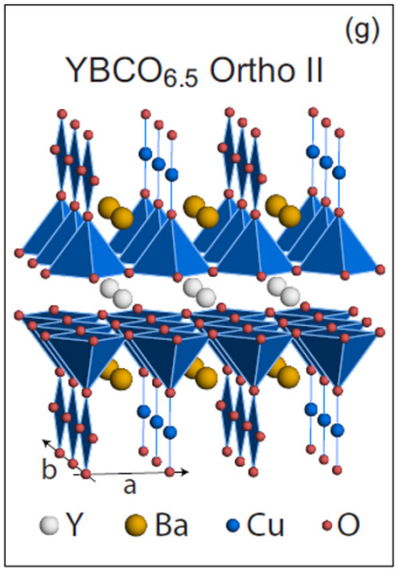

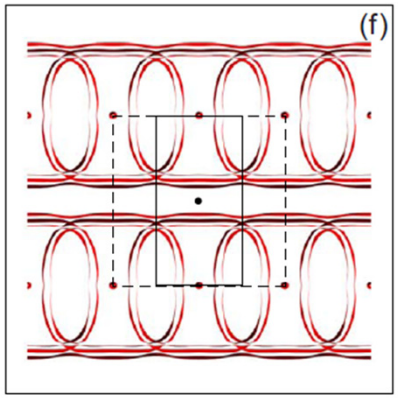

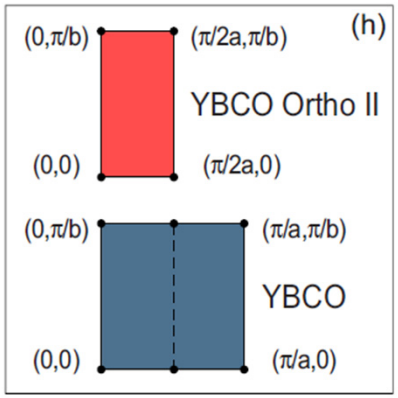

Elfimov, Sawatzky, Damascelli, PRB **77**, 060504(R) (2008)

Fermiology of Underdoped YBCO

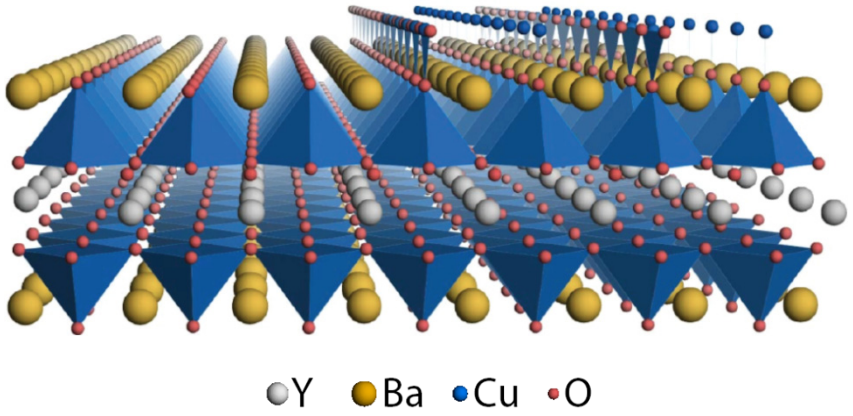

Elfimov, Sawatzky, Damascelli PRB **77**, 060504 (2008)

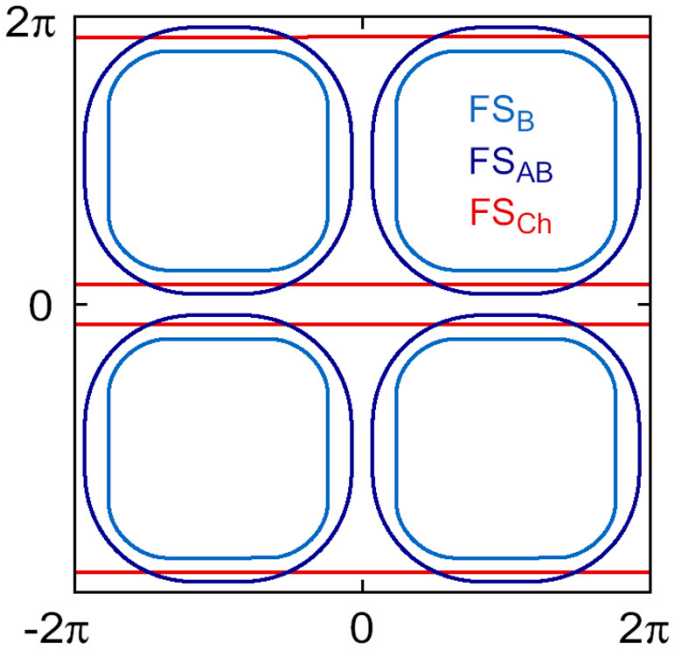

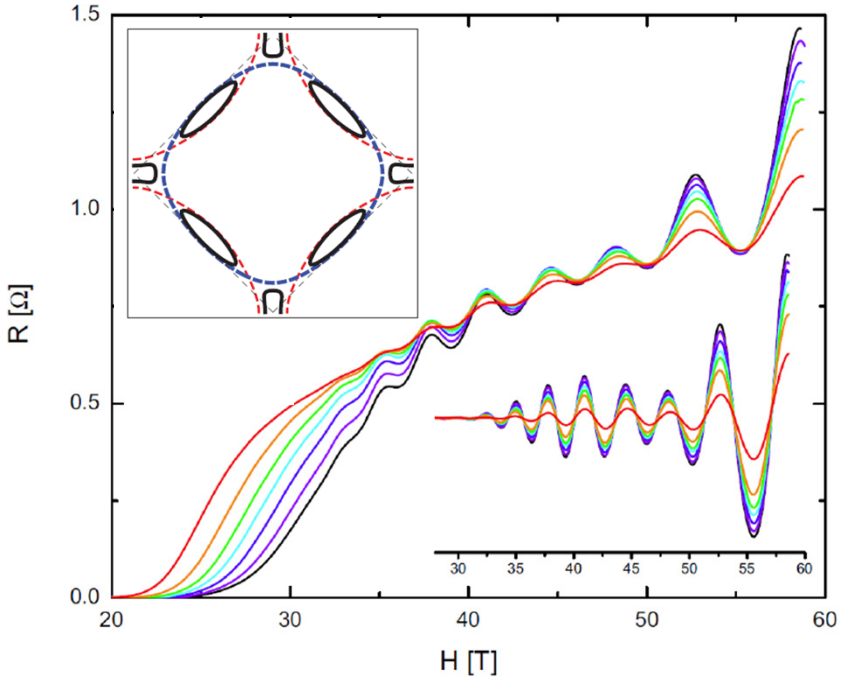

QO suggest Fermi liquid behavior in the very underdoped regime

Small pockets are also not in LDA

Competing ordering?

B.J. Ramshaw et al., Nature Physics (2010)

Ordered Phases of CuO Chain Layer in YBCO

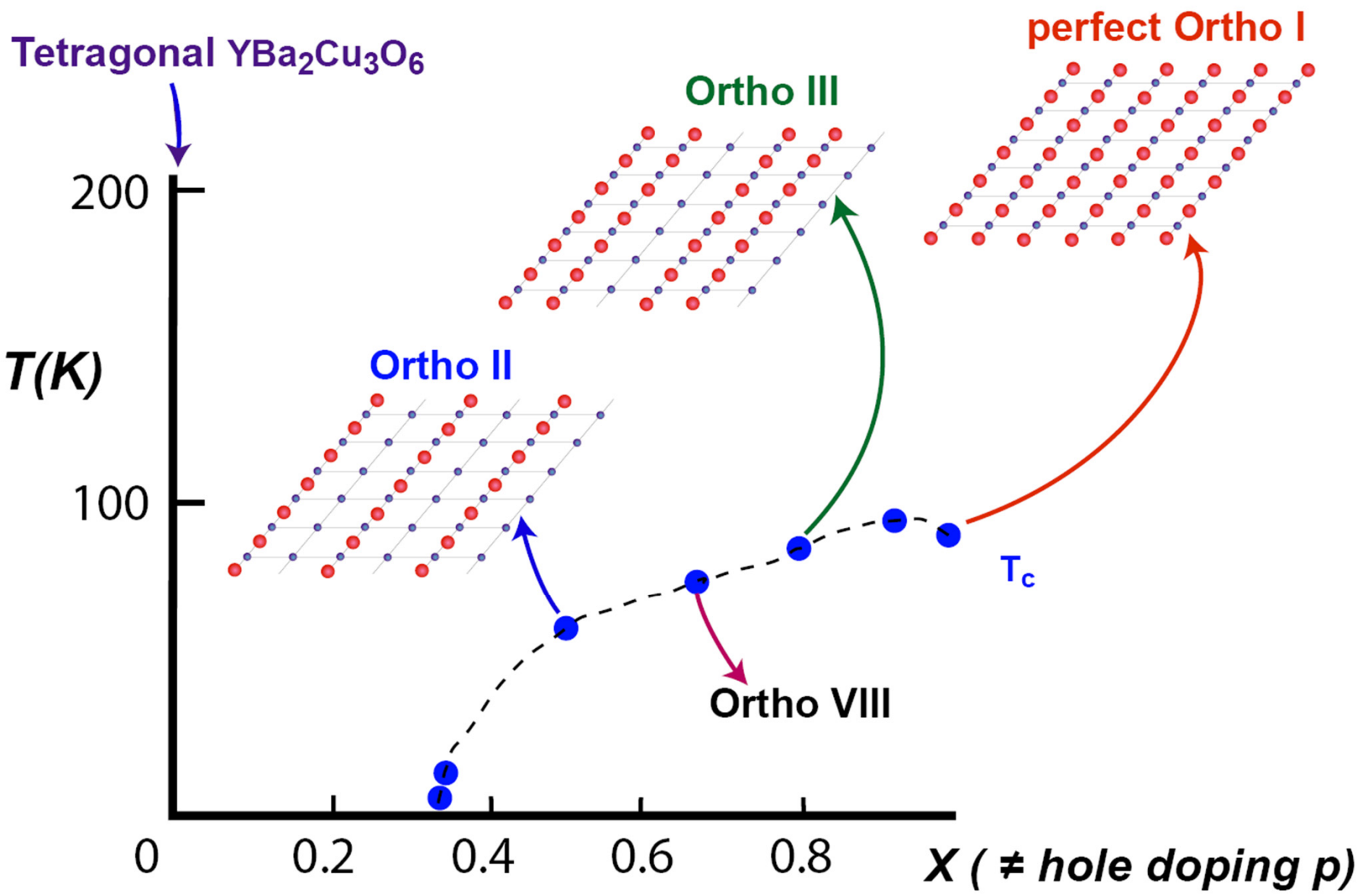

Hole Doping by CuO Chain Oxygen in YBCO

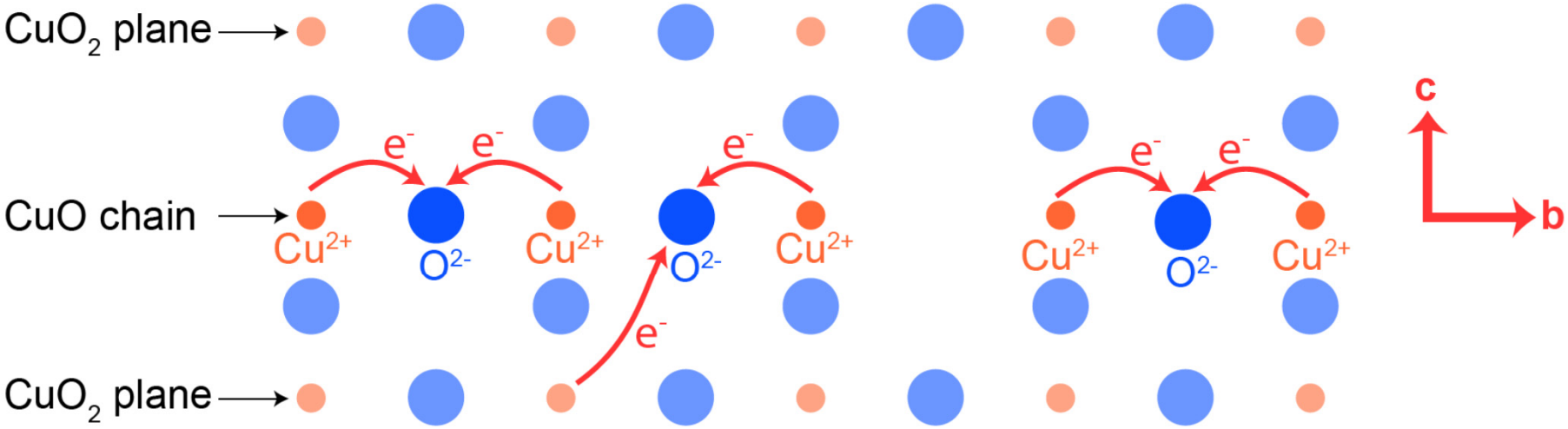

Chainlets of CuO_x are required for doping of holes on the CuO_2 planes.

Problem: **Hole doping *p* depends on the average chain length as well as the oxygen content *x*.**

Advantage: **CuO_x chain oxygen ions are mobile at room temperature and slowly form ordered superstructures.**

Advantage: **At a fixed oxygen content *x*, hole doping *p* can vary over time.**

Fermiology of YBCO by ARPES

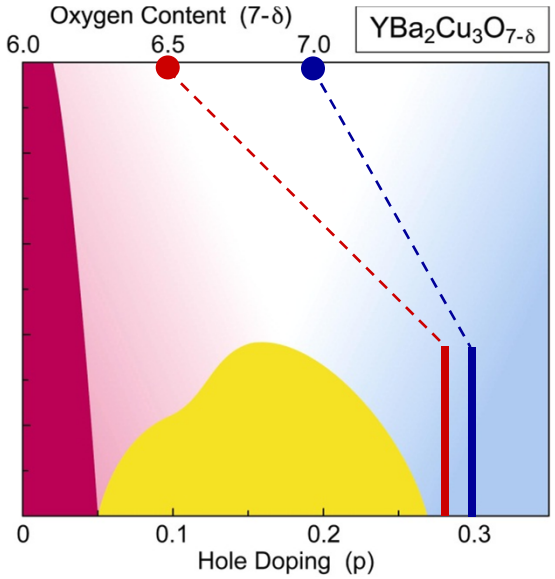

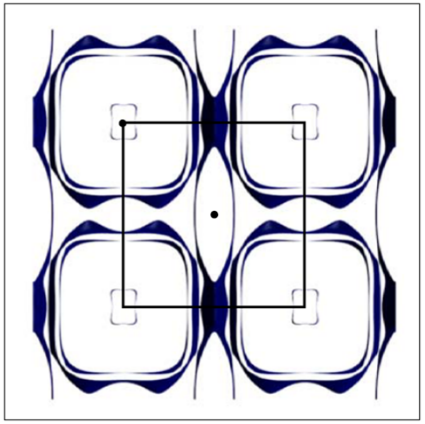

Elfimov, Sawatzky, Damascelli
PRB **77**, 060504 (2008)

Large doping almost independent of oxygen content

Fermi surface of twinned $YBa_2Cu_3O_{6.51}$

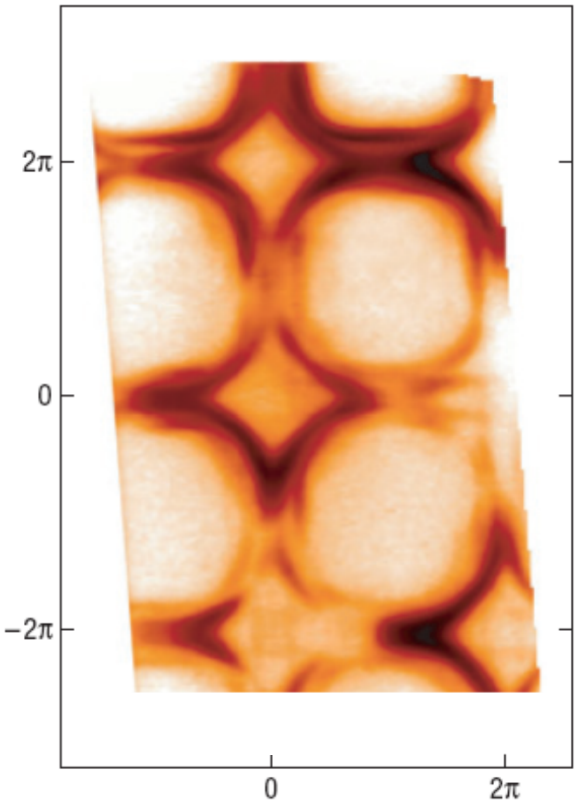

Hossain et al.
Nature Physics **4**, 527 (2008)

Fermi surface of detwinned $YBa_2Cu_3O_{6.99}$

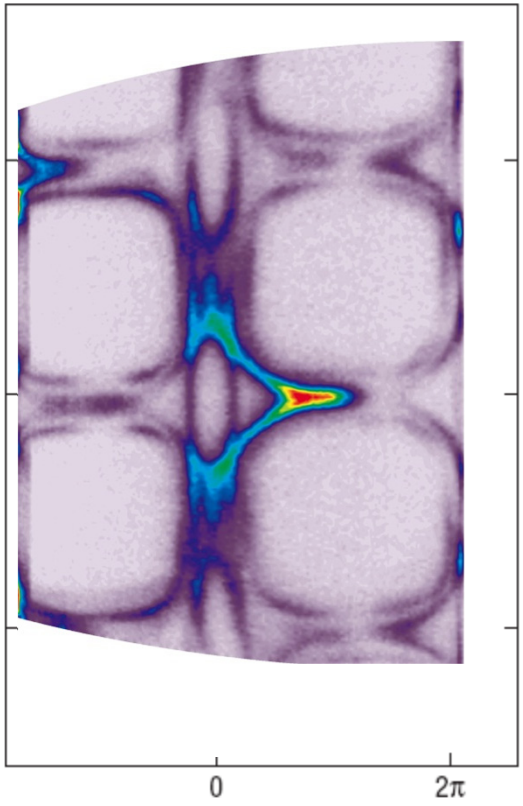

Fournier et al.
Nature Physics **6**, 905 (2010)

Whither Oxide Electronics?

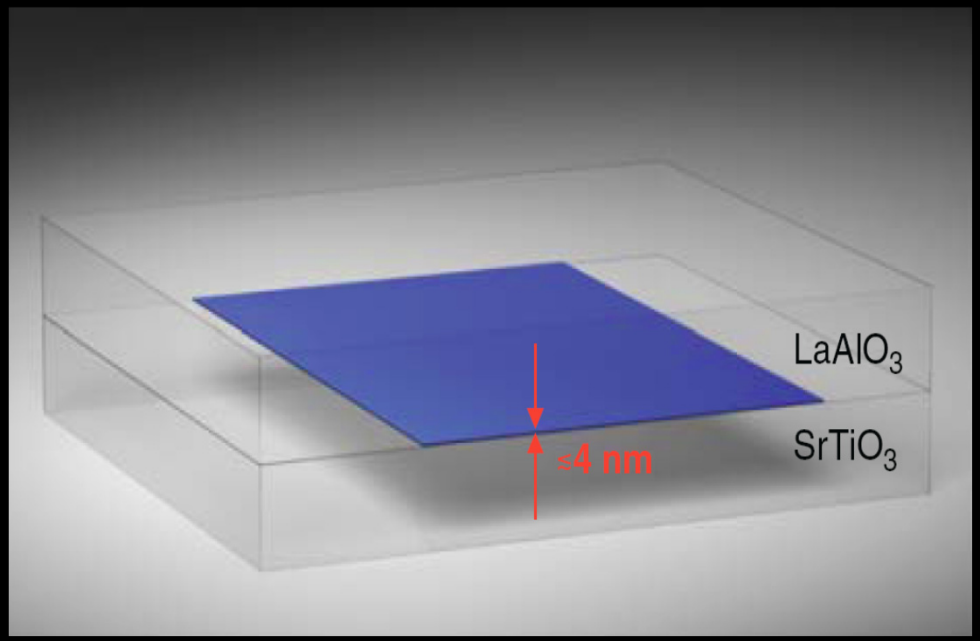

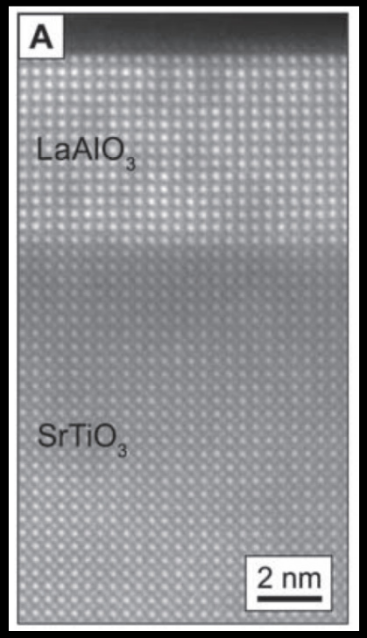

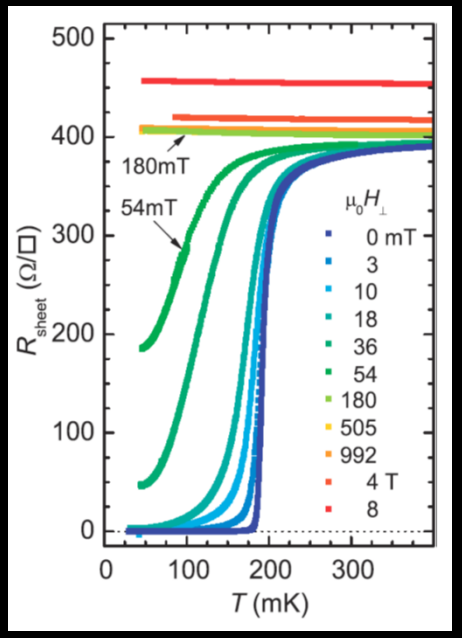

Carrier mobility 10^4 $cm^2/(Vs)$

2DEG, superconductivity, magnetism, orbital ordering, etc.

J. Mannhart, D.H.A. Blank, H.Y. Hwang, A.J. Millis, J.-M. Triscone, MRS Bulletin **33**, 1027 (2008)

Electronic Reconstruction at the Interface

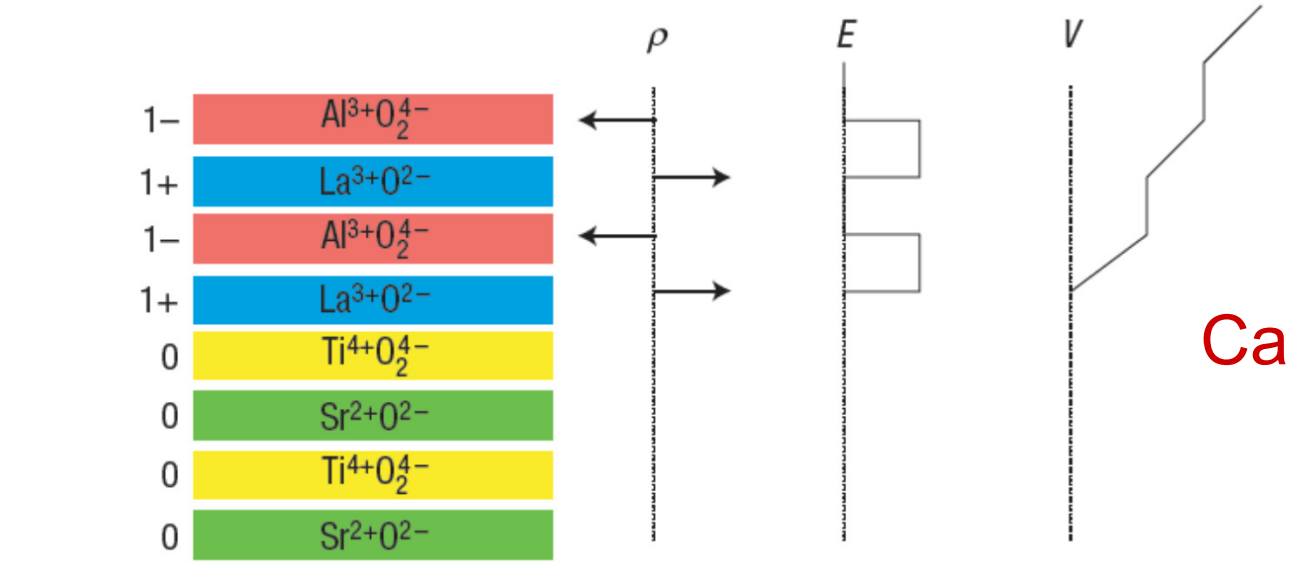

Polar Catastrophe

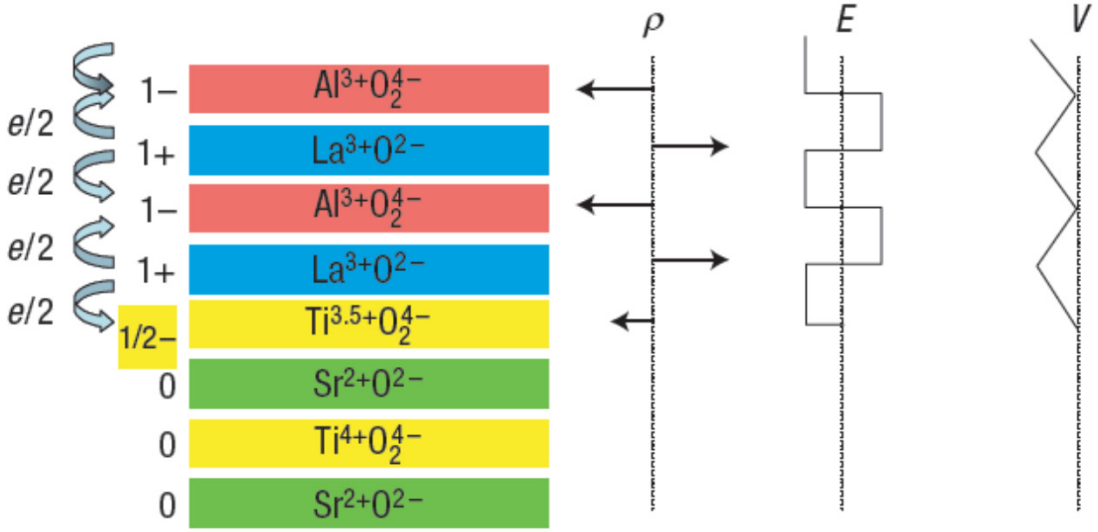

Electronic Reconstruction

Nakagawa, Hwang, Muller, Nature Materials **5**, 204 (2006)

Electronic Surface Reconstruction in $YBa_2Cu_3O_{6.0}$

Polar catastrophe

Self-doping of YBCO surface

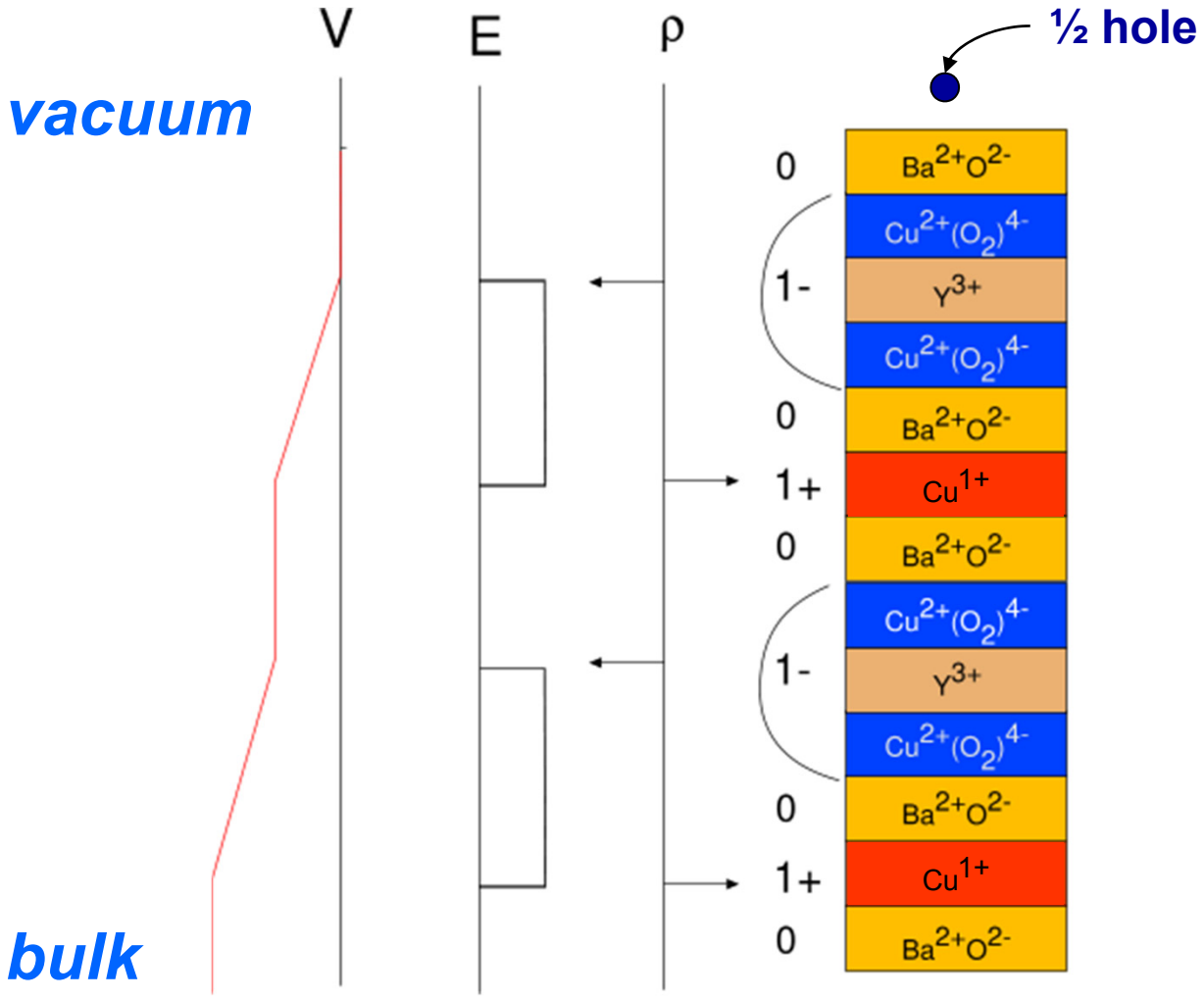

Electronic Surface Reconstruction in $YBa_2Cu_3O_{6.0}$

Polar catastrophe

Self-doping of YBCO surface

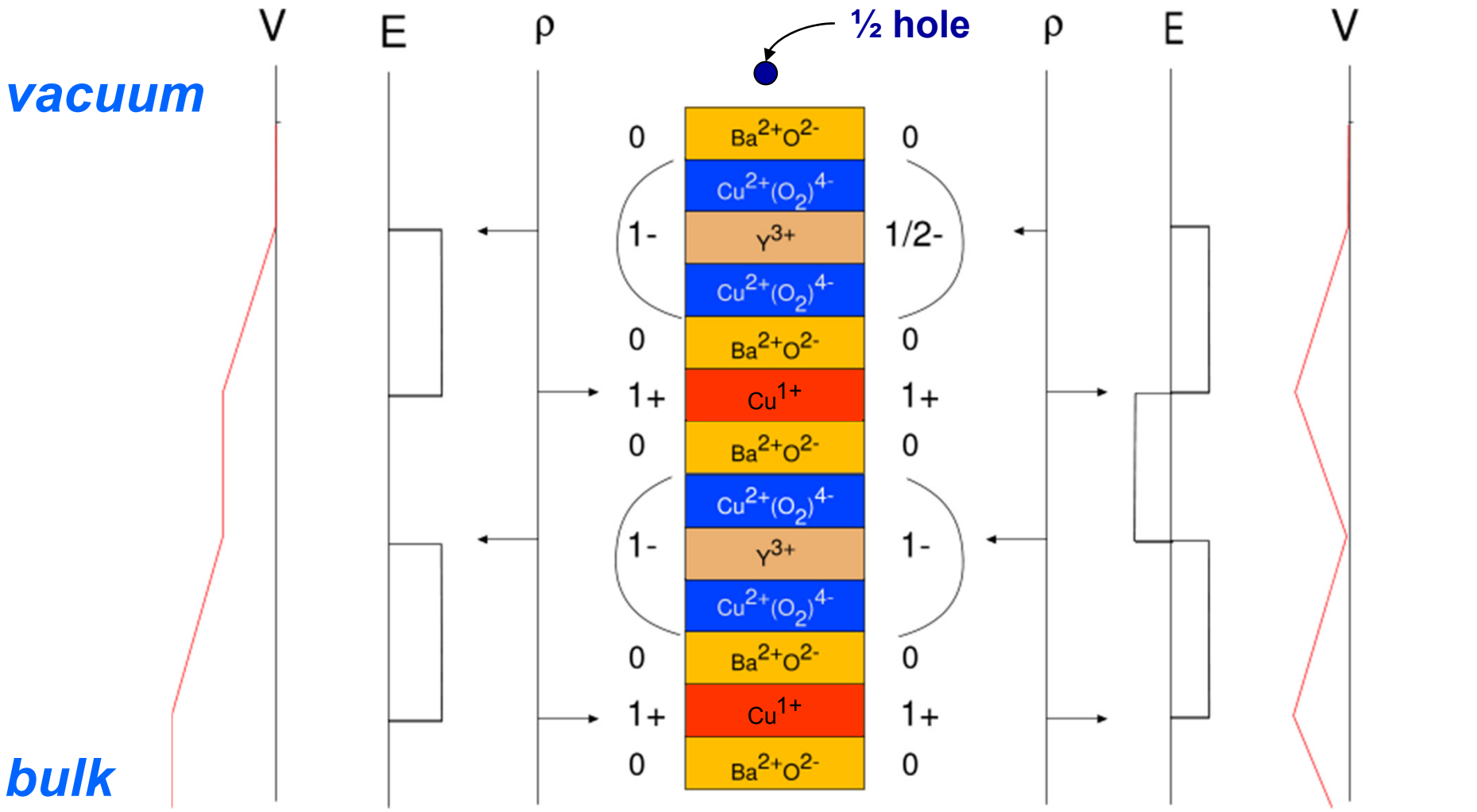

Electronic Surface Reconstruction in $YBa_2Cu_3O_{6.0}$

Self-doping of YBCO surface

Self-doping

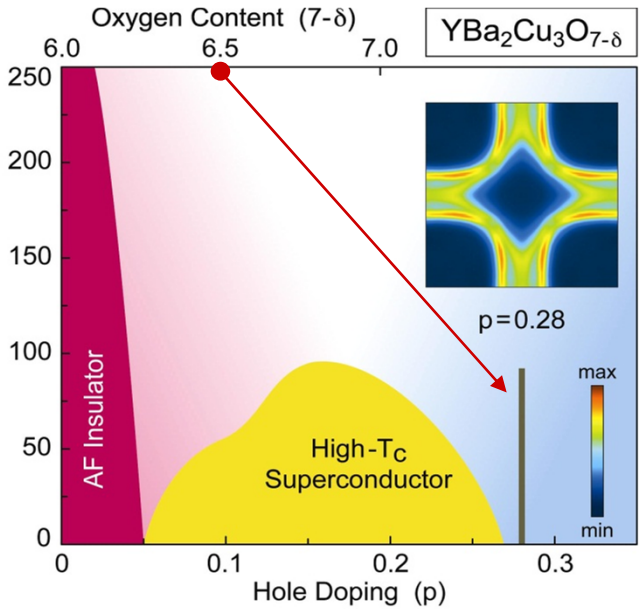

Overdoping

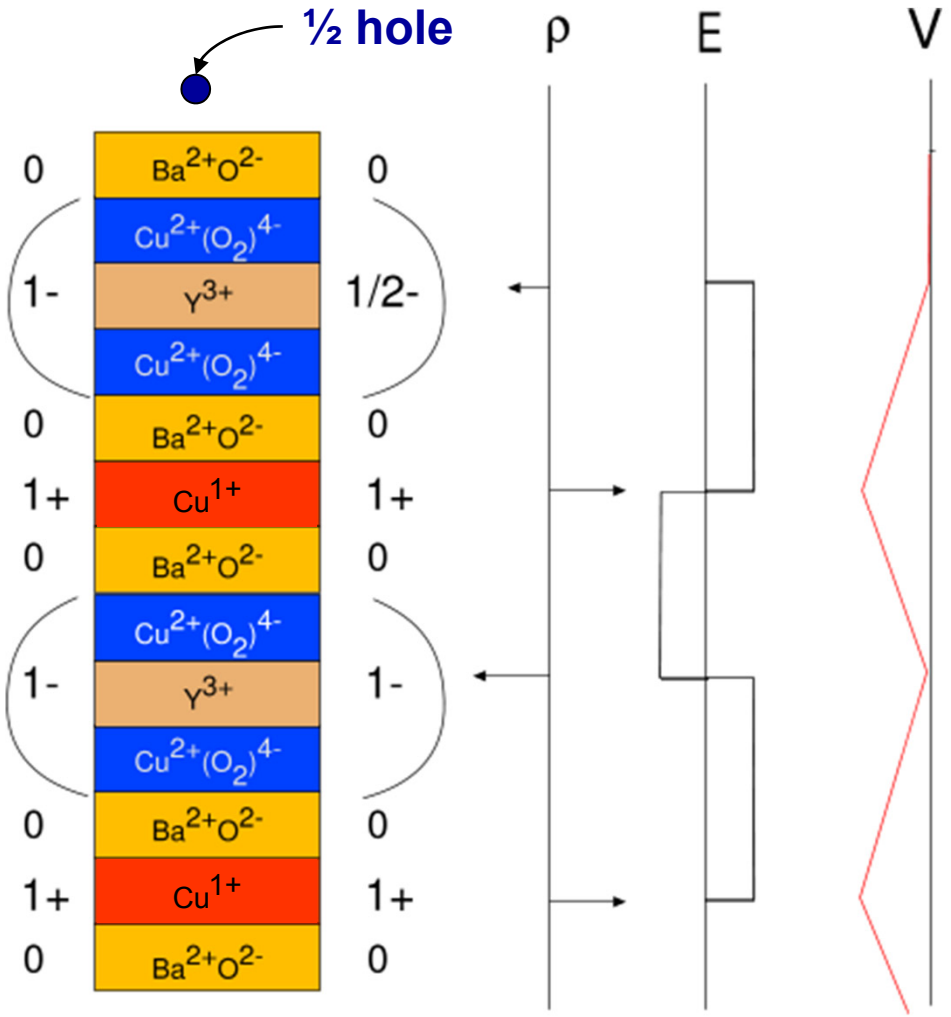

Fixing the YBCO surface self-doping by K deposition

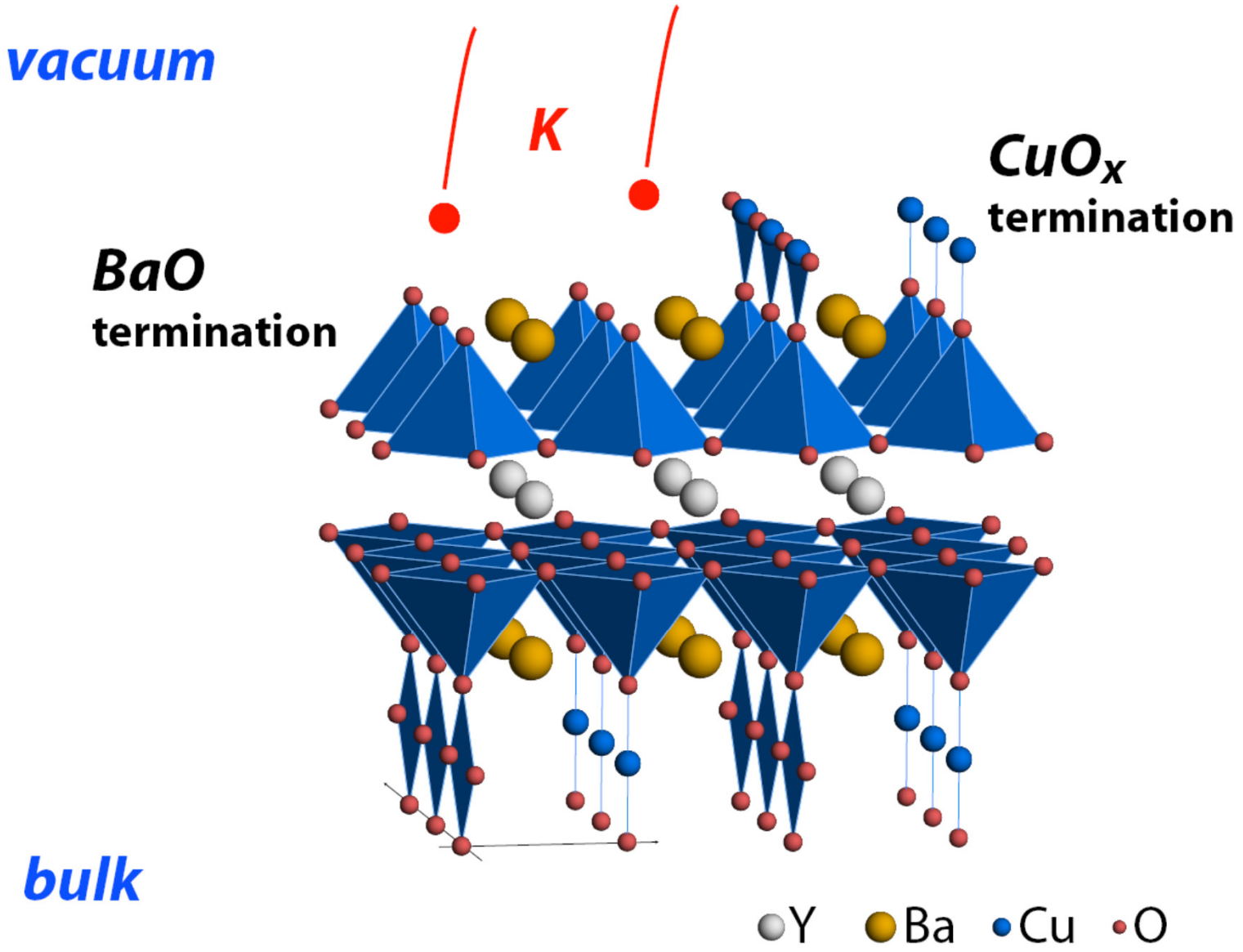

Hossain et al., Nature Physics **4**, 527 (2008)

Is the Surface of $Tl_{2-y}Ba_2Cu_{1+y}O_{6+x}$ polar? NO!!

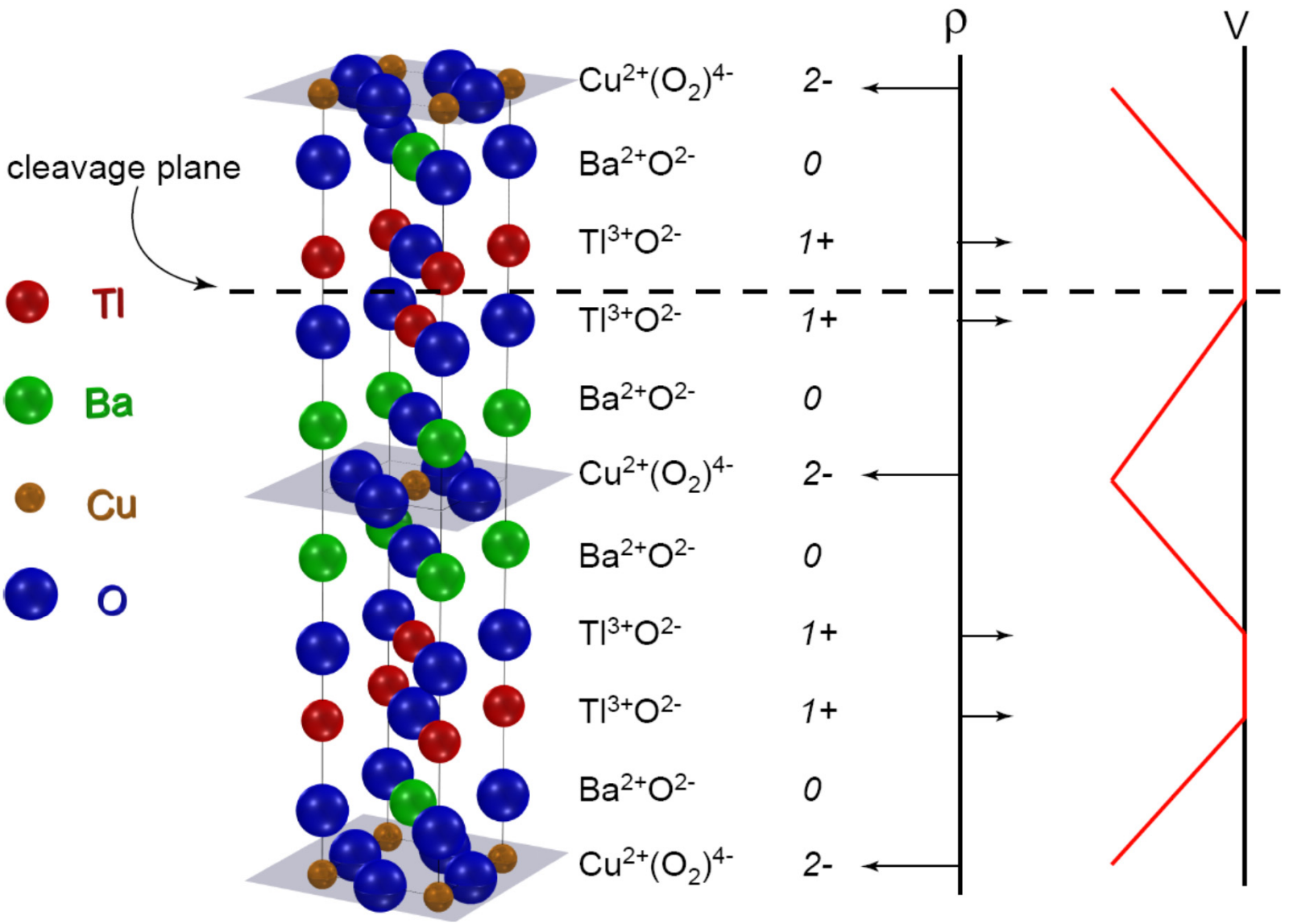

ARPES on K-deposited YBCO: counting carriers

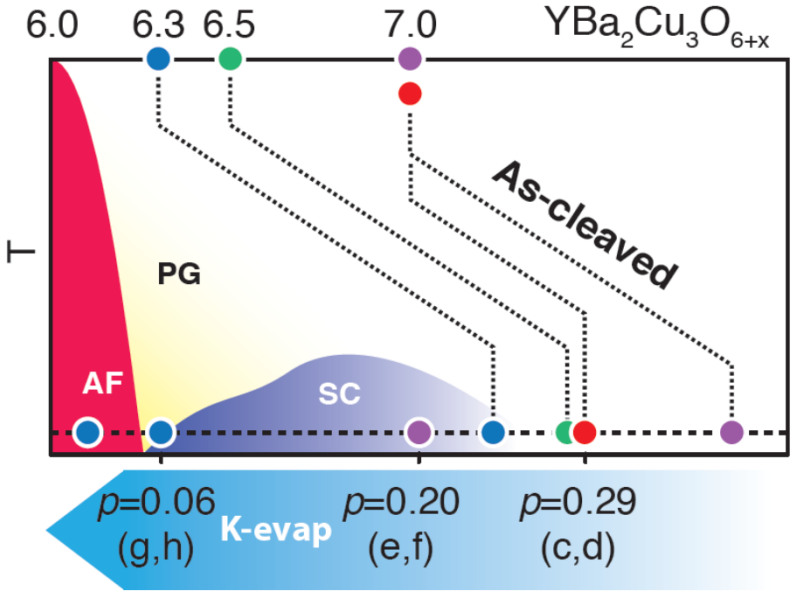

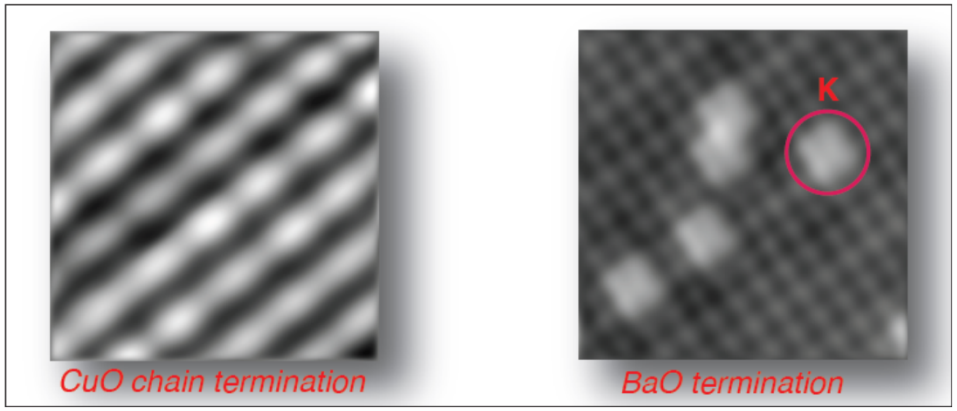

D. Fournier, Nature Physics **6**, 905 (2010)

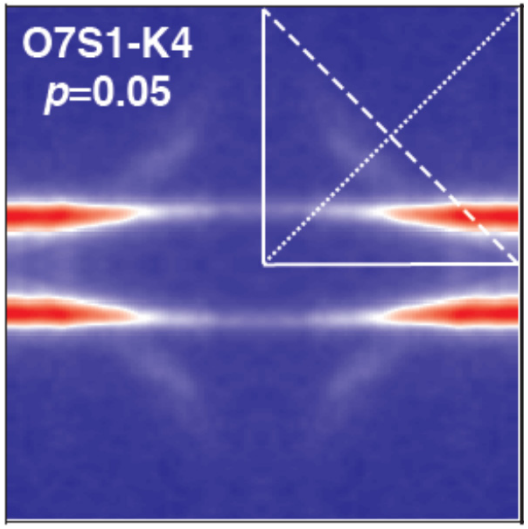

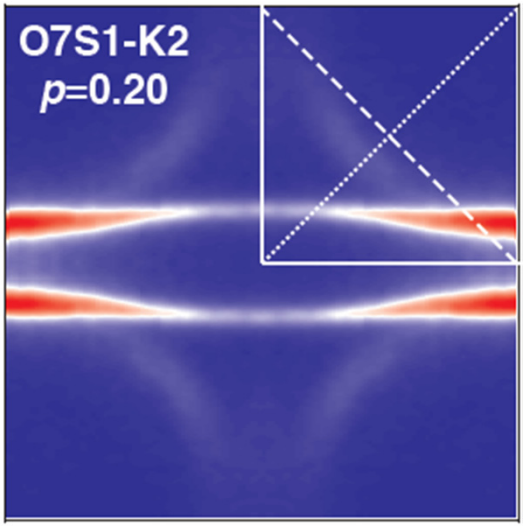

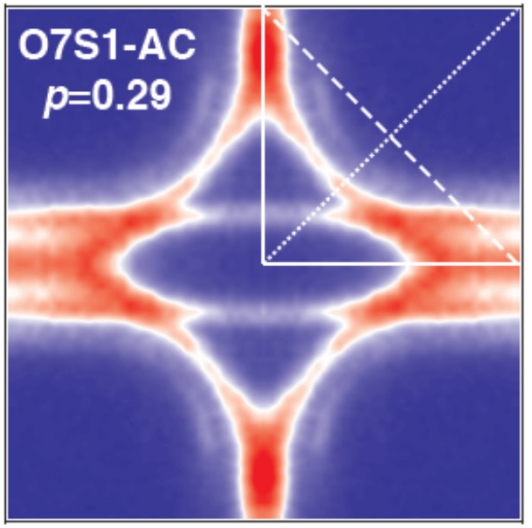

ARPES on K-deposited YBCO: arcs vs. pockets

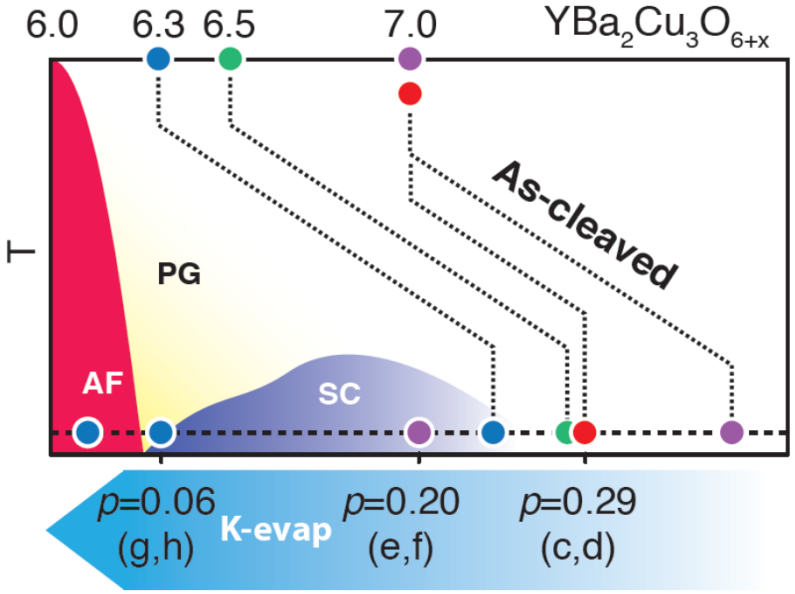

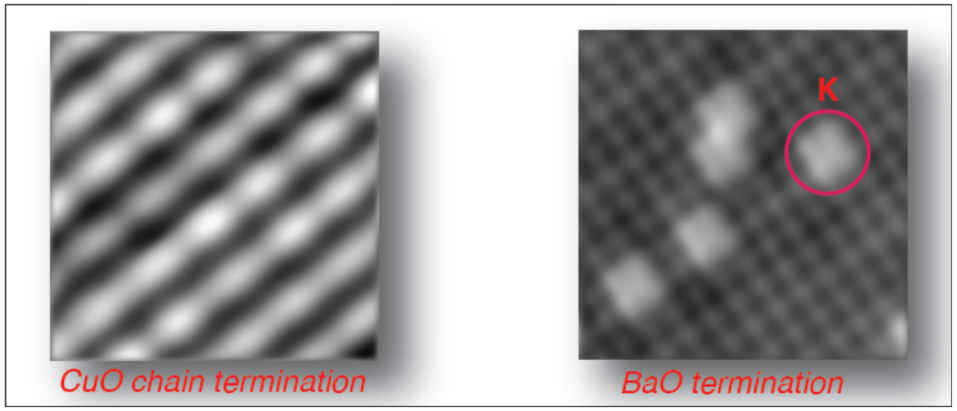

Fournier et al., Nature Physics **6**, 905 (2010)

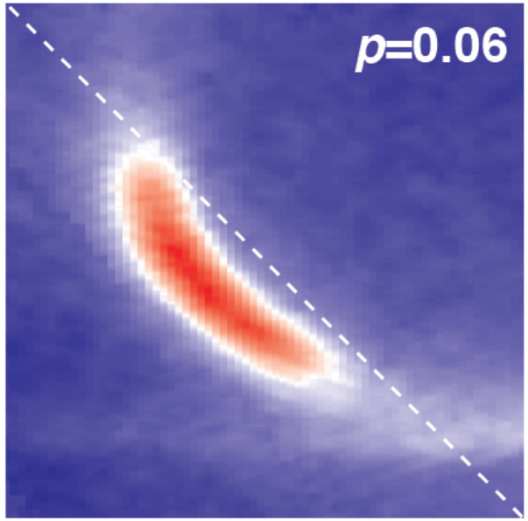

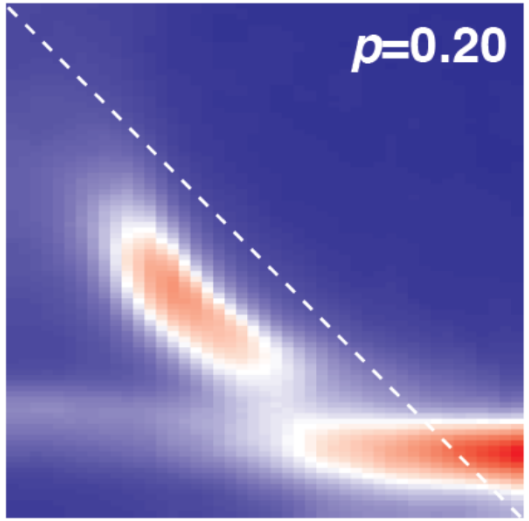

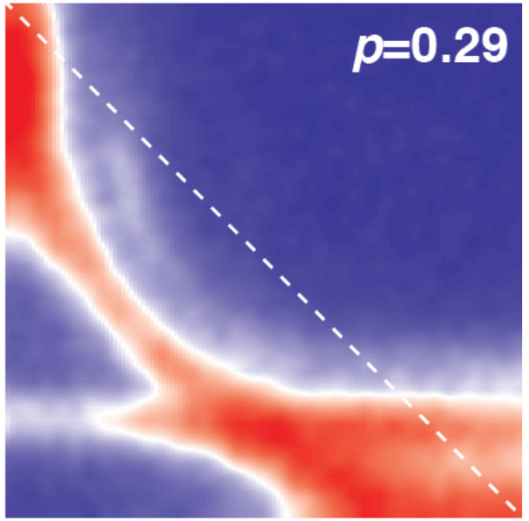

ARPES on K-deposited YBCO: SP and pseudogap

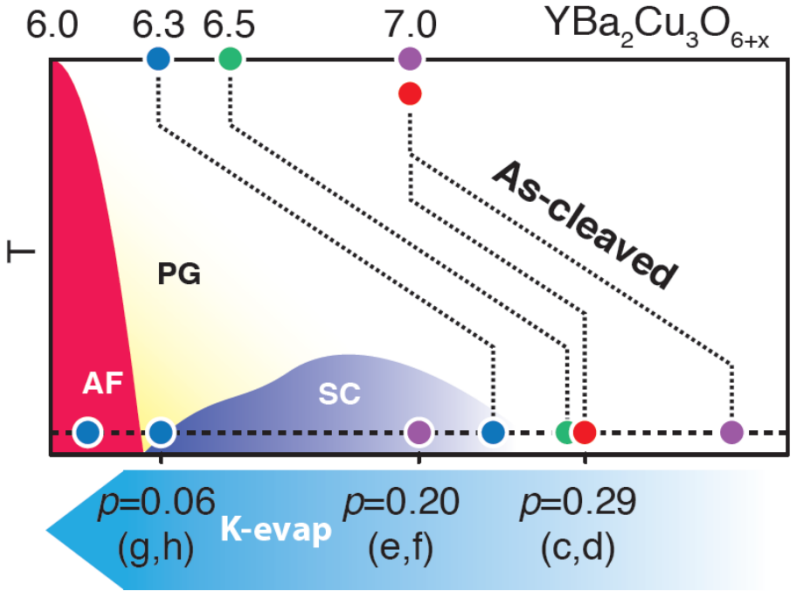

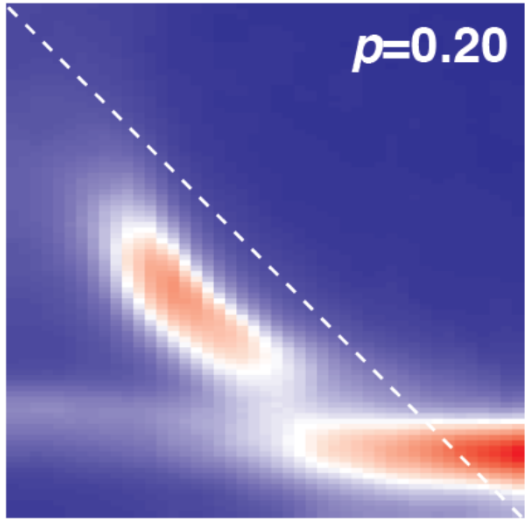

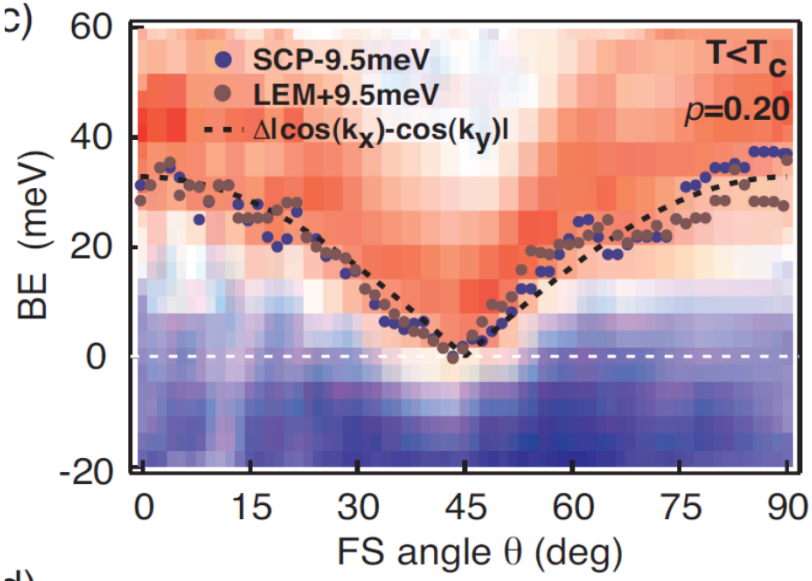

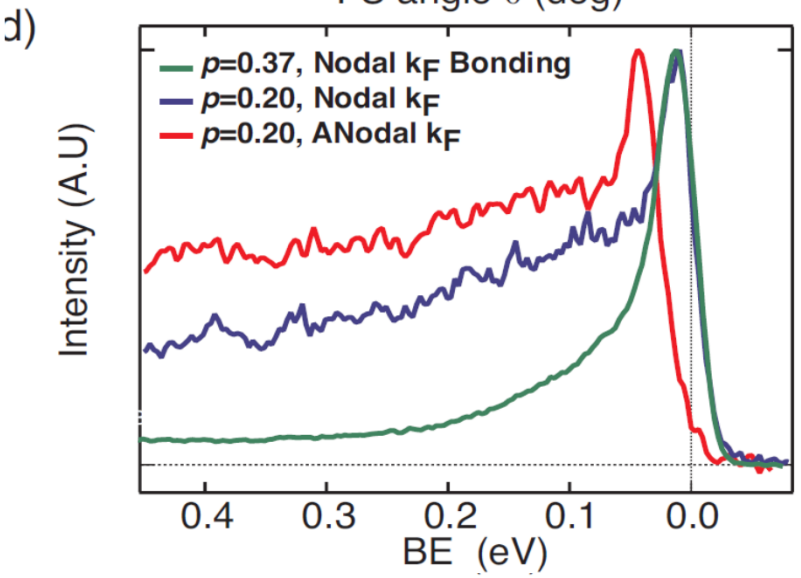

ARPES on K-deposited YBCO: SP and pseudogap

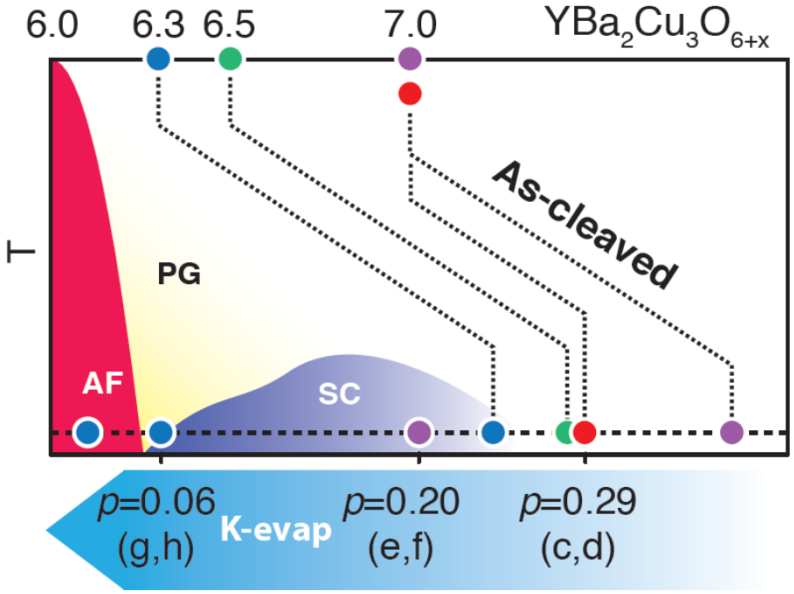

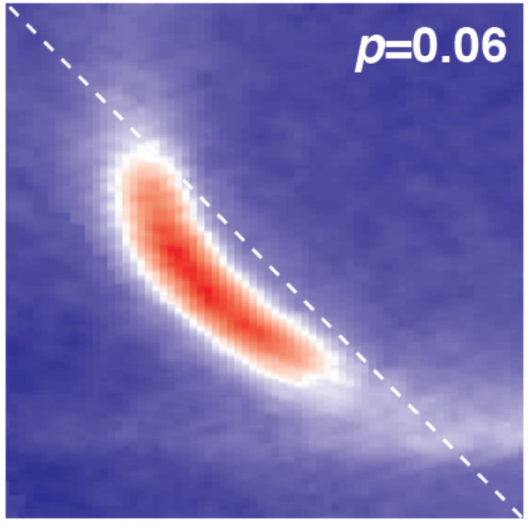

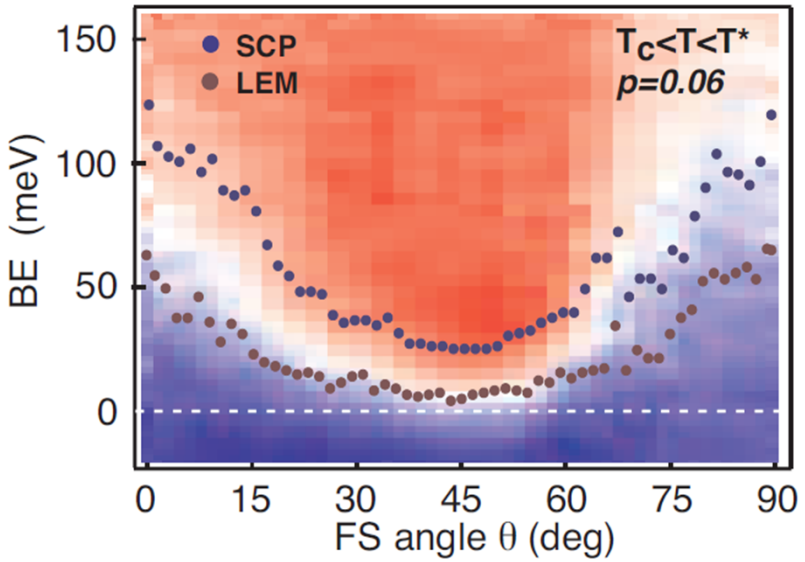

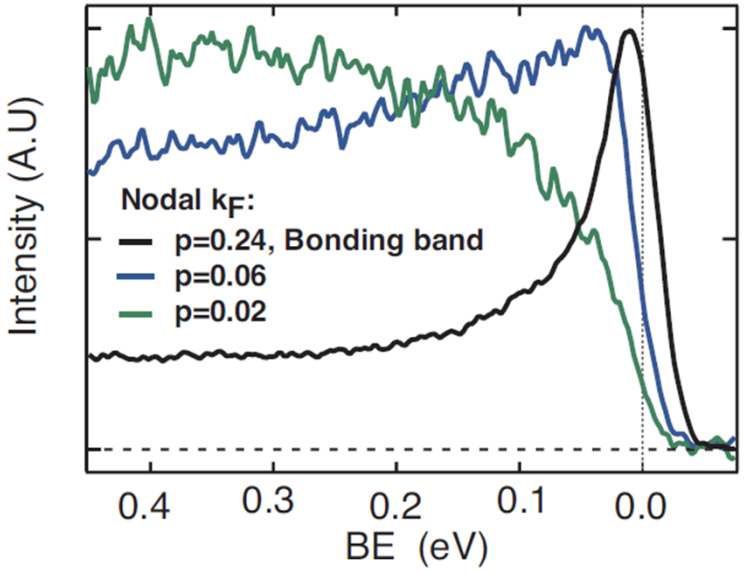

ARPES on K-deposited YBCO: SP and pseudogap

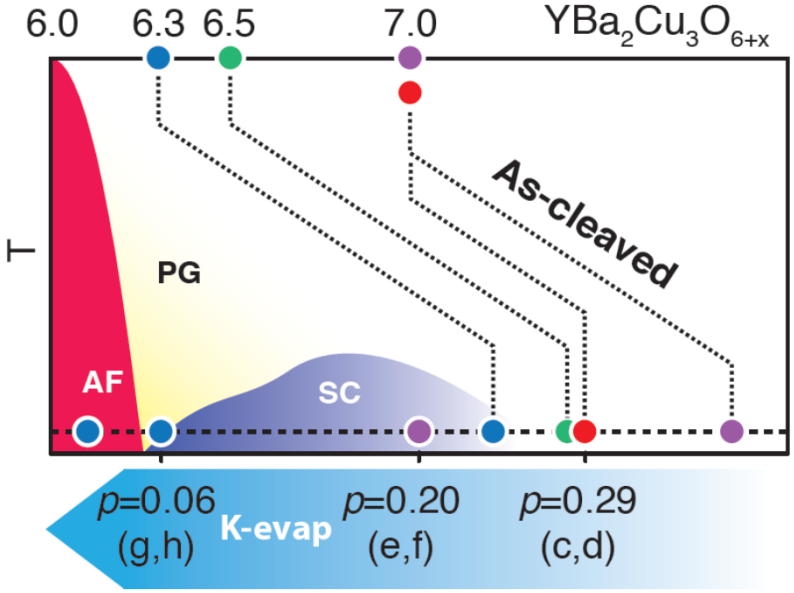

K doping provides access to the whole phase diagram (FS, dispersion, SC gap)

The FS collapses in 4 disconnected arcs

NO evidence for pockets in ARPES !!

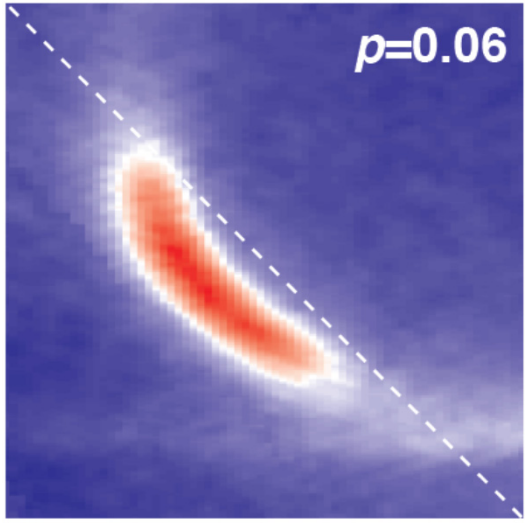

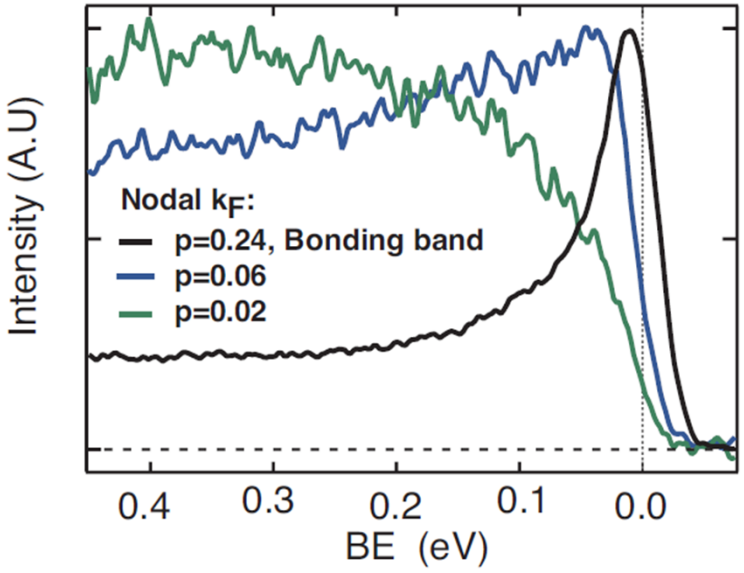

ARPES: The One-Particle Spectral Function

A. Damascelli, Z. Hussain, Z.-X Shen, Rev. Mod. Phys. **75**, 473 (2003)

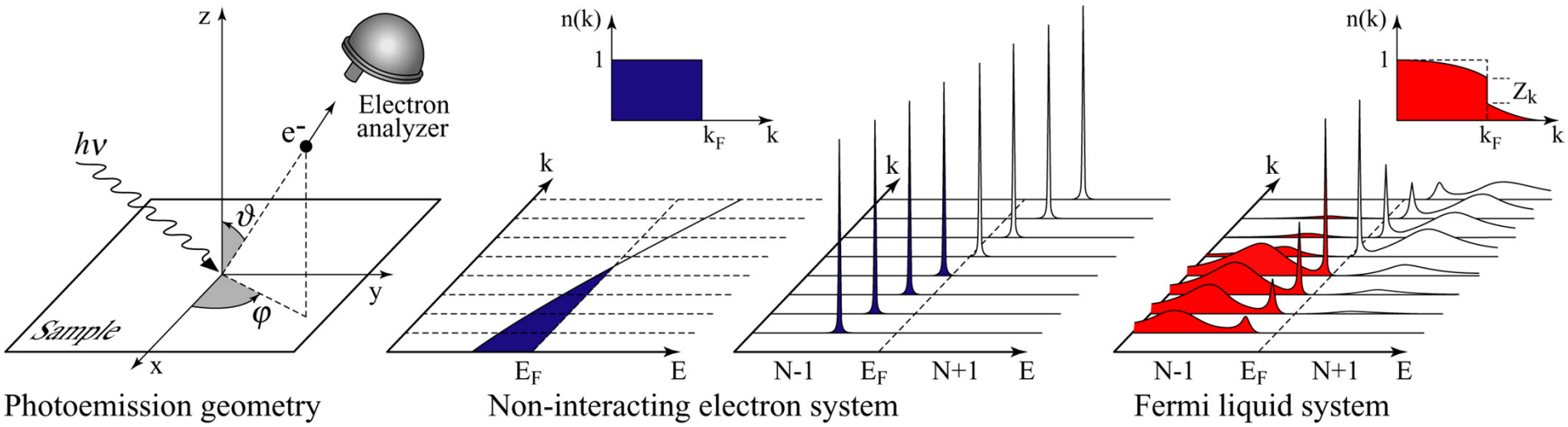

Photoemission intensity: $I(k,\omega) = I_0 \, |M(k,\omega)|^2 f(\omega) \, A(k,\omega)$

Single-particle spectral function

$$A(\mathbf{k},\omega) = -\frac{1}{\pi} \frac{\Sigma''(\mathbf{k},\omega)}{[\omega - \epsilon_{\mathbf{k}} - \Sigma'(\mathbf{k},\omega)]^2 + [\Sigma''(\mathbf{k},\omega)]^2}$$

$\Sigma(k,\omega)$: the "self-energy" captures the effects of interactions

Renormalization of Polaronic Quasiparticles

$$\mathcal{H} = \sum_k \varepsilon_k^b c_k^\dagger c_k + \Omega \sum_Q b_Q^\dagger b_Q + \frac{g}{\sqrt{N}} \sum_{k,Q} c_{k-Q}^\dagger c_k (b_Q^\dagger + b_{-Q})$$

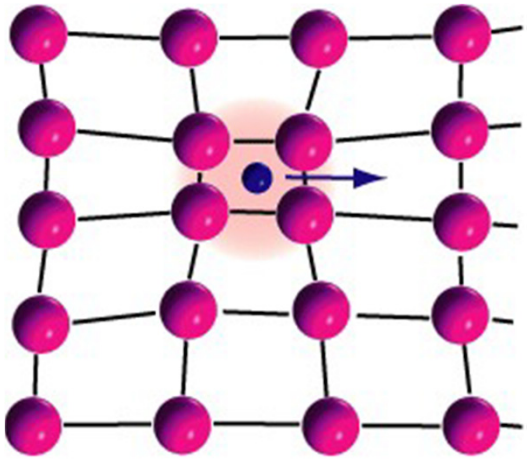

$$A(\mathbf{k},\omega) = Z_\mathbf{k} \frac{\Gamma_\mathbf{k}/\pi}{(\omega - \varepsilon_\mathbf{k})^2 + \Gamma_\mathbf{k}^2} + A_{inc}$$

$$m^* > m \qquad |\varepsilon_\mathbf{k}| < |\epsilon_\mathbf{k}|$$

$$\tau_\mathbf{k} = 1/\Gamma_\mathbf{k}$$

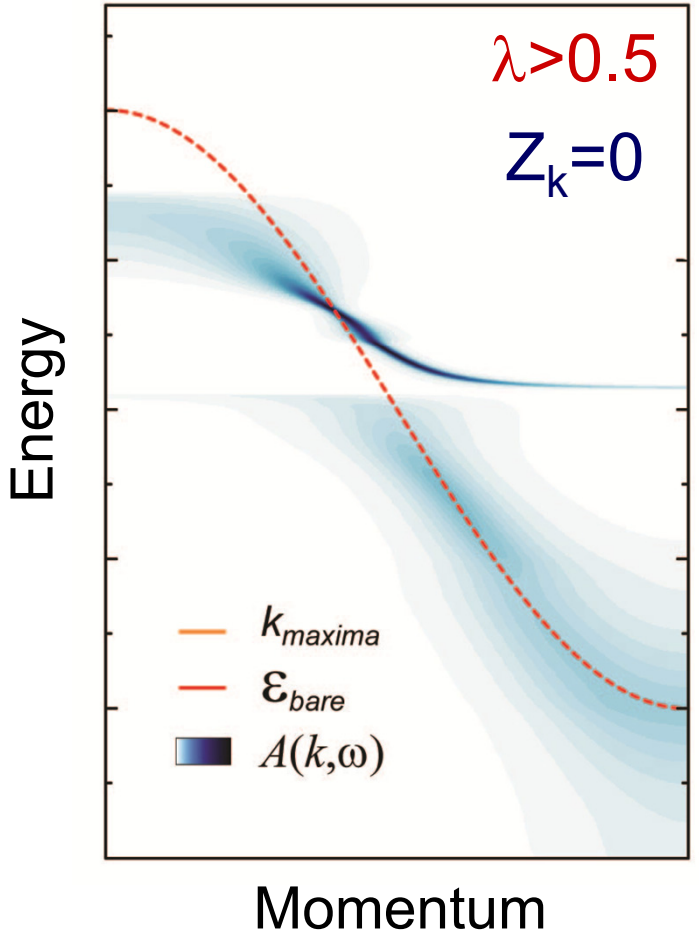

Veenstra, Goodvin, Berciu, Damascelli, PRB **82**, 012504 (2010)

Renormalization of Polaronic Quasiparticles

$$\mathcal{H} = \sum_k \varepsilon_k^b c_k^\dagger c_k + \Omega \sum_Q b_Q^\dagger b_Q + \frac{g}{\sqrt{N}} \sum_{k,Q} c_{k-Q}^\dagger c_k (b_Q^\dagger + b_{-Q})$$

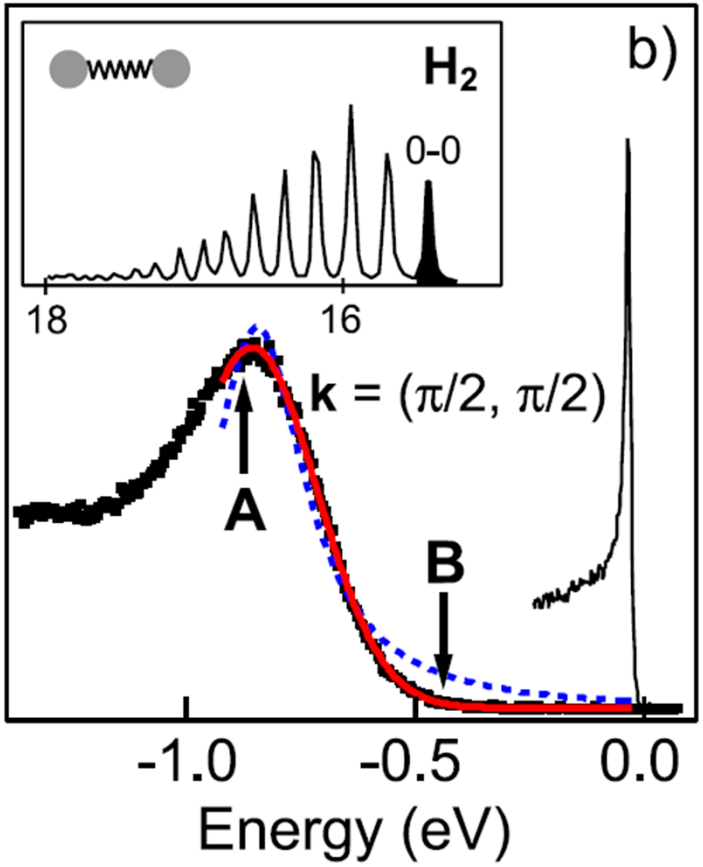

K.M. Shen et al., PRL **93,** 267002 (2004)

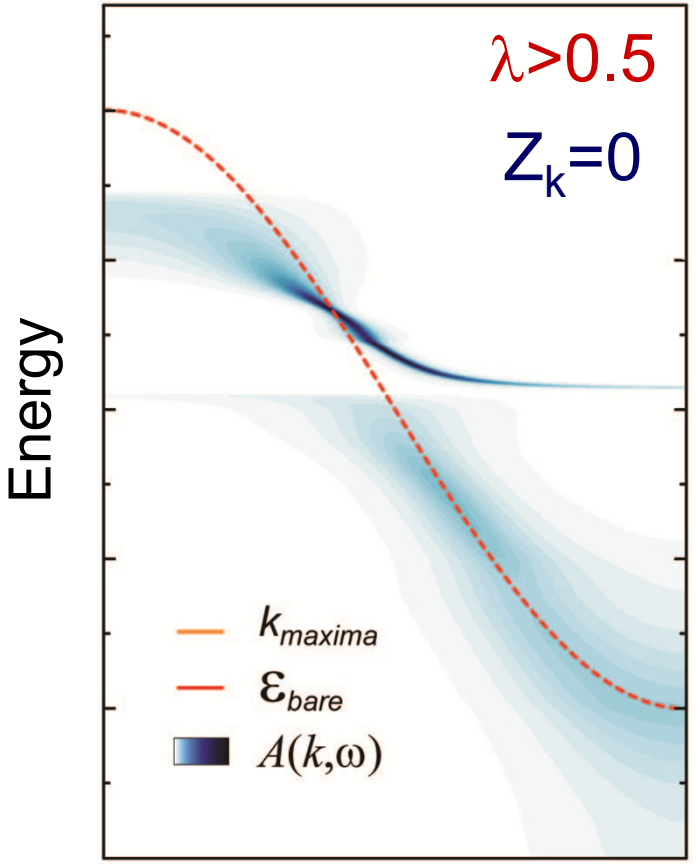

Veenstra, Goodvin, Berciu, Damascelli, PRB **82**, 012504 (2010)

Quasiparticle Coherence across the Phase Diagram

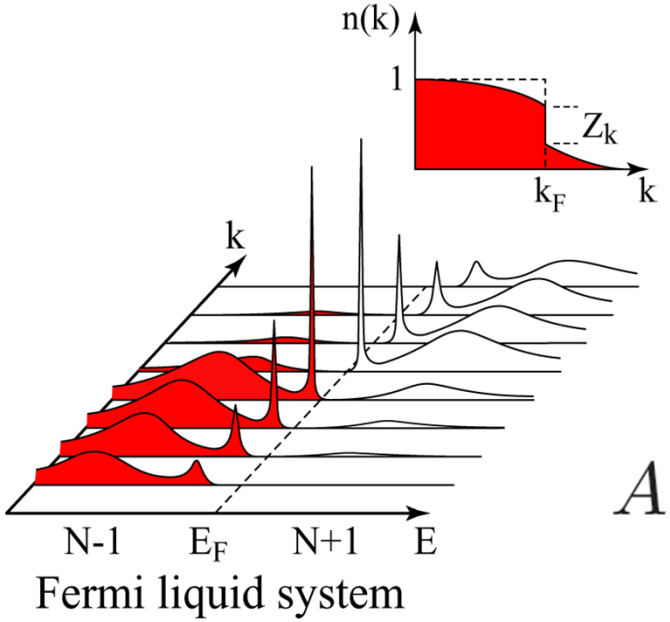

Fermi liquid system

$$Z_k = \int A_{coh}(k,\omega)\, d\omega$$

$$I(k,\omega) = I_0(k) f(\omega) A(k,\omega)$$

$$A(k,\omega) \equiv A_{coh}(k,\omega) + A_{incoh}(k,\omega)$$

$$Z_k = \int I_{coh}(k,\omega)\, d\omega / \int I(k,\omega)\, d\omega$$

Quasiparticle Coherence across the Phase Diagram

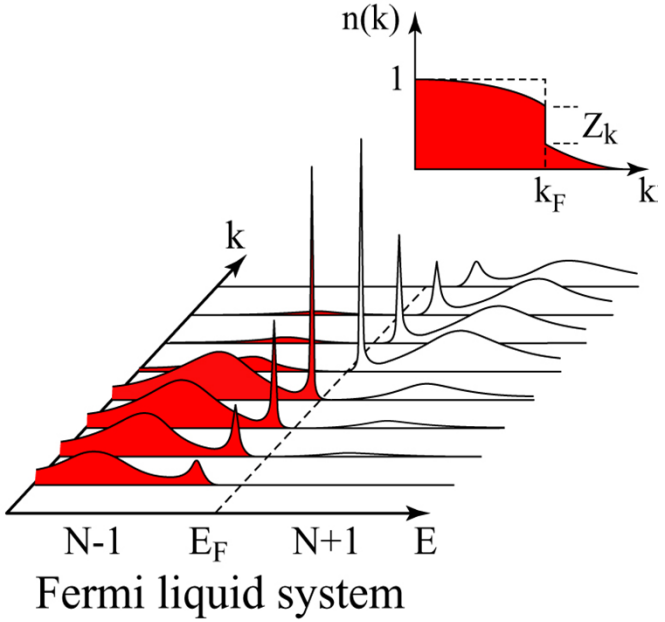

Fermi liquid system

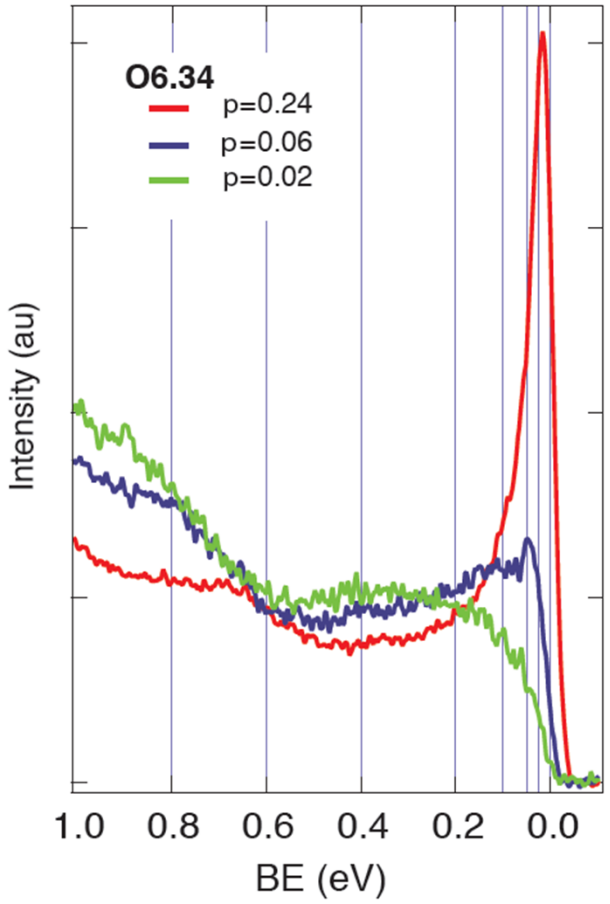

$$Z_k = \int I_{coh}(k,\omega)\, d\omega / \int I(k,\omega)\, d\omega$$

Quasiparticle Coherence across the Phase Diagram

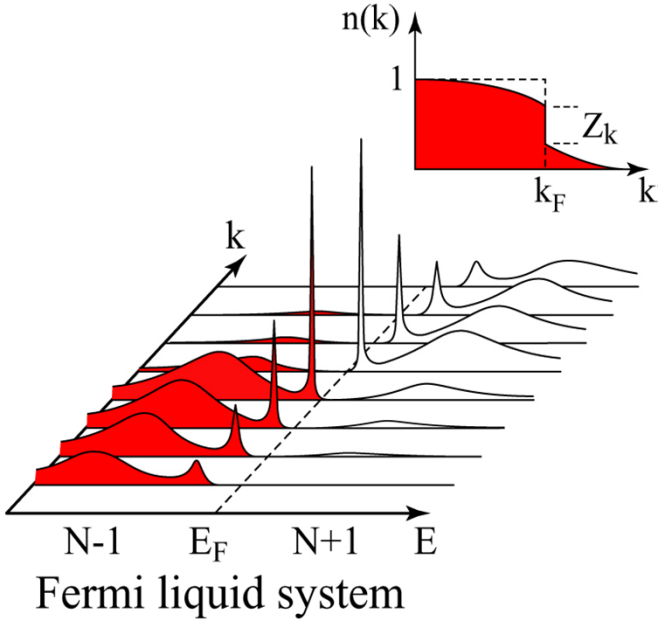

Fermi liquid system

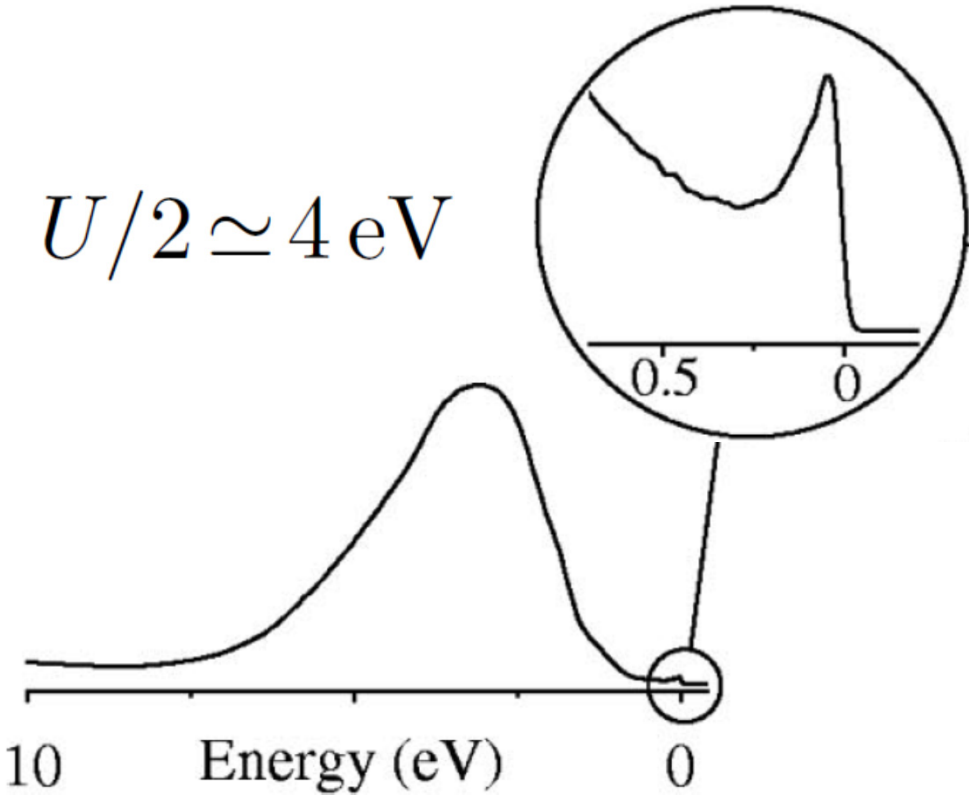

$$Z_k = \int I_{coh}(k,\omega)\, d\omega / \int I(k,\omega)\, d\omega$$

Quasiparticle Coherence across the Phase Diagram

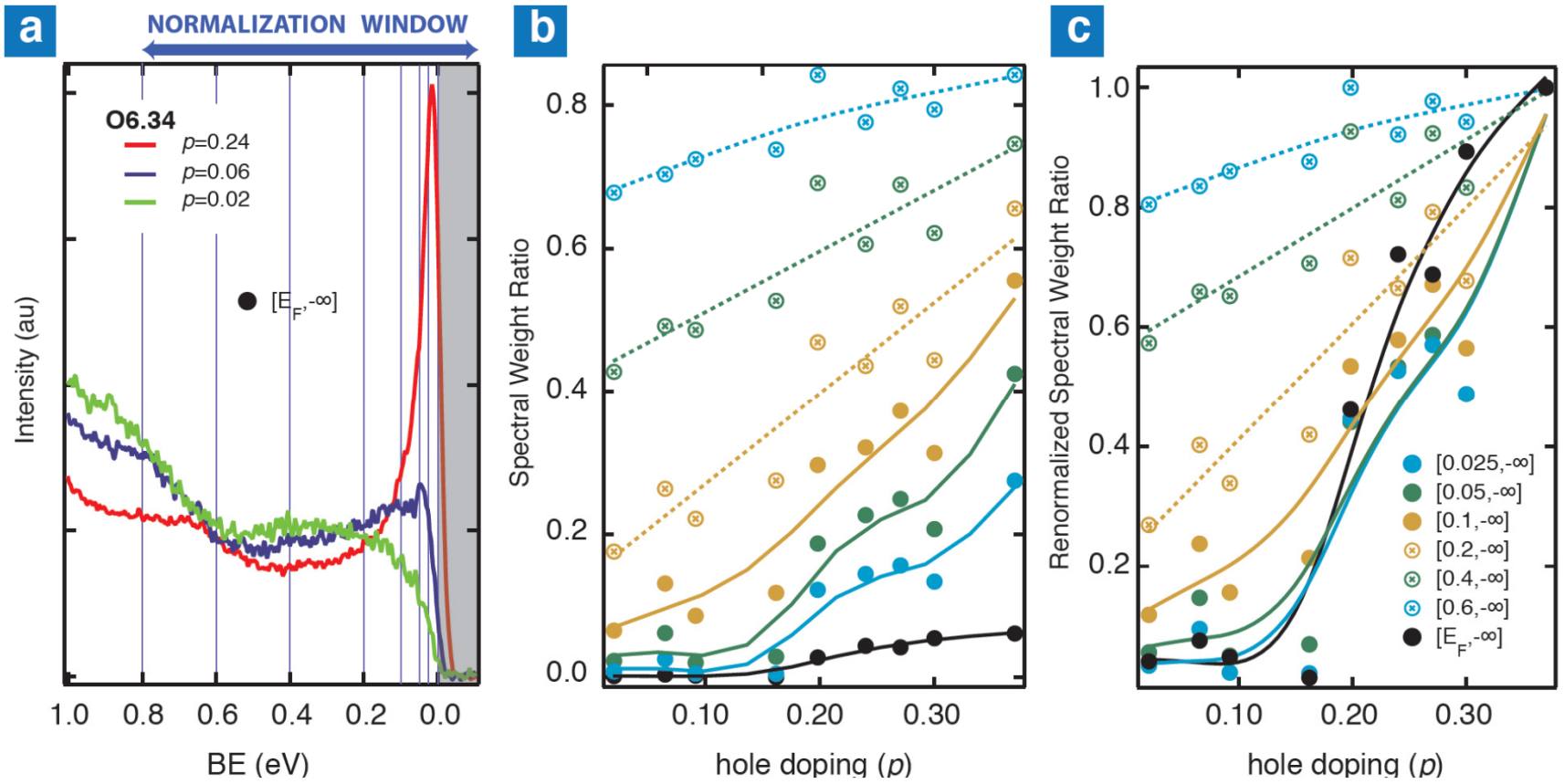

$$Z_N = \int_{BE_{min}}^{-\infty} I(k_{F,N},\omega)\,d\omega \Big/ \int_{0.8\,eV}^{-\infty} I(k_{F,N},\omega)\,d\omega$$

David Fournier, Nature Physics (2010)

Bilayer Band Splitting and Quasiparticle Integrity

$$\epsilon^{B,AB}(k) = \epsilon(k) \mp t_{\perp}^{eff}(k) = \epsilon(k) \mp Z_k t_{\perp}^{LDA}(k)$$

Bilayer band splitting
Anti-bonding & Bonding

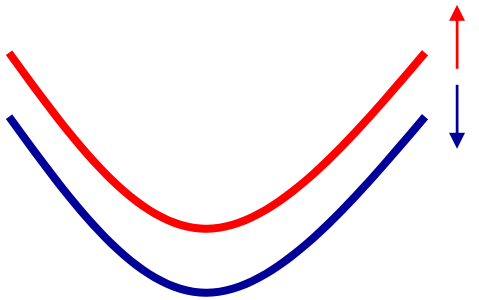

FS with bilayer splitting

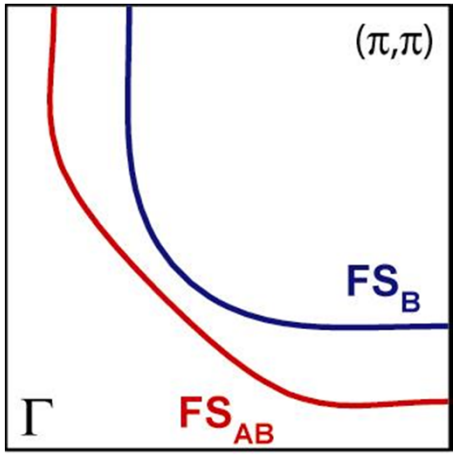

Correlations suppress Z_k

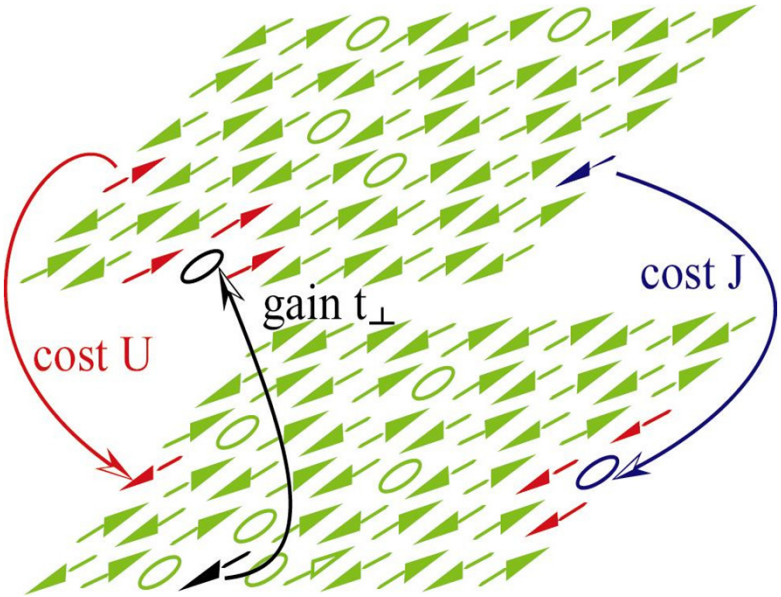

$$Z \simeq 2p/(p+1)$$

Sawatzky, Anderson, Randeria, Rice, et al.

Bilayer band splitting and quasiparticle coherence

$$Z_N = \Delta\epsilon_N^{B,AB}/2t_\perp^{LDA}(N)$$

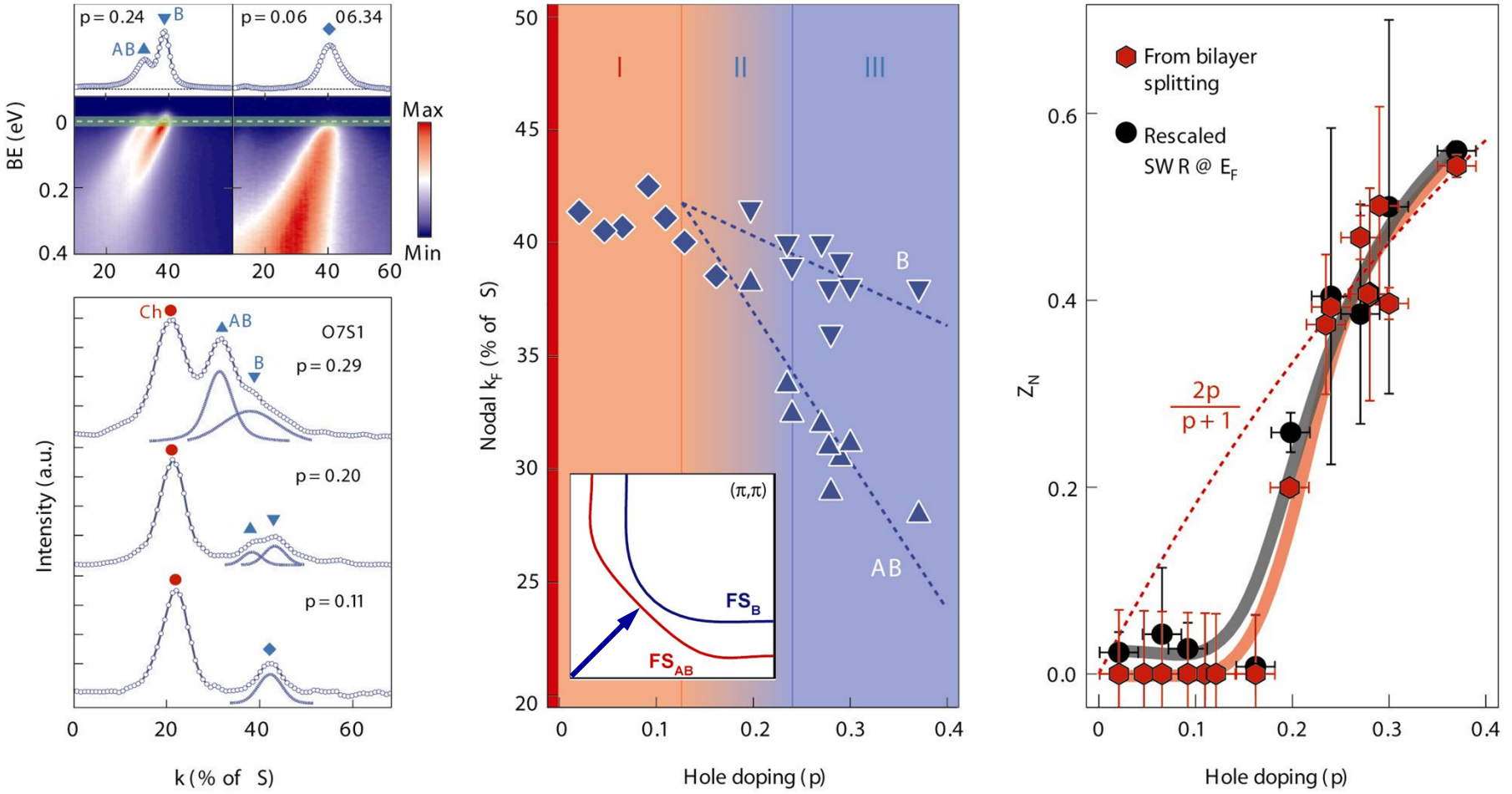

Fournier et al., Nature Physics **6**, 905 (2010)

Bilayer band splitting and quasiparticle coherence

$$Z_N = \Delta\epsilon_N^{B,AB} / 2t_\perp^{LDA}(N)$$

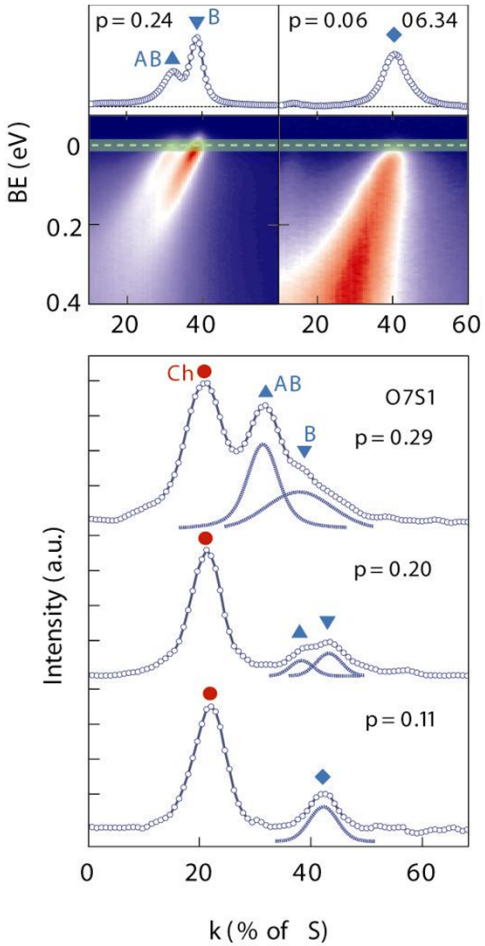

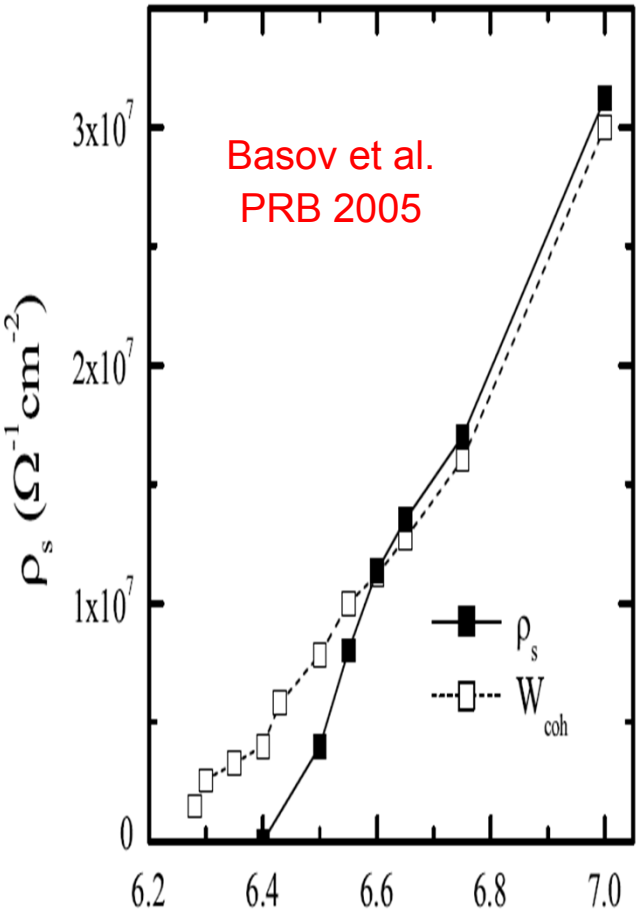

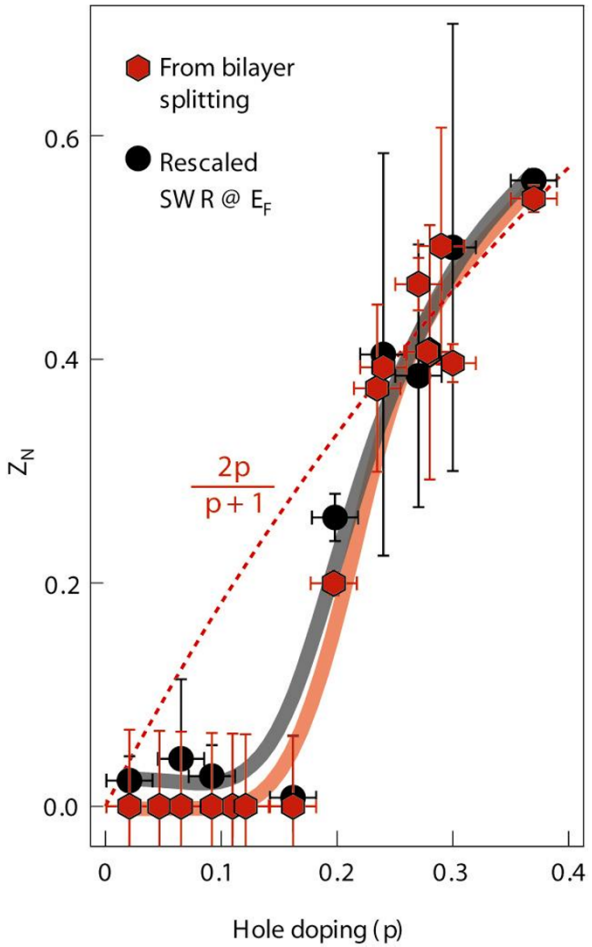

Fournier et al., Nature Physics **6**, 905 (2010)

Bilayer band splitting and quasiparticle coherence

$$Z_N = \Delta\epsilon_N^{B,AB} / 2t_\perp^{LDA}(N)$$

- Quantitative estimate of Z
- Agreement with 2p/(p+1) for x>0.23
- Isotropic Z_N~0.54 and Z_{AN}~0.50
- Vanishing Z_N below 15-10%
- $t_\perp$~10meV consistent with QO
- Z even smaller for pockets' "other side"
- Pseudogap? Loss of coherent SW
- Fermi surface? Luttinger's counting?

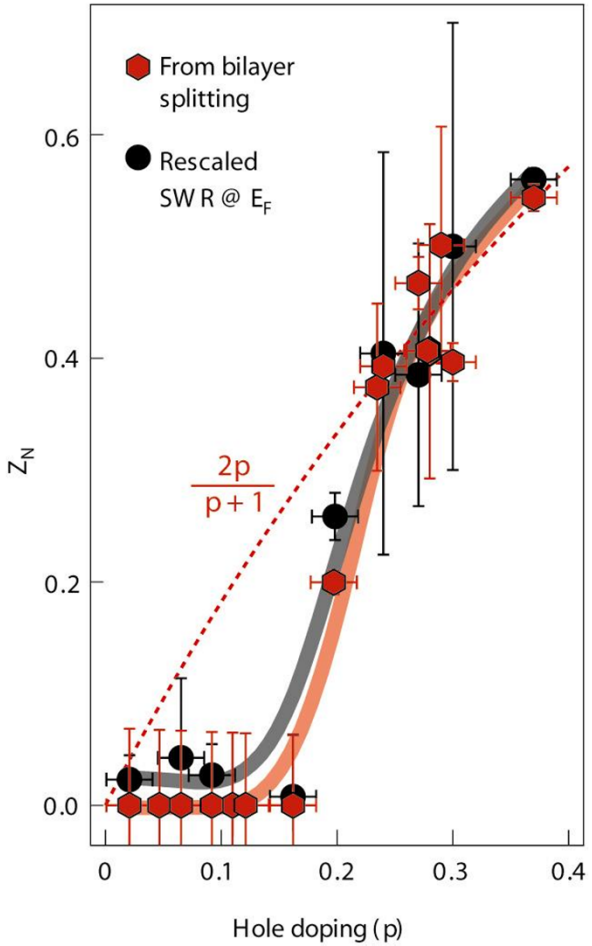

Fournier et al., Nature Physics **6**, 905 (2010)

Outline Part II

References, slides, and lecture notes

CUSO Lecture – Lausanne 02/2011

http://www.physics.ubc.ca/~quantmat/ARPES/RESEARCH/ARPES_intro.html

Physica Scripta. Vol. T109, 61–74, 2004

Probing the Electronic Structure of Complex Systems by ARPES

Andrea Damascelli

Department of Physics & Astronomy, University of British Columbia, 6224 Agricultural Road, Vancouver, British Columbia V6T 1Z1, Canada

Received June 18, 2003; accepted June 30, 2003

PACS Ref: 79.60.i, 71.18.+y; 71.20.−b

Abstract

Angle-resolved photoemission spectroscopy (ARPES) is one of the most direct methods of studying the electronic structure of solids. By measuring the kinetic energy and angular distribution of the electrons photoemitted from a sample illuminated with sufficiently high-energy radiation, one can gain information on both the energy and momentum of the electrons propagating inside a material. This is of vital importance in elucidating the connection between electronic, magnetic, and chemical structure of solids, in particular for those complex systems which cannot be appropriately described within the independent-particle picture. The last decade witnessed significant progress in this technique and its applications, thus ushering in a new era in photoelectron spectroscopy; today, ARPES experiments with 2 meV energy resolution and 0.2° angular resolution are a reality even for photoemission on solids. In this paper we will review the fundamentals of the technique and present some illustrative experimental results; we will show how ARPES can probe the momentum-dependent electronic structure of solids providing detailed information on band dispersion and Fermi surface as well as on the strength and nature of many-body correlations, which may profoundly affect the one-electron excitation spectrum and in turn the macroscopic physical properties.

photoemission event is decomposed in three independent steps: optical excitation between the initial and final *bulk* Bloch eigenstates, *travel* of the excited electron to the surface, and escape of the photoelectron into vacuum after transmission through the *surface* potential barrier. This is the most common approach, in particular when photoemission spectroscopy is used as a tool to map the electronic band structure of solids. However, from the quantum-mechanical point of view photoemission should not be described in terms of several independent events but rather as a *one-step* process (Fig. 1(b)): in terms of an optical transition (with probability given by Eq. (12)) between initial and final states consisting of many-body wave functions that obey appropriate boundary conditions at the surface of the solid. In particular (see Fig. 2), the initial state should be one of the possible N-electron eigenstates of the semi-infinite crystal, and the final state must be one of the

http://www.physics.ubc.ca/~quantmat/ARPES/RESEARCH/ARPES_intro.html

ARPES ON COMPLEX SYSTEMS

home
people
research
projects
ARPES intro
open positions
facilities
publications
presentations
pictures
contact

Electronic and Magnetic Interactions in Novel Complex Systems

Angle-resolved photoemission spectroscopy (ARPES) is one of the most direct methods of studying the electronic structure of solids and is the only truly momentum-resolved probe, which is essential for the investigation of low dimensional and strongly anisotropic systems. By measuring momentum and kinetic energy of the electrons photoemitted from a sample illuminated with radiation of energy larger than the material work function, it is possible to gain information on both energy and the momentum of the electronic excitations inside the solid.

As the intensity measured in photoemission experiments is proportional to the single-particle spectral function $A(\mathbf{k},\omega)=-(1/\pi)\mathrm{Im}G(\mathbf{k},\omega)$, ARPES provides direct insights on the Green's function $G(\mathbf{k},\omega)$ which describes the propagation of an electron in a many-body system. This is of vital importance in elucidating the connection between electronic, magnetic, and chemical structure of solids, in particular for those complex systems which cannot be described within the independent-particle picture.

The last decade witnessed significant progress in this technique and its applications, thus ushering in a new era in photoelectron spectroscopy. Today, ARPES experiments with 2 meV energy resolution and 0.2 degree angular resolution are a reality even for photoemission on solids, providing detailed information on band dispersion and Fermi surface, as well as on the strength and nature of those many-body correlations which may profoundly affect the one-electron excitation spectrum and, in turn, determine the macroscopic physical properties.

The Photoelectric Effect

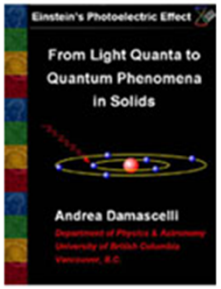

ARPES: Introduction

ARPES on HTSC's

ARPES: Viewgraphs

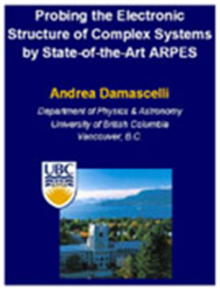

Andrea Damascelli

UBC-MPI Quantum Matter Institute

Thank you!

CUSO Lecture – Lausanne 02/2011